Universidade de Aveiro Departamento de Biologia
2014

MIGUEL ALBUQUERQUE COSTA LEAL

Trophic plasticity in the cnidarian-dinoflagellate symbiosis

Plasticidade trófica na simbiose entre cnidários e dinoflagelados

Universidade de Aveiro Departamento de Biologia
2014

MIGUEL ALBUQUERQUE COSTA LEAL

Trophic plasticity in the cnidarian-dinoflagellate symbiosis

Plasticidade trófica na simbiose entre cnidários e dinoflagelados

Tese apresentada à Universidade de Aveiro para cumprimento dos requisitos necessários à obtenção do grau de Doutor em Biologia, realizada sob a orientação científica do Doutor Ricardo Calado, Investigador Principal do Departamento de Biologia da Universidade de Aveiro, e do Professor Doutor João Serôdio, Professor Auxiliar do Departamento de Biologia da Universidade de Aveiro.

Miguel C. Leal was supported by a PhD scholarship (SFRH/BD/63783/2009) funded by Fundação para a Ciência e Tecnologia Portugal (QREN-POPH – Type 4.1 – Advanced Training, subsidized by the European Social Fund and national funds MCE)

The unknown should be protected for unknown reasons

o júri

presidente

Professor Doutor Vasile Staicu
Professor Catedrático da Universidade de Aveiro

vogais

Professor Doutor Henrique Manuel Roque Nogueira Cabral
Professor Catedrático da Faculdade de Ciências da Universidade de Lisboa

Professor Doutor Amadeu Mortágua Velho da Maia Soares
Professor Catedrático da Universidade de Aveiro

Professora Doutora Maria Ester Tavares Álvares Serrão
Professora Auxiliar com Agregação da Faculdade de Ciências e Tecnologia da Universidade do Algarve

Doutor Rui Afonso Bairrão da Rosa
Investigador Principal da Faculdade de Ciências da Universidade de Lisboa

Doutor Ricardo Jorge Guerra Calado (Orientador)
Investigador Principal do CESAM-Centro de Estudos do Ambiente e do Mar da Universidade de Aveiro

acknowledgments

This is my attempt to thank those who have been pivotal during my PhD. I start with a special acknowledgment to Ricardo Calado, who I first met in 2006. Later in 2009, Ricardo gave me the opportunity to apply to a PhD grant under his supervision, which was later approved. Since then, our similar working methods and ambitions were, and will be, definitely important in my life. I truly thank Ricardo for his friendship, patience and support. I'd also like to thank João Serôdio for his trust, encouragement, and important role in this learning process. A special thanks goes also to Jens Nejstgaard, for being crazy enough to accept me as a PhD student. I followed him to Savannah and his friendship and guidance have been very important. Also thanks to Jens I had the opportunity to meet and work with Marc Frischer, who has been critical in my development as a scientist, particularly by teaching me to think "Why?" instead of "How?". I'm sure that without Marc and Jens Savannah wouldn't be as meaningful to me as it is today. Also from Savannah, I'd like to thank Stella, everyone at the business office (Christel, Levon and Gail) and in the lab, especially Megan and Tina. My lab mates and friends in Aveiro have also been important, particularly Rui, Jörg, Martin, Gi, Sónia, Ana, João and Silja. I also want to thank Bruno Jesus and Rafael Mendes for their friendship and fruitful discussions.

A very very special thanks goes to Christine Ferrier-Pagès from Monaco. Christine was also crazy enough to accept me as a non-official PhD student. She ended up being the only coral expert among my advisors and her critical thinking and scientific discussions have been extremely important. I also had the opportunity to meet and work with great people that I'd like to thank: Igor Cruz, Mark Warner, Tye Pettay, Kenny Hoadley, Ronald Osinga and Tim Wijgerde. I'm especially thankful to meet and be friends with Christopher Sheridan, who has been a great friend and scientific collaborator, to Vasco Mota, João Puga, Mª João and Fernando Albuquerque for all the friendship and support.

My family, for the unconditional support, concern, patience, love and care that were critical to make me what I am today.

At last, but truly the first, to Marta for being my source of motivation, for helping me being a better person, for being there even when I wasn't, for sharing life and show me how great this life can be.

palavras-chave Corais; Simbiose; *Symbiodinium*; Ecologia trófica; *Aiptasia*; Fotossíntese

resumo

Os recifes de coral são ecossistemas de elevada importância ecológica e económica. Contudo, encontram-se em declínio global devido ao efeito das alterações climáticas e outras perturbações de origem antropogénica. Os corais, tal como outros cnidários, vivem em simbiose com dinoflagelados fotossintéticos do género *Symbiodinium*. Esta associação permite ao hospedeiro dispor de vias metabólicas alternativas, uma vez que os simbiontes fixam carbono fotossinteticamente e translocam-no para o hospedeiro. Para além deste modo de nutrição autotrófico, estes cnidários também se alimentam de matéria orgânica disponível no meio ambiente (heterotrofia). O balanço nutricional entre auto- e heterotrofia é fundamental para o funcionamento, capacidade adaptativa e resiliência da simbiose entre cnidários e dinoflagelados. No presente trabalho foram utilizadas novas abordagens metodológicas para investigar a importância da auto- e heterotrofia na ecofisiologia de cnidários em simbiose com *Symbiodinium* e as implicações ecológicas desta plasticidade trófica. Os métodos aqui desenvolvidos estão relacionados com a fotofisiologia, produção de biomassa do organismo modelo *Aiptasia pallida* e métodos moleculares para investigar heterotrofia na simbiose entre cnidários e dinoflagelados. Foram utilizados métodos não invasivos para avaliar padrões espaciais fotofisiológicos em cnidários associados com *Symbiodinium* e explorar a relação entre a fluorescência da clorofila e a abundância relativa de clorofila *a* e proteínas verdes fluorescentes. As condições de cultivo que maximizam a produção de *Aiptasia* sp. foram identificadas, bem como as respetivas implicações na sua composição em ácidos gordos. A utilização de marcadores tróficos moleculares permitiu identificar que o tempo de digestão em cnidários associados com *Symbiodinium* varia entre 1 e 3 dias e que depende da espécie de predador e de presa, bem como do historial trófico do predador. O mesmo método molecular permitiu concluir que as microalgas são uma presa potencialmente importante para a nutrição de corais simbióticos. Adicionalmente, os resultados obtidos através da utilização de isótopos estáveis *in situ*, para avaliar a ecologia trófica do coral simbiótico facultativo *Oculina arbuscula*, confirmaram a importância que os organismos pico- e nanoplanctónicos, principalmente autotróficos, podem representar para a nutrição de corais simbióticos. Por fim, o efeito da diversidade funcional de *Symbiodinium* na plasticidade trófica da simbiose entre cnidários e dinoflagelados foi investigado. Concluiu-se que a identidade do simbionte define esta plasticidade através dos seus requisitos metabólicos individuais, capacidade para fixar carbono, quantidade de carbono translocado e a capacidade de ingestão e digestão de presas do cnidário hospedeiro.

keywords Corals; Symbiosis; *Symbiodinium*; Trophic ecology; *Aiptasia*; Photosynthesis

abstract

Coral reefs are of utmost ecological and economical importance but are currently in global decline due to climate change and anthropogenic disturbances. Corals, as well as other cnidarian species, live in symbiosis with photosynthetic dinoflagellates of the genus *Symbiodinium*. This relationship provides the cnidarian host with alternative metabolic pathways, as the symbionts translocate photosynthetic carbon to the animal. Besides this autotrophic nutrition mode, symbiotic cnidarians also take up organic matter from the environment (heterotrophy). The nutritional balance between auto- and heterotrophy is critical for the functioning, fitness and resilience of the cnidarian-dinoflagellate symbiosis. New methodological approaches were developed to better understand the role of auto- and heterotrophy in the ecophysiology of cnidarians associated with *Symbiodinium*, and the ecological implications of this trophic plasticity. Specifically, the new approaches were developed to assess photophysiology, biomass production of the model organism *Aiptasia* sp. and molecular tools to investigate heterotrophy in the cnidarian-dinoflagellate symbiosis. Using these approaches, we were able to non-invasively assess the photophysiological spatial heterogeneity of symbiotic cnidarians and identify spatial patterns between chlorophyll fluorescence and relative content of chlorophyll *a* and green-fluorescent proteins. Optimal culture conditions to maximize the biomass production of *Aiptasia pallida* were identified, as well as their implications on the fatty acid composition of the anemones. Molecular trophic markers were used to determine prey digestion times in symbiotic cnidarians, which vary between 1-3 days depending on prey species, predator species and the feeding history of the predator. This method was also used to demonstrate that microalgae is a potential food source for symbiotic corals. By using a stable isotope approach to assess the trophic ecology of the facultative symbiotic *Oculina arbuscula in situ*, it was possible to demonstrate the importance of pico- and nanoplanktonic organisms, particularly autotrophic, in the nutrition of symbiotic corals. Finally, we showed the effects of functional diversity of *Symbiodinium* on the nutritional plasticity of the cnidarian-dinoflagellate symbiosis. Symbiont identity defines this plasticity through its individual metabolic requirements, capacity to fix carbon, quantity of translocated carbon and the host's capacity to feed and digest prey.

Table of contents

List of Figures

List of Tables

Chapter 1 Introduction

1.1 General Introduction

Coral reefs play a key ecological role as they harbour diverse and productive biological communities, mainly in shallow tropical marine ecosystems (Hoegh-Guldberg 1999). While these are dynamic systems subject to natural disturbances (Buddemeier & Smith 1999), the nature and temporal pattern of disturbances affecting coral reefs have changed dramatically over the past few decades, matching global climate change and increasing anthropogenic activities in coastal areas (Hoegh-Guldberg et al. 2007, De'ath et al. 2012). As the extent of disturbances affecting these ecosystems generally exceed their regenerative capacity, a global degradation of coral reefs has been recorded worldwide followed by critical losses of marine biodiversity (Pandolfi et al. 2005, 2011).

Cnidarians from order Scleractinia and Alcyonacea (class Anthozoa) are generally known as stony and soft corals, respectively. Corals are colonial organisms composed of individual polyps and are present in a wide range of environments, from warm tropical waters to temperate and polar environments (Veron 2000). While stony corals are not necessarily the most abundant or diverse animal group inhabiting coral reefs, they are especially important as they form the structural foundation of these ecosystems by producing the majority of the habitat structure for other reef organisms (Richmond 1993).

Numerous coral species live in symbiosis with unicellular dinoflagellates of genus *Symbiodinium* (popularly known as zooxanthellae), which are located in vacuoles within the endoderm cells of the zooxanthellate cnidarian (Trench 1993, Furla et al. 2005). The cnidarian-dinoflagellate symbiosis is likely the most prevalent and ecologically important relationship in tropical marine environments as it forms the basis of tropical coral reef ecosystems, and is one of the best-known and most widely distributed photosynthetic symbiosis in the oceans (Rowan 1998, Coffroth & Santos 2005, Weis et al. 2008). Interactions between cnidarian and *Symbiodinium* species array along a mutualism-parasitism continuum that rely on the specificity and compatibility of each partner, complexity of community-level interactions and environmental drivers (Lesser et al. 2013, Thornhill et al. 2013). Also important is the disruption of this symbiotic association, a process popularly known as bleaching. This process involves the dissociation of the cnidarian host and its symbionts and is a stress response commonly triggered by thermal and/or light stress, as well as diseases (Brown 1997). Bleaching has dramatic consequences for the host, such as a reduction in growth, tissue biomass, fecundity and nutrition.

1.1.1 Nutrition of zooxanthellate cnidarians

In coral biology and marine tropical ecology it has long been accepted that the success of zooxanthellate cnidarians in oligotrophic environments originates from its association with *Symbiodinium* (Dubinsky & Jokiel 1994). The cnidarian-dinoflagellate symbiosis is especially important as the symbiont provides the host with alternative metabolic pathways (Fig. 1.1) that contribute to overcome environmental food limitation (Muscatine & Porter 1977). Endosymbionts use light energy to fix inorganic carbon in form of bicarbonate (HCO_3^-) as organic compounds, such as glycerol, glucose and amino acids. A notable fraction of these photosynthetic products, which may account for more than 90% of the carbon fixed by zooxanthellae, is transferred to the cnidarian host and used to fuel its metabolism (Muscatine & Porter 1977, Muscatine 1980, Tremblay et al. 2014). Translocated photosynthates, i.e. autotrophic acquired carbon, have been considered “junk food” to the cnidarian host, as they are mostly respired or released to the surrounding environment rather than stored as energy reserves or to increase the tissue biomass of the cnidarian (Falkowski

et al. 1984). However, others have noted the relevant contribution of photosynthates to lipid reserves of the cnidarian host (Rodrigues & Grottoli 2006).

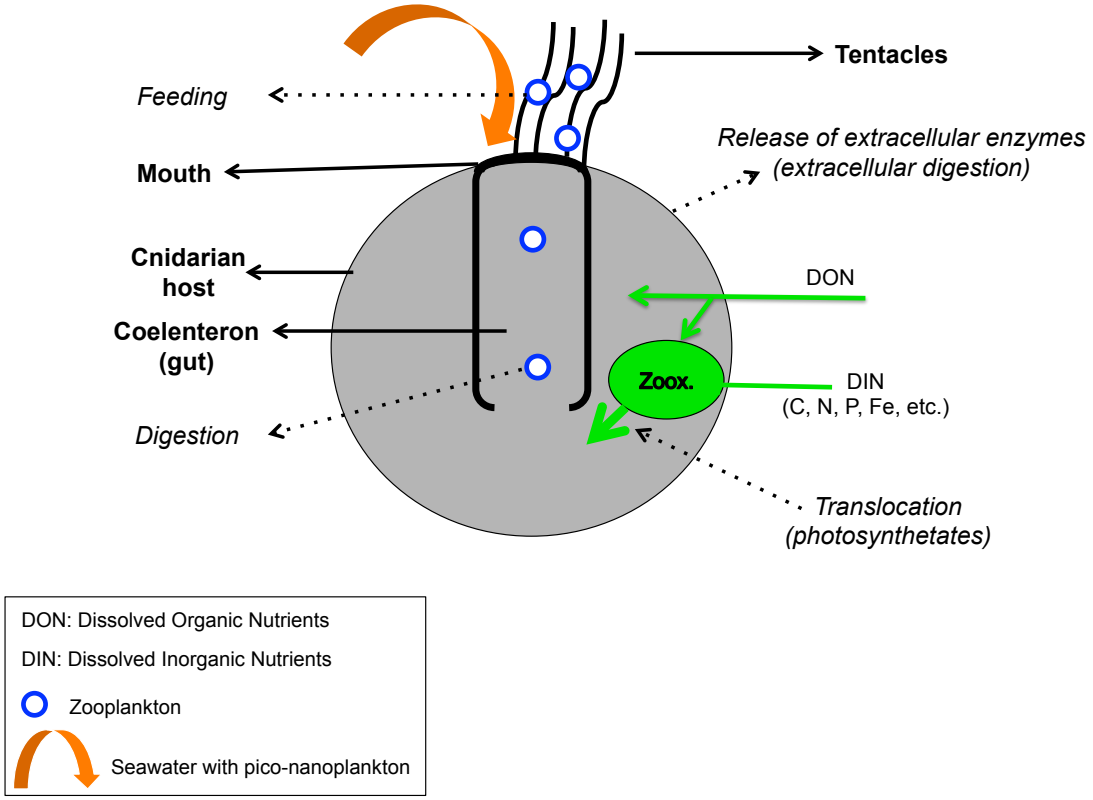

Fig. 1.1 Most important nutritional sources potentially used by zooxanthellate cnidarians. Straight lines denote different components of the coral. Dashed lines indicate processes of nutrient acquisition, either through the zooxanthellae (Zoox.) or the coral tissue (inside or outside the coelenteron).

Carbon fixation by photosynthetic symbionts is only one of several possible sources of carbon for the cnidarian host (Fig. 1.1). Other mechanisms available include feeding on planktonic organisms (ranging in size from pico- and nanoplankton to zooplankton), uptake of particulate and dissolved organic matter available in the sediment and water column, mucus feeding, and feeding on microorganisms associated with detritus and mucus (reviewed by Houlbrèque & Ferrier-Pagès 2009). These mechanisms are usually considered heterotrophic food sources. Together with autotrophy (Godinot et al. 2011), heterotrophy is currently accepted as a significant source of nitrogen, phosphorus and other nutrients that cannot be supplied by autotrophy (Porter 1976, Muscatine & Porter 1977, Davies 1991). This nutritional plasticity between auto- and heterotrophy, i.e. mixotrophy, is critical for the functioning, health, fitness, resilience and stress recovery of the cnidarian-dinoflagellate symbiosis (Grottoli et al. 2006, Hughes & Grottoli 2013, Tremblay et al. 2014).

1.1.2 Factors affecting trophic plasticity

Several factors may affect the contribution of auto- and heterotrophy to the cnidarian-dinoflagellate symbiosis. Because autotrophy is associated with the translocation of photosynthetic products, light plays a key role in the bioenergetics of zooxanthellate cnidarians and is a major factor limiting their distribution to the photic zone of subtropical and tropical marine environments (Kaiser et al. 2011). Variations in light availability affect the amount and fate of translocated products, either through

symbiont concentration within the host tissue or photosynthetic and translocation capacity of individual symbiont cells (Tremblay et al. 2012a, Tremblay et al. 2012b, Tremblay et al. 2014). As different *Symbiodinium* species may associate with cnidarians and each species may have different photophysiological capacities, symbiont diversity also affects the trophic plasticity of the association (Loram et al. 2007, Starzak et al. 2014).

Any factor that induces stress to the cnidarian-dinoflagellate symbiosis and causes bleaching will also affect the trophic plasticity of the association (Grottoli et al. 2006). However, not all corals display the same nutritional strategy to cope with bleaching. Some corals, such as *Porites compressa*, maintain their heterotrophic efforts when bleached but rely on the consumption of stored energy reserves to maintain its calcification rates and fuel zooxanthellae recovery (Grottoli et al. 2006, Rodrigues & Grottoli 2006, Hughes et al. 2010). Other corals, such as *Montipora captitata*, increase their heterotrophic carbon acquisition when bleached and use this to maintain their energy reserves, and to sustain its host tissue and zooxanthellae population (Rodrigues & Grottoli 2007, Palardy et al. 2008).

Besides bleaching status and diversity of endosymbiotic community, heterotrophy is also affected by water flow rate (Sebens et al. 1997, Wijgerde et al. 2012), coral shape (Sebens et al. 1997, Todd 2008), prey density (reviewed by Osinga et al. 2011), prey type (Piniak 2002, Houlbrèque et al. 2004), and other factors (see review by Houlbrèque & Ferrier-Pagès 2009). All these factors may affect feeding rates, and therefore the role of heterotrophy in the nutrient budget of zooxanthellate cnidarians (Tremblay et al. 2014). Although the study of auto- and heterotrophy in the cnidarian-dinoflagellate symbiosis has been investigated over the past decades, methodological issues are still limiting our in depth knowledge on trophic plasticity of this association.

1.1.3 Methodological constraints

Most studies addressing the simultaneous contribution of auto- and heterotrophy to the cnidarian-dinoflagellate symbiosis have used radiolabeling methods (e.g. Bachar et al. 2007, Hughes et al. 2010), stable isotope analysis (e.g. Muscatine et al. 1989, Ferrier-Pagès et al. 2011), or estimation of auto- and heterotrophic carbon contribution to daily animal respiration (CZAR and CHAR, respectively) through photosynthetically fixed carbon, prey capture and respiration rates (e.g. Grottoli et al. 2006, Starzak et al. 2014). The use of radiolabels has limitations, especially because translocated products might be rapidly metabolized, thus releasing radiolabel from the system and leading to an underestimation of the translocation of metabolites (Davy et al. 2012). In addition, metabolized products may be refixed by photosynthesis, thus biasing translocation measurements. Nevertheless, radiolabelling techniques are used to assess the autotrophic contribution to the nutrition of the cnidarian host (Tremblay et al. 2012c). Stable carbon and nitrogen isotope ratios ($\delta^{13}C$ and $\delta^{15}N$) have been used to assess the relative importance of auto- and heterotrophy in coral nutrition (e.g. Muscatine et al. 1989, Alamaru et al. 2009, Ferrier-Pagès et al. 2011). While isotopes provide information on the trophic level and potential nutritional sources of the coral host, this method does not provide quantitative estimates of auto- and heterotrophy. Furthermore, although it is possible to assess the theoretical heterotrophic food sources of the coral, this information is not accurate at a low taxonomic level (e.g. Ferrier-Pagès et al. 2011). However, stable isotope analyses provide a time-integrated signal of the food sources, which is important in field studies.

Estimations of CZAR and CHAR have been used to assess energy budgets in the cnidarian-algal symbiosis (Muscatine et al. 1981, Falkowski et al. 1984, Grottoli et al. 2006). The formulas to calculate both contributions assume that respiration rates are proportional to animal and algal biomass. However, heterotrophic feeding and prey digestion have metabolic costs to the cnidarian

host that affect respiration rates (Sebens 2002) and, ultimately, CZAR and CHAR estimates. CZAR estimates may decrease with increasing animal respiration associated with heterotrophic processes (Muscatine et al. 1981). Moreover, CHAR estimates assume a constant feeding over 8 h (Grottoli et al. 2006), which may be an unrealistic premise (Wijgerde et al. 2011).
The investigation of coral feeding on planktonic organisms has been mostly performed using a couple of methodologies, such as clearance rate and polyp dissection, which are known to have important limitations (e.g. Sebens et al. 1997, Houlbrèque et al. 2004, Palardy et al. 2008). Clearance rate is an indirect estimate of maximal prey ingestion as it builds on the assumption that all prey that disappears during incubation has been ingested. However, prey may also be lost from the suspension due to other mechanisms or artefacts such as adhering to other parts of the body, experimental walls or aggregate formation outside the organisms' gut. Prey clearance further fails to reveal the dynamics of prey capture, digestion and release, possibly obscuring realistic estimates of nutrient input from zooplankton. Another approach that has been used is identification of visual prey content in organisms. Microscopic analysis of gut contents is uncertain because of its reliance on the recognition of small and highly amorphous partially digested prey, as has been concluded for a wide range of organisms (see Nejstgaard et al. 2008 for a general discussion).
Most studies on coral heterotrophy have not quantified the fraction of organic matter utilised by corals after prey capture, but rather assumed various quantities of carbon assimilation from prey items (Fabricius et al. 1995a, Grottoli et al. 2006, Starzak et al. 2014). Such assumptions prevent realistic estimates of nutrient input through heterotrophy. This constraint is mostly due to our lack of knowledge on the ability that corals have to digest prey after they are captured, in part due to current limitations of the methods available to assess heterotrophic feeding. Prey digestion has been estimated by visual observations with reported digestion times of less than a day (Fabricius et al. 1995b, Sebens et al. 1996) but it has several limitations associated with soft and small prey items. Nonetheless, to accurately assess the role of heterotrophy in the cnidarian-dinoflagellate symbiosis, prey capture, ingestion and digestion must be reliably quantified.

1.1.4 General aim and research questions

Based on the important gaps of knowledge outlined above, the aim of this thesis was to increase the understanding on the role of autotrophy and heterotrophy in the ecophysiology of cnidarians associated with *Symbiodinium*, and the ecological implications of this trophic plasticity.
The research questions for this thesis were:

1. How can we non-invasively assess the photophysiological spatial heterogeneity within the cnidarian-dinoflagellate symbiosis? (**Chapter 2**)
2. How can we maximize biomass production of the model organism *Aiptasia pallida* to use in the study of the cnidarian-dinoflagellate symbiosis, and what are the biochemical implications of culturing these organisms in laboratory? (**Chapter 3 and 4**)
3. Can we use molecular methods to improve the study of heterotrophy in zooxanthellate cnidarians, and what ecological insights can these methods provide? (**Chapter 5**)
4. Are symbiotic corals able to feed on phytoplankton under laboratory and field conditions? (**Chapter 6 and 7**)
5. How does *Symbiodinium* diversity affect trophic plasticity of the cnidarian-dinoflagellate symbiosis? (**Chapter 8**)

1.1.5 Thesis outline

This thesis is composed of a general introduction (**Chapter 1**), seven research chapters (**Chapter 2-8**) and a general discussion with final considerations (**Chapter 9**). **Chapter 2** illustrates a novel

methodological approach to study the spatial heterogeneity of the photophysiology of zooxanthellate cnidarians. Particularly, this study investigates the association between different key-parameters that are often measured in photobiological studies of the cnidarian-zooxanthellate symbiosis, namely photochemical efficiency, chlorophyll *a* content and GFPs. In order to produce large numbers of individuals to use in laboratory experiments, **Chapter 3** describes a factorial experiment to assess the effect of light, feeding and temperature on the production of *Aiptasia pallida*. This sea anemone, which is a model organism to study the cnidarian-dinoflagellate symbiosis (Weis et al. 2008), was further used in **Chapter 4**. As light, feeding and temperature have been identified as key factors affecting the production of *A. pallida*, **Chapter 4** reports a factorial experiment where the fatty acid profile of *A. pallida* reared under different conditions was analysed. Both *A. pallida* and the facultative symbiotic coral *Oculina arbuscula* are used in **Chapter 5** to show the use of molecular trophic markers to study heterotrophy in zooxanthellate cnidarians, and assess the effect of predator and prey species, along with heterotrophic starvation, in feeding and digestion processes. These molecular methods were used in **Chapter 6** to investigate whether symbiotic corals feed on microalgae under laboratory conditions, a prey item that has been overlooked by coral ecologists. **Chapter 7** shows the assessment of coral herbivory *in situ* for the facultative symbiotic coral *O. arbuscula* through the analysis of the stable isotopic signature of different coral fractions (coral host and symbionts) and the potential food sources (sediment organic matter and different-sized fractions of particulate organic matter). Lastly, the effect of *Symbiodinium* diversity on the trophic plasticity of the cnidarian-dinoflagellate symbiosis is investigated using the model *A. pallida* in **Chapter 8**. This chapter combines measurements of carbon fixation and translocation from the symbionts to the host with molecular methods to assess prey ingestion and digestion. Finally, the conclusions of **Chapters 2-8** are discussed and integrated in **Chapter 9** to note ecological implications of these findings and provide recommendations for future research.

1.1.6 References

Alamaru A, Yam R, Shemesh A, Loya Y (2009) Trophic biology of *Stylophora pistillata* larvae: evidence from stable isotope analysis. Mar Ecol Prog Ser 383:85-94

Bachar A, Achituv Y, Pasternak Z, Dubinsky Z (2007) Autotrophy versus heterotrophy: The origin of carbon determines its fate in a symbiotic sea anemone. J Exp Mar Biol Ecol 349:295-298

Brown BE (1997) Coral bleaching: causes and consequences. Coral Reefs 16:S129-S138

Buddemeier RW, Smith SV (1999) Coral adaptation and acclimatization: a most ingenious paradox. Am Zool 39:1-9

Coffroth MA, Santos SR (2005) Genetic diversity of symbiotic dinoflagellates in the genus *Symbiodinium*. Protist 156:19-34

Davies P (1991) Effect of daylight variations on the energy budgets of shallow-water corals. Mar Biol 108:137-144

Davy SK, Allemand D, Weis VM (2012) Cell biology of cnidarian-dinoflagellate symbiosis. Microbiol Mol Biol Rev 76:229-261

De'ath G, Fabricius KE, Sweatman H, Puotinen M (2012) The 27-year decline of coral cover on the Great Barrier Reef and its causes. Proc Natl Acad Sci USA 109:17995-17999

Dubinsky Z, Jokiel PL (1994) Ratio of energy and nutrient fluxes regulates symbiosis between zooxanthellae and corals. Pac Sci 48:313-324

Fabricius KE, Benayahu Y, Genin A (1995a) Herbivory in asymbiotic soft corals. Science 268:90-92

Fabricius KE, Genin A, Benayahu Y (1995b) Flow-dependent herbivory and growth in zooxanthellae-free soft corals. Limnol Oceanogr 40:1290-1301

Falkowski P, Dubinsky Z, Muscatine L, Porter J (1984) Light and the bioenergetics of a symbiotic coral. BioScience 34:705-709

Ferrier-Pagès C, Peirano A, Abbate M, Cocito S, Negri A, Rottier C, Riera P, Rodolfo-Metalpa R, Reynaud S (2011) Summer autotrophy and winter heterotrophy in the temperate symbiotic coral *Cladocora caespitosa*. Limnol Oceanogr 56:1429-1438

Furla P, Allemand D, Shick JM, Ferrier-Pagès C, Richier S, Plantivaux A, Merle P-F, Tambutté S (2005) The symbiotic anthozoan: a physiological chimera between alga and animal. Integr Comp Biol 45:595-604

Grottoli AG, Rodrigues LJ, Palardy JE (2006) Heterotrophic plasticity and resilience in bleached corals. Nature 440:1186-1189

Hoegh-Guldberg O (1999) Climate change, coral bleaching and the future of the world's coral reefs. Mar Freshwat Res 50:839-866

Hoegh-Guldberg O, Mumby PJ, Hooten AJ, Steneck RS, Greenfield P, Gomez E, Harvell CD, Sale PF, Edwards AJ, Caldeira K, Knowlton N, Eakin CM, Iglesias-Prieto R, Muthiga N, Bradbury RH, Dubi A, Hatziolos ME (2007) Coral Reefs Under Rapid Climate Change and Ocean Acidification. Science 318:1737-1742

Houlbrèque F, Tambutte E, Richard C, Ferrier-Pages C (2004) Importance of a micro-diet for scleractinian corals. Mar Ecol Prog Ser 282:151-160

Houlbrèque F, Ferrier-Pagès C (2009) Heterotrophy in tropical scleractinian coral. Biol Rev 84:1-17

Hughes AD, Grottoli AG, Pease TK, Matsui Y (2010) Acquisition and assimilation of carbon in non-bleached and bleached corals. Mar Ecol Prog Ser 420:91-101

Hughes AD, Grottoli AG (2013) Heterotrophic compensation: a possible mechanism for resilience of coral reefs to global warming or a sign of prolonged stress? PLoS One 8:e81172

Kaiser MJ, Attrill MJ, Jennings S, Thomas DN, Barnes DKA, Brierley AS, Hiddink JG, Kaartokallio H, Polunin NVC, Raffaelli DG (2011) Marine Ecology: Processes, Systems, and Impacts. Oxford University Press, Oxford, 528 p.

Lesser MP, Stat M, Gates RD (2013) The endosymbiotic dinoflagellates (*Symbiodinium* sp.) of corals are parasites and mutualists. Coral Reefs 32:603-611

Loram JE, Trapido-Rosenthal HG, Douglas AE (2007) Functional significance of genetically different symbiotic algae *Symbiodinium* in a coral reef symbiosis. Mol Ecol 16:4849-4857

Muscatine L, Porter J (1977) Reef corals - Mutualistic symbioses adapted to nutrient-poor environments. BioScience 27:454-460

Muscatine L (1980) Productivity of zooxanthellae. In: Falkowski PG (ed) Primary production in the sea. Plenum, New York, pp. 649-658

Muscatine L, McCloskey L, Marian R (1981) Estimating the daily contribution of carbon from zooxanthellae to coral animal respiration. Limnol Oceanogr 26:601-611

Muscatine L, Porter JW, Kaplan IR (1989) Resource partitioning by reef corals as determined from stable isotope composition. I. δ13C of zooxanthellae and animal tissue vs depth. Mar Biol 100:185-193

Nejstgaard JC, Frischer ME, Simonelli P, Troedsson C, Brakel M, Adiyaman F, Sazhin AF, Artigas LF (2008) Quantitative PCR to estimate copepod feeding. Mar Biol 153:565-577

Osinga R, Delft S, Lewaru M, Janse M, Verreth J (2011) Determination of prey capture rates in the stony coral *Galaxea fascicularis*: a critical reconsideration of the clearance rate concept. J Mar Biol Assoc UK:1-7

Palardy JE, Rodrigues LJ, Grottoli AG (2008) The importance of zooplankton to the daily metabolic carbon requirements of healthy and bleached corals at two depths. J Exp Mar Biol Ecol 367:180-188

Pandolfi J, Jackson J, Baron N, Bradbury R, Guzman H, Hughes T, Kappel C, Micheli F, Ogden J, Possingham H, Sala E (2005) Are US coral reefs on the slippery slope to slime? Science 307:1725-1731

Pandolfi JM, Connolly SR, Marshall DJ, Cohen AL (2011) Protecting coral reef futures under global warming and ocean acidification. Science 333:418-422

Piniak G (2002) Effects of symbiotic status, flow speed, and prey type on prey capture by the facultatively symbiotic temperate coral *Oculina arbuscula*. Mar Biol 141:449-455

Porter JW (1976) Autotrophy, heterotrophy, and resource partitioning in Caribbean reef-building corals. Am Nat 110:731-742

Richmond RH (1993) Coral Reefs: Present problems and future concerns resulting from anthropogenic disturbances. Am Zool 33:524-536

Rodrigues L, Grottoli A (2006) Calcification rate and the stable carbon, oxygen, and nitrogen isotopes in the skeleton, host tissue, and zooxanthellae of bleached and recovering Hawaiian corals. Geochim Cosmochim Ac 70:2781-2789

Rodrigues L, Grottoli A (2007) Energy reserves and metabolism as indicators of coral recovery from bleaching. Limnol Oceanogr 52:1874-1882

Rowan R (1998) Diversity and Ecology of Zooxanthellae on Coral Reefs. J Phycol 34:407-417

Sebens KP, Vandersall KS, Savina LA, Graham KR (1996) Zooplankton capture by two scleractinian corals, *Madracis mirabilis* and *Montastrea cavernosa*, in a field enclosure. Mar Biol 127:303-317

Sebens KP, Witting J, Helmuth B (1997) Effects of water flow and branch spacing on particule capture by the reed coral *Madracis mirabilis* (Duchassaing and Michelotti). J Exp Mar Biol Ecol 211:1-28

Sebens KP (2002) Energetic contraints, size gradients, and size limits in benthic marine invertebrates. Integr Comp Biol 42:853-861

Starzak DE, Quinnell RG, Nitschke MR, Davy SK (2014) The influence of symbiont type on photosynthetic carbon flux in a model cnidarian-dinoflagellate symbiosis. Mar Biol 161:711-724

Thornhill DJ, Xiang Y, Pettay DT, Zhong M, Santos SR (2013) Population genetic data of a model symbiotic cnidarian system reveal remarkable symbiotic specificity and vectored introductions across ocean basins. Mol Ecol 22:4499-4515

Todd PA (2008) Morphological plasticity in scleractinian corals. Biol Rev 83:315-337

Tremblay P, Ferrier-Pagès C, Maguer JF, Rotier C, Legendre L, Grover R (2012a) Controlling effects of irradiance and heterotrophy on carbon translocation in the temperate coral *Cladocora caespitosa*. PLoS One 7:e44672

Tremblay P, Naumann MS, Sikorski S, Grover R, Ferrier-Pagès C (2012b) Experimental assessment of organic carbon fluxes in the scleractinian coral *Stylophora pistillata* during a thermal and photo stress event. Mar Ecol Prog Ser 453:63-77

Tremblay P, Grover R, Maguer JF, Legendre L, Ferrier-Pages C (2012c) Autotrophic carbon budget in coral tissue: a new 13C-based model of photosynthate translocation. The Journal of Experimental Biology 215:1384-1393

Tremblay P, Grover R, Maguer JF, Hoogenboom M, Ferrier-Pagès C (2014) Carbon translocation from symbiont to host depends on irradiance and food availability in the tropical coral *Stylophora pistillata*. Coral Reefs 33:1-13

Trench RK (1993) Microalgal-invertebrate symbioses - a review. Endocyt Cell Res 9:135-175

Veron JEN (2000) Corals of the World. Australian Institute of Marine Science, Townsville, Qld, Australia. 1382 p.

Weis V, Davy S, Hoegh-Guldberg O, Rodriguez-Lanetty M, Pringle J (2008) Cell biology in model systems as the key to understanding corals. Trends Ecol Evol 23:369-376

Wijgerde T, Diantari R, Lewaru MW, Verreth JAJ, Osinga R (2011) Extracoelenteric zooplankton feeding is a key mechanism of nutrient acquisition for the scleractinian coral *Galaxea fascicularis*. J Exp Biol 214:3351-3357

Wijgerde T, Spijkers P, Karruppannan E, Verreth JAJ, Osinga R (2012) Water flow affects zooplankton feeding by the scelractinian coral *Galaxea fascicularis* on a polyp and colony level. J Mar Biol 2012:1-7

Chapter 2 Concurrent imaging of chlorophyll fluorescence, chlorophyll *a* content and GFP-like proteins of symbiotic cnidarians

Abstract

Research on photosynthetic cnidarians has been mainly focused on the symbiosis established between the cnidarian host and its dinoflagellates endosymbionts from genus *Symbiodinium*. Despite the potential of imaging techniques for assessing the spatial distribution of key parameters of cnidarian photobiology, such as photochemical activity, chlorophyll *a* content or green fluorescent proteins-like proteins (GFPs), to our best knowledge, no study has ever attempted to simultaneous map these three features. In this study, we developed a modified imaging pulse amplitude fluorometer by applying excitation light of different wavelengths and selectively detecting short spectral bands through bandpass filters. The imaging system was used to sequentially excite and quantify chlorophyll variable fluorescence (maximum quantum yield of photosystem II, F_v/F_m), chlorophyll *a* content (Normalized Difference Vegetation Index) and relative content of GFPs. The spatial distribution of these photophysiological parameters was mapped both horizontally, across the surface of the soft corals *Sarcophyton* cf. *glaucum* and *Sinularia flexibilis* and the zoanthid *Protopalythoa* sp., and vertically, throughout a vertical section of *S*. cf. *glaucum*. Results showed bleached areas within each individual coral colony and registered photophysiological changes with *S*. cf. *glaucum* tissue depth. Analysis of *Protopalythoa* sp. polyps' expansion revealed differential surface patterns of NDVI and GFPs concentration, and a negative relation between these latter parameters within each polyp. This novel non-invasive approach allowed a high-resolution characterization of the spatial relationship between these key parameters through the analysis of image information on a pixel-by-pixel basis, which has great potential for investigating the physiological state of symbiotic associations.

Keywords

Symbiosis; Imaging-PAM; Fluorescence; Chlorophyll *a*; *Symbiodinium*.

In publication: Leal MC, Jesus B, Ezequiel J, Calado R, Rocha RJM, Cartaxana P, Serôdio J (in press) Concurrent imaging of chlorophyll fluorescence, Chlorophyll *a* content and green fluorescent proteins-like proteins of symbiotic cnidarians. Marine Ecology (doi: 10.111/maec.12164)

2.1 Introduction

The symbiotic relationship between corals and photosynthetic dinoflagellates within genus *Symbiodinium* is of paramount importance for both the structure and function of coral reefs (Hoegh-Guldberg 1999). The algal endosymbionts contribute to the nutrition of the cnidarian host by providing photosynthetically fixed carbon, and the coral host provides a sheltered and light rich environment, in addition to a pool of inorganic nutrients (Muscatine & Porter 1977, Muscatine et al. 1989).

Corals often show a heterogeneous distribution of photochemical activity that varies across scales from a few millimetres up to the whole colony (Kühl et al. 1995, Helmuth et al. 1997, Ralph et al. 2002, Hill et al. 2004, Roff et al. 2008). Ultimately, changes in symbiont photobiology affect the coral host physiology and its response to biotic and abiotic factors (Venn et al. 2008). Although several studies have already employed imaging tools to study cnidarian photophysiology, most efforts have investigated microscopic and environmental scales through the use of microscopy (e.g. Salih et al. 1995, Hanley et al. 2006) and satellite imaging (e.g. Kutser et al. 2006, Ziskin et al. 2011), respectively. Some studies have also developed techniques to assess surface heterogeneity of photosynthetic activity, particularly photosynthesis rates and effective quantum yield of photosystem II (PSII) (Hill et al. 2004, Ralph et al. 2005). Other studies have used imaging tools to study oxygen dynamics in coral tissues (Kühl et al. 2008, Fabricius-Dyg et al. 2012). Curiously, imaging techniques have not been used to monitor chlorophyll (Chl) *a* content and green fluorescent proteins-like proteins (GFPs) at the colony scale. Furthermore, to our best knowledge, no study has ever attempted to simultaneously take these measurements together with other photobiological parameters in living coral tissues.

The possibility to study *in vivo* and in detail the relationship between photochemical activity through Chl *a* fluorescence, Chl *a* content and GFPs, as well as their spatial distribution in anthozoan tissues, may provide a solid approach to address physiological and photobiological processes. Moreover, as the role of GFPs is still largely debated (Matz et al. 2006, Alieva et al. 2008, Kenkel et al. 2011), its spatial distribution in the coral and association with other photobiological parameters may provide new insights on the physiological and ecological role of GFPs.

The present study describes a method that enables the simultaneous *in vivo* quantification of the distribution of photochemical activity, Chl *a* content and GFPs, using a modified imaging Pulse Amplitude Modulated fluorometer. The potential applications of this method are shown through mapping these photophysiological parameters both horizontally, across the surface of corals, as well as vertically, throughout a longitudinal section of coral tissue. The application of this imaging method is illustrated using the symbiotic soft corals *Sarcophyton* cf. *glacum* and *Sinluaria flexibilis*, and the symbiotic zoanthid *Protopalythoa* sp. to investigate the following questions: what is the spatial heterogeneity of photochemical activity, Chl *a* content and GFPs of the symbiotic cnidarians? How do these physiological parameters change during polyp expansion? Are these parameters homogenous throughout a polyp cross-section?

2.2 Materials and Methods

2.2.1 Cnidarian species

Colonies of *Sarcophyton* cf. *glaucum* (subclass Octocorallia, order Alcyonacea), *Sinularia flexibilis* (subclass Octocorallia, order Alcyonacea) and *Protopalythoa* sp. (subclass Hexacorallia, order Zoanthidea) were stocked in a recirculating aquarium system using synthetic saltwater (prepared

by mixing Tropic Marin Pro Reef salt (Tropic Marine, Germany) with freshwater purified by a reverse osmosis unit). The system was composed of a 200 L glass tank holding the coral colonies connected to a 100 L filter tank equipped with a protein skimmer (APF-600 Deltec, Delmenhorst, Germany) and a biological filter (composed by approximately 20 kg of live rock). Salinity in the aquarium system was maintained at 35 through automatic compensation of evaporated water with freshwater purified by a reverse osmosis unit, using an osmoregulator (Deltec Aquastat 1000, Delmenhorst, Germany). Temperature was maintained at 26 ± 0.5 ºC using a submersible heater (Eheim Jäger 300 W, Germany). Partial water changes (10% of total system volume) were performed once a week.
The tank holding the cnidarians was illuminated from above with a 250 W (10000 K) Hydrargyrum Quartz Iodide (HQI) lamp (BLV, Germany) under a 12h light: 12h dark photoperiod. The Photosynthetic Active Radiation (PAR) at the surface of the colonies was 50 µmol quanta m^{-2} s^{-1}. Four months before performing the measurements using the imaging system, one colony of each species was moved to a different area of the tank with a PAR level of 250 µmol quanta m^{-2} s^{-1} in order to show the applicability of this imaging system to explore the effects of coral photoacclimation. PAR values were measured at the level of the colonies using a Quantum Flux meter with a submergible sensor (Apogee MQ-200, Logan, UT, USA).

2.2.2 Imaging system

Images were acquired using a FluorCAM 800MF, open version (PSI, Brno, Czech Republic), with a computer-operated control unit (SN-FC800-082, PSI) and a CCD camera (CCD381, PSI) with an F1.2 (2.8-6 mm) objective (Eneo, Japan) (Fig. 2.1). The camera had a 2/3" CCD with a wavelength range between 400-1000 nm and generated 12 bit images with 512 x 512 pixels dimension at a maximum frequency of 50 images per second. A filter wheel, with capacity for eight filters, was located between the camera lenses and the CCD. Different filters and light sources were used for the different measurements performed (details in the following sections). All images were captured using the Fluorcam 7 software (PSI, Brno, Czech Republic). The software allowed user-defined measuring sequences (protocols) of fluorescence and reflectance images with the ability to define shutter speed of the camera and sensitivity (Nebdal et al. 2000). The images were taken with the colonies out of seawater because they were relatively small and their structure was stable during measurements. The only exception was *Protopalythoa* sp. that was analysed in seawater (10 mm of water above the zoanthid surface) to allow polyp expansion (see Image analysis section). Preliminary trials showed a minor effect of the presence of this thin water layer between the zoanthid surface and the excitation light sources and detection devices in the measurements taken using these particular excitation wavelengths (see sections below). The effect of water was unimportant as the same specimen was analysed throughout polyp expansion with the same layer of water above the zoanthid surface.

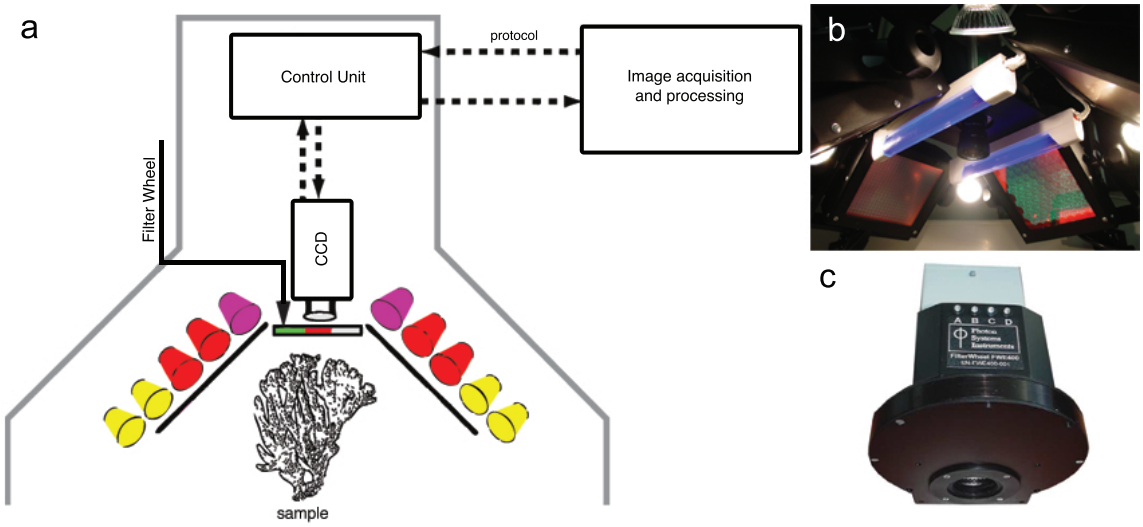

Fig. 2.1 FluorCAM 800MF with the modifications used in the present study (a). Four LED panels (red) provide measuring, actinic and saturating lights for photophysiology measurements. Four halogen lamps (yellow) and two UVa lamps (purple) were added to generate light for the NDVI and GFP measurements, respectively. Photograph of the equipment (b) and filter wheel (c; located between the CCD camera and the lenses, allowed the acquisition of the desired wavelengths).

2.2.3 Chlorophyll *a* fluorescence and PSII maximum quantum yield

Chl *a* fluorescence images were taken using the standard imaging PAM fluorometry (Schreiber et al. 1986) functions of the FluorCAM provided by the manufacturer without any customized modifications. The FluorCAM Chl *a* fluorescence filter system comprised a high (695 nm) and low pass filter (780 nm). Two red LED panels (MLS13x13, PSI) provided the measuring non-actinic light (0.1 µmol m^{-2} s^{-1}) and two other red LED panels provided the saturating pulse (7500 µmol m^{-2} $s^{-1;}$ SL3500, PSI). All red panels had an emission peak at 621 nm and a 40 nm bandwidth.
Maximum PSII quantum yield (F_v/F_m) is one of the best known and most used photophysiology parameters to estimate photochemical efficiency (Maxwell & Johnson 2000, Baker & Rosenquist 2004). A user-defined protocol, with a total duration of 2 s, was employed to measure the minimum fluorescence yields (F_o) in the first 1.4 s and the maximum fluorescence values (F_m) after a saturating pulse of 0.6 s. F_v/F_m was calculated as $(F_m-F_o)/F_m$ (Kitajima & Butler 1975). Measurements were performed 1 h before tank lights were switched on in order to assure that corals were properly dark-adapted.

2.2.4 Chlorophyll *a* content

Chl *a* content in the coral tissue was estimated using the Normalized Difference Vegetation Index (NDVI; Rouse et al. 1973). NDVI is based on the difference between the red and infrared (IR) reflectance caused by Chl *a* presence. NDVI was established in the 1970s and has been one of the most widely used indices for estimating Chl *a* content in different organisms and different ecosystems. Besides its use in terrestrial plants, it has been successfully used in a range of aquatic organisms including microalgae-dominated biofilms (Serôdio et al. 2009, Perkins et al. 2010), photosymbiotic sea slugs (Serôdio et al. 2010, Costa et al. 2012), and macroalgae and seagrasses (Peñuelas et al. 1993). Similarly to NDVI, Ralph et al. (2005) have used the same principle to measure absorptivity of corals, also using red and IR light, but using a slightly different formula:

Absorptivity = 1 – (red /IR).

As the application of NDVI to corals has been limited to airborne and spatial remote sensing studies (Yamaguchi et al. 2008, Collin et al. 2012, Hamilton 2012, Phinn et al. 2012) and laboratory-based experiments (Rocha et al. 2013a, 2013b), we performed preliminary investigations to validate the use of NDVI as a proxy of Chl *a* content. Fifteen coral nubbins (approximately 4 cm) of *S.* cf *glaucum* were prepared as described in Rocha et al. (2013c) and acclimated to different light levels (120, 85 and 55 µmol quanta m^{-2} s^{-1}) in separate tanks to induce a large range of Chl *a* content. After 60 days, the diffusion reflectance spectra were measured over a 330-1000 nm bandwidth, with a spectral resolution of 0.33 nm, using a USB2000 spectrometer (USB2000-VIS-NIR, grating #3, Ocean Optics, Dunedin, FL, USA) connected to 400 µm diameter fiberoptic (QP400-2-VIS/NIR-BX, Ocean Optics, Dunedin, FL, USA) following the methods described in Rocha et al. (2013b). In summary, the measurements were taken under a constant irradiance of 200 µmol m^{-2} s^{-1}, provided by a halogen lamp (Volpi Intraluz 5000-1; Volpi International, Schlieren, Switzerland). The light spectrum reflected from each coral was normalized to the spectrum reflected from a reference white panel (WS-1-SL Spectralon Reference Standard, Ocean Optics). The reflectance spectrum measured in the dark was subtracted to both spectra to account for the dark current noise of the spectrometer. The NDVI was calculated as follows:

$$NDVI = (R_{750} - R_{675})/(R_{750} + R_{675})$$

where R_{675} and R_{750} represent the average diffusive reflectance in the intervals of the red and IR bandpass filters used in the FluorCAM (R_{675}: 676 ± 29; R_{750}: 747 ± 33; see below). The filters' bandwidths were chosen as a compromise between wavelength selectivity and signal detection by the camera. In other words, the bandwidth should be narrow to select the targeted wavelengths, but large enough to maximize the signal reaching the sensor.

After performing the reflectance measurements, coral nubbins were frozen in liquid nitrogen and freeze-dried for pigment analysis using High Performance Liquid Chromatography (HPLC). Samples were extracted with 3-5 mL of 95% cold buffered methanol (2% ammonium acetate) for 30 min at –20 °C in the dark. Samples were sonicated (Bransonic, model 1210) for 30 s at the beginning of the extraction period. Extracts were filtered (Fluoropore PTFE filter membranes, 0.2 µm pore size) and injected in a Shimadzu HPLC system with photodiode array (SPD-M10AVP) detector. Chromatographic separation was carried out using a C18 column for reverse phase HPLC chromatography (Supelcosil; 25 cm length; 4.6 mm in diameter; 5 µm particles) and 35 min elution programme. The solvent gradient followed Kraay et al. (1992) with a flow rate of 0.6 mL min^{-1} and an injection volume of 100 µL. Chl *a* was identified from absorbance spectrum and retention time and concentrations calculated from signals in the photodiode array detector. Calibration of Chl *a* was performed using a commercial standard from DHI (Institute for Water and Environment, Hørsholm, Denmark). Concentrations of Chl *a* were expressed per gram of dry weight.

In order to map the NDVI using the FluorCAM, the coral colonies were illuminated with four halogen lamps (50 W, Auchan JD 230V/GU 10; Fig. 2.1), which provided a light spectrum with a strong emission in the red and IR regions. Two bandpass filters were installed in the filter wheel of the imaging system: a red filter (FF01-676/29-25, Semrock, Rochester, NY, USA) with a transmission peak at 676 nm and a 29 nm bandwidth, and a IR filter (FF01-747/33-25, Semrock, Rochester, NY, USA) with a transmission peak at 747 nm and a 33 nm bandwidth. A user-defined protocol was run during sample illumination to allow the acquisition of one red and one IR image during one second of exposure time, each. Images were captured using the Fluorcam 7 software (PSI, Brno, Czech Republic) and NDVI images were calculated (Image analysis section).

2.2.5 GFP-like proteins

GFPs fluorescence images were acquired by exposing the samples to UV light, provided by two UV lamps (Blink F6T5/BLB) with a maximum emission peak at 365 nm and 40 nm bandwidth (Fig. 2.1). A green bandpass filter (NT67-030, Edmund Optics, Barrington, NJ, USA) with a transmission peak at 520 nm and 36 nm bandwidth was installed in the filter wheel for GFPs image acquisition. A user-defined protocol was run for 1 second, which allowed GFPs emission image to be captured by the Fluorcam 7 software. As the GFPs fluorescence signal increases with GFPs concentration (Roth et al. 2010), the GFPs signal (image pixel values) was taken as a relative quantification of GFPs content. However, it is important to note that further validation is needed in order to use the fluorescence signal to accurately measure the absolute concentration of GFPs in cnidarians.

2.2.6 Image acquisition

All measurements performed in the present study were taken in the following order: Chl *a* fluorescence (F_o and F_v/F_m), red and IR reflectance (for NDVI calculation) and GFPs fluorescence. Every time a measurement was taken for each sample, an image of an 18% grey standard (Neutral Grey Card 4963, FOTOWAND-Technic Dietmar Meisel) was also captured in order to assess and correct eventual light differences between measurements (see Image analysis section). Preliminary investigations confirmed that placing the grey standard at different heights had no effect in the normalized image.
Images of tissue vertical profiles were only obtained for *S.* cf. *glaucum*, as this coral species is relatively rigid and allows a more precise vertical cut (performed using a scalpel through the centre of the tissue). Spatial differences in the coral surface throughout polyp expansion were recorded for *Protopalythoa* sp., with images for NDVI and GFPs analysis being taken every 15 min over a total period of 60 min. F_v/F_m images were only taken at the beginning (0 min) and at the end of polyp expansion (60 min).

2.2.7 Image analysis

Image analysis was carried out using ImageJ software (Schneider et al. 2012). Images obtained using the Fluorcam 7 software were exported in the PSI native “fcimg” format. This is a compressed file that contains all files with the information acquired during the execution of the FluorCAM protocols. Amongst these files, the ones with the extension “dunn” contained the images in a 12-bit format. Each image was then imported into ImageJ as a 16-bit image, allowing the calculation of 32-bit NDVI and F_v/F_m images with double-precision floating-point format. After importing to ImageJ, each image was converted to relative reflectance by normalizing each pixel to the 18% grey reflectance photographic standard that was always photographed together with the coral specimens surveyed:

$$\rho\,(\text{image}) = DN\,(\text{image}) \times 18 / DN\,(\text{standard})$$

where: ρ (image) is the reflectance at each image pixel; 18 is the reflectance of the reflectance standard; DN (image) digital number of each image pixel; DN (standard) average digital number of the grey reflectance standard. NDVI and F_v/F_m images were calculated using the ImageJ image calculator functions as follow:

$$NDVI = (\text{InfraRed image} - \text{Red image})/(\text{InfraRed image} + \text{Red image})$$

F_v/F_m = (F_m image- F_o image)/ F_m image

Pixel values were extracted from NDVI, F_o, F_v/F_m, and GFPs images in three different ways: i) by defining polygon areas of interest (AOIs) surrounding the colonies and extracting mean values and standard deviations from these AOIs; ii) by defining evenly distributed transects throughout the coral tissue in the case of vertical profiles (80 and 86 vertical transects for the high and low light adapted *S*. cf *glaucum*, respectively); and iii) by defining AOIs and extracting all pixels values and cross-analysing these AOIs within R software as numerical matrices.

2.2.8 Statistical analysis

The correlation between Chl *a* content and NDVI for *S.* cf *glaucum* was calculated using Pearson's correlation coefficient (*r*). Results recorded for F_v/F_m, NDVI and GFPs on the colonies' surface and vertical sections of coral tissue (for *S.* cf. *glaucum* only) were compared between light treatments using Student's *t* test. When the assumptions of homogeneity of variances and homoscedasticity for the parametric analysis were not met, the nonparametric Mann-Whitney U test was performed. These tests were also used to compare bleached and non-bleached areas present in *S.* cf. *glaucum* surface tissue. Coefficients of variation (CV = SD / mean) were used as a measure of variability to analyse the different results recorded for the vertical sections of *S.* cf. *glaucum*. The Pearson correlation coefficient (*r*) was used to investigate the association of different variables measured for the same areas through pixel data. All statistical analyses were performed with R software (R Development Core Team 2012). It is important to note that although only one colony was investigated for each measurement, with the exception of the validation of NDVI, the purpose of this imaging method is to analyse spatial patterns within the same colony and the relationship between the measured parameters (F_v/F_m, NDVI and GFPs). The goal of this investigation was to illustrate the potential of this method through several examples in individual colonies (horizontal mapping, vertical section and polyp expansion) and not to provide conclusive statements on the ecology and physiology of the symbiosis.

2.3 Results

2.3.1 NDVI *vs* Chl *a* content

A significant linear relationship was observed between NDVI and Chl *a* content in *S. cf. glaucum* (r = 0.95, p<0.001). This correlation was established for a NDVI range between 0.35 and 0.62, and a Chl *a* range between 105.9 and 435.4 µg Chl *a* g^{-1} coral dry weight (Fig. 2.2).

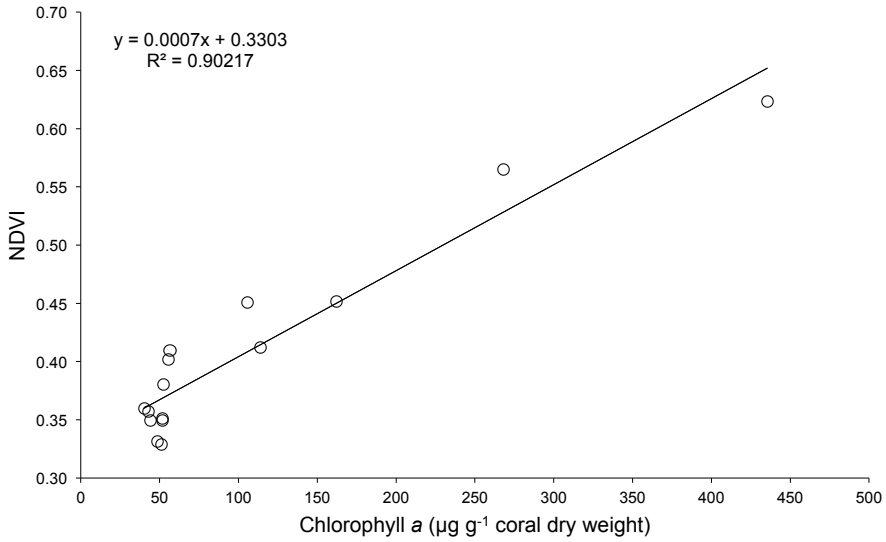

Fig. 2.2 Correlation between chlorophyll *a* and normalized difference vegetation index (NDVI) measured for the soft coral *Sarcophyton* cf. *glaucum*. Each point corresponds to a different coral organism (n = 15). Linear regression line and the coefficient of determination (R^2) are presented.

2.3.2 Mapping spatial heterogeneity of coral surface

The surface of *S.* cf. *glaucum* acclimated to low light (LL) and high light (HL) were analysed for F_v/F_m, F_o and NDVI (Fig. 2.3a-d). GFPs distribution was also analysed, with no GFPs being observed on *S.* cf. *glaucum* surface (data not shown). Surface F_v/F_m values in *S.* cf. *glaucum* acclimated to LL and HL were similar and relatively homogeneous (LL: 0.456 ± 0.042; HL: 0.476 ± 0.042; mean ± SD). Average surface (± SD) F_o and NDVI also showed similar patterns between light treatments (F_o: LL, 21.42 ± 6.48, HL: 20.49 ± 5.48; NDVI: LL, 0.65 ± 0.09; HL, 0.61 ± 0.06). However, surface heterogeneity was observed in *S.* cf. *glaucum* acclimated to HL, as the coral edges were relatively bleached (Fig. 2.3a), which was revealed through the lower values of F_o and NDVI recorded in the coral edges (Fig. 2.3c,d). To explore differences within *S.* cf. *glaucum* acclimated to HL, five AOIs were selected in the bleached and non-bleached region of *S.* cf. *glaucum* and the pixel values extracted. Significant differences between bleached and non-bleached AOIs (n = 124 pixels) were observed for F_v/F_m (bleached: 0.500 ± 0.052; non-bleached: 0.468 ± 0.038; p<0.05, df = 1427.4, t = 13.89) and for NDVI (bleached: 0.387 ± 0.053; non-bleached: 0.656 ± 0.054; p<0.05, df = 1577.1, t = -99.14).

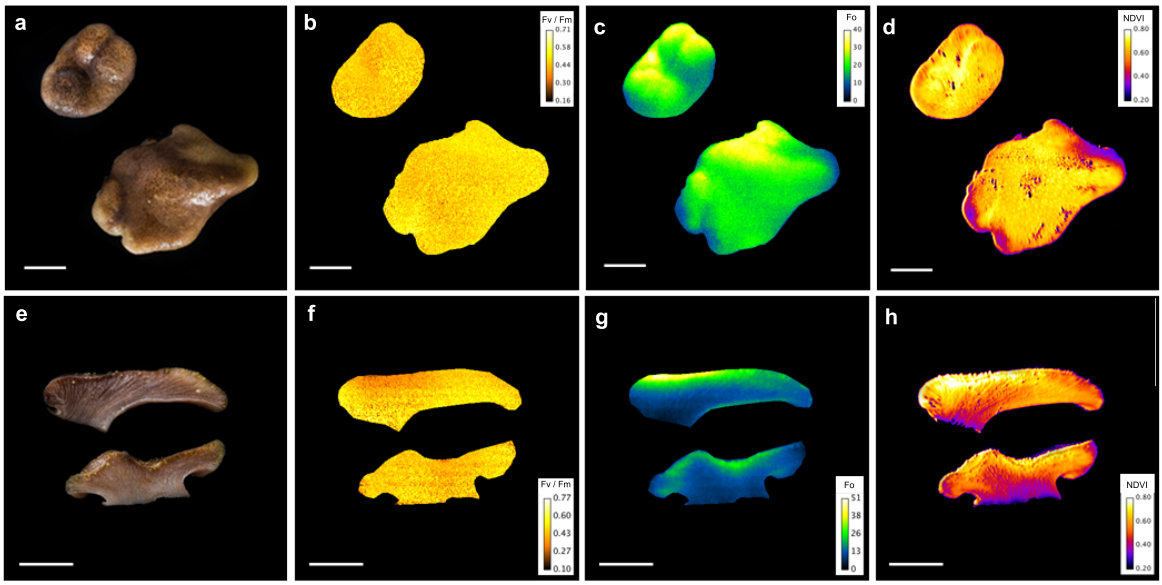

Fig. 2.3 Image analysis of surface (a-d) and vertical sections (e-h) of *Sarcophyton* cf. *glaucum* acclimated to low light (top coral in each image) and high light (bottom coral in each image). Different coral specimens were used for the imaging analysis of the coral surface and vertical sections. Images show a picture taken with a regular photographic camera (a, e) F_v/F_m (b, f) F_o (c, g) and NDVI (d, h). Scale bar (white): 10 mm.

S. flexibilis acclimated to HL and LL were also analysed for surface heterogeneity. However, all parameters measured in *S. flexibilis* exhibited a homogeneous surface (data not shown). Similar values were observed between *S. flexibilis* acclimated to HL and LL for the F_v/F_m (LL: 0.581 ± 0.049; HL: 0.515 ± 0.048) and NDVI (LL: 0.683 ± 0.095; HL: 0.668 ± 0.063). In contrast, GFPs were significantly higher in *S. flexibilis* acclimated to HL (LL: 1259 ± 135; HL: 1356 ± 350; mean ± SD; p<0.05, df = 1974.53, t = -10.19). Although pixel data obtained from the different images taken for each coral were used to test for correlations between different parameters, no correlation was observed between NDVI and F_v/F_m (*S.* cf. *glaucum*: LL r = -0.01; HL r = -0.22).

2.3.3 Vertical profiling

The vertical sections of *S.* cf. *glaucum* acclimated to HL and LL are presented in Fig. 2.3e-h. A vertical pattern was observed for both F_o and NDVI, with higher values found near the coral surface. Large variability was observed within the vertical section, as detected by the relatively high coefficients of variation, in particular for F_o and NDVI (F_v/F_m: LL 13.7%, HL 9.7%; F_o: LL 52.6%, HL 32.5%; NDVI: LL 20.4%, HL 20.8%).

Fig. 2.4 shows the vertical profile of F_v/F_m and NDVI using the pixel data obtained from transects defined throughout the vertical section of *S.* cf. *glaucum*. The vertical pattern recorded for the coral acclimated to LL exhibited an increasing F_v/F_m with depth, i.e., lower at the coral surface and higher at the coral foot (Fig. 2.4a). In contrast, the coral acclimated to HL showed a relatively homogenous F_v/F_m vertical profile. The NDVI decreased with depth and displayed a similar pattern between specimens of *S.* cf. *glaucum* under HL and LL. Overall, higher NDVI values were observed for corals exposed to LL conditions. Corals acclimated to either HL or LL showed similar NDVI profiles, which were characterized by a sub-superficial increase followed by a notable reduction in the first millimetre, a new increase after the first millimetre and finally a steady uniform decrease until the end of the vertical profile (Fig. 2.4b).

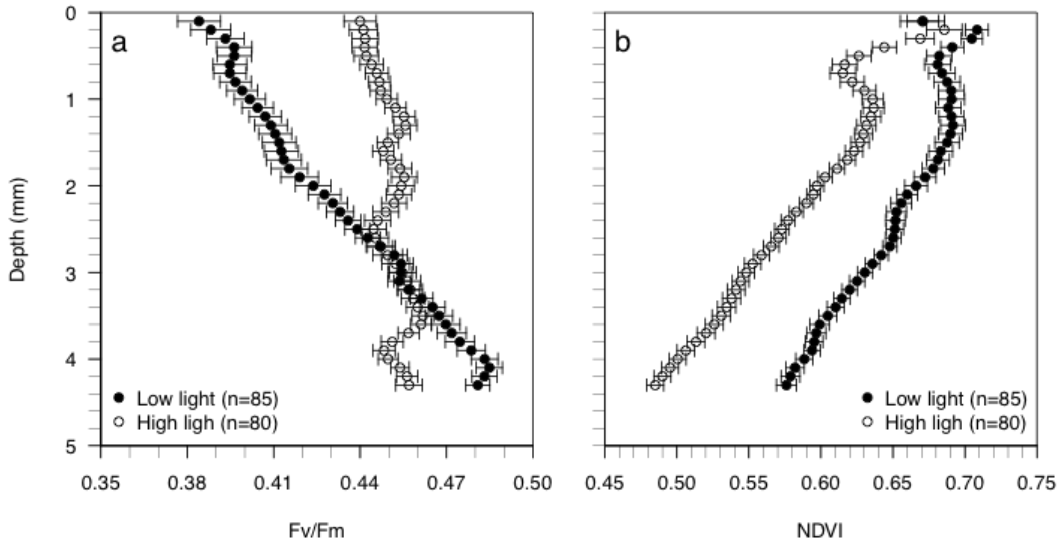

Fig. 2.4 Vertical profile of F_v/F_m (a) and NDVI (b) of *Sarcophyton* cf. *glaucum* acclimated to low and high light. Average (± SE) results of all transects analysed throughout the vertical profile starting at the coral surface (0 mm depth).

2.3.4 Variation of surface heterogeneity with polyp expansion

Fig. 2.5 shows the NDVI and GFPs images of the *Protopalythoa* sp. colony acclimated to HL while expanding its polyps (0, 30 and 60 min). NDVI became more heterogeneous with time, as the area of open polyps showed lower NDVI when compared to the coral tissue surrounding the polyps. Contrasting results were observed for GFPs. The coral tissue surrounding the polyps showed no GFPs, whereas higher GFPs values were observed in the centre of the polyps (i.e. mouth). Closed (0 min) and expanded polyps (60 min) showed similar F_v/F_m (0 min: 0.465 ± 0.057; 60 min: 0.474 ± 0.050), but slightly different NDVI (0 min: 0.477 ± 0.072; 60 min: 0.403 ± 0.099) and GFPs (0 min: 928.584 ± 766.656; 60 min: 679.835 ± 372.900).

The analysis of pixel data for the whole *Protopalythoa* sp. surface revealed a significant negative correlation between NDVI and GFPs for both 0 min (r = -0.10, p<0.001, n = 262144) and 60 min (r = -0.22, p<0.001, n = 262144), but only explained 1 and 5% of the variance (r^2 = 0.01 and 0.05, respectively for 0 and 60 min). The analysis of pixel data for the whole colony revealed no correlations for the other parameters at any time point (data not shown). The correlation between NDVI and GFPs was more pronounced when individual polyp areas were analysed at 0 or 60 min (0 min: r = -0.61, p<0.001, n = 3402; 60 min: r = -0.762, p<0.001, n = 3584).

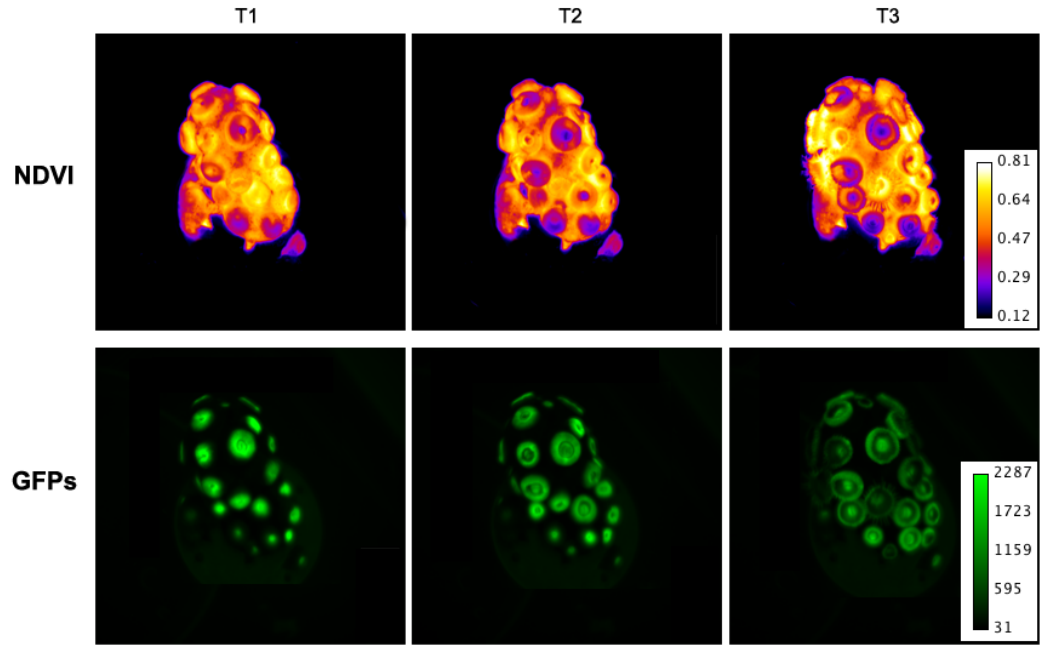

Fig. 2.5 NDVI and GFP-fluorescence time sequence images taken with the modified FluorCAM of *Protopalythoa* sp. polyp expansion through time. Closed polyps: T1 – 0 min; polyp expansion: T2 – 30 min; expanded polyps: T3 – 60 min.

The use of pixel data from individual polyps allowed the detailed analysis of the horizontal profile of F_v/F_m, NDVI and GFPs through defining a transect from one edge of the polyp to the opposite edge, passing through the polyp's mouth in the middle of the drawn diameter (Fig. 2.6). NDVI and GFPs showed a significant contrasting pattern throughout the polyp surface (r = -0.93, p<0.001, n = 136); NDVI decreased in the centre of the oral disk (mouth) while GFPs increased. F_v/F_m showed a relatively homogenous pattern throughout the coral polyp. No significant correlation was observed between F_v/F_m and NDVI (r = 0.11, p = 0.2, n = 136) or between F_v/F_m and GFPs (r = -0.14, p = 0.1, n = 136).

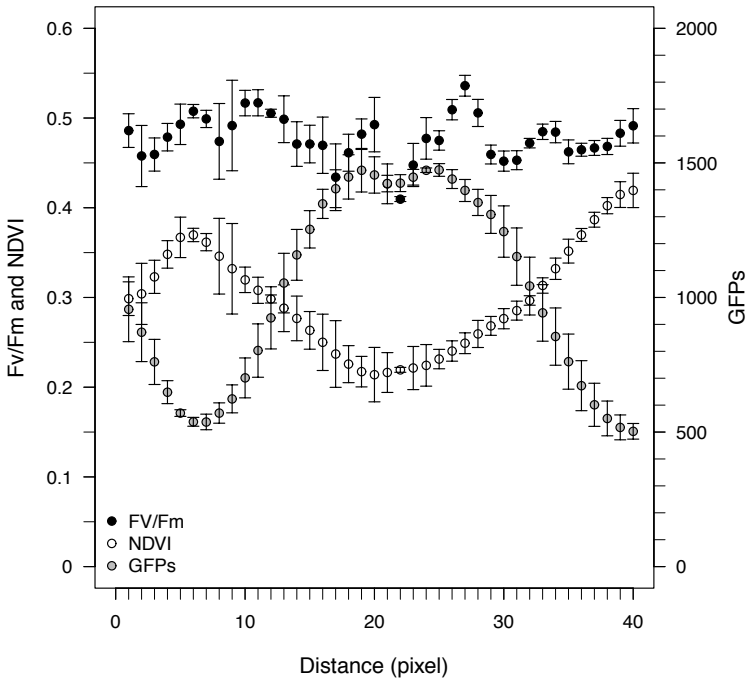

Fig. 2.6 Horizontal profile of F_v/F_m, NDVI and GFP-fluorescence of a *Protopalythoa* sp. open polyp. Average (± SE) results of three transects analysed in the same coral polyp (with 40-pixel width).

2.4 Discussion

High-resolution imaging of Chl *a* fluorescence has already demonstrated that the complex morphology of corals can influence the photobiology of localized regions within the coral (Ralph et al. 2005, Cox et al. 2007, Roff et al. 2008). The Chl *a* fluorescence images here produced are similar to previous results obtained by similar imaging methods applied to corals (Ralph et al. 2005). In addition, the method used in this study included various light sources and bandpass filters, which enabled the production of NDVI and GFPs images concurrent with Chl *a* fluorescence images, and consequently analyse the relationship between these measurements using pixel data. The possible applications of this approach were illustrated in three symbiotic cnidarian species used as biological models (*Sarcophyton* cf. *glaucum*, *Sinularia flexibilis* and *Protopalythoa* sp.) exhibiting contrasting morphological features. While being a soft coral, *S.* cf. *glaucum* tissue is relatively rigid, which allowed performing a well-defined cut over its vertical section. Furthermore, the surface of this species is relatively flat in small colonies, which avoids problems in image analysis associated with self-shading, a common constraint when analysing 3-dimensional structures. In contrast, *S. flexibilis* commonly exhibits a bush-like shape and has very soft tissue. These characteristics prevented us to perform a precise vertical cutting and replicate the study described above for *S*. cf. *glaucum*.

2.4.1 NDVI as a proxy of Chl *a* content

NDVI is often used as a proxy of Chl *a* in microalgae-dominated biofilms (Serôdio et al. 2001, Honeywill et al. 2002, Coelho et al. 2009, Perkins et al. 2010), as well as in photosynthetic animals (seaslugs; Serôdio et al. 2010). This study shows that NDVI values were significantly correlated with Chl *a* content in the soft coral *S*. cf *glaucum*. Curiously, the use of NDVI in symbiotic corals has been relatively scarce (EJ Hochberg pers. comm.; Phinn et al. 2012, Rocha et al. 2013b). Joyce and Phinn (2003), Enríquez et al. (2005) and Ralph et al. (2005) used reflectance data as a

proxy of Chl *a* content in corals. These studies report some issues associated with the application of reflectance as a proxy of Chl *a*. Joyce and Phinn (2003) note the low range of Chl *a* concentration in their study, as well as the influence of scale variations among the different measurements (spectrometer and pigment measurements). Enríquez et al. (2005) note the increase in the absorption capacity of the coral associated with multiple scattering processes that take place in the coral structure. However, it must be noted that the latter study investigated scleractinian corals. The present study focused on soft corals and zoanthids, which have soft tissues and no hard and white skeleton affecting reflectance measurements. Another important difference is associated with the use of information in the IR region by NDVI. Whereas reflectance measurements by Joyce and Phinn (2003) and Enríquez et al. (2005) only considered the red region of the spectrum (675 nm), Ralph et al. (2005) used both red and IR region of the spectrum but a relatively different calculation from NDVI. Indices based on both red and IR reflectance, such as NDVI, provide a more accurate proxy of Chl *a* because it includes information about the light reflected in the IR region that is not absorbed by chlorophyll molecules. Nonetheless, several symbiotic coral species have GFPs that may lead to increased light absorption by Chl *a* (Schlichter et al. 1994, Salih et al. 2000). Future studies should be carried out to assess the effect of GFPs content on NDVI measurements, particularly because our validation of NDVI was performed with *S*. cf. *glaucum*, which showed no GFPs content. The use of this single species to validate NDVI is associated with: i) this coral species has a relatively flat surface without a complex three dimensional structure that could affect the excitation and reflection of light; ii) the distribution of Chl *a* in the surface tissue of this species is very homogenous and, therefore, the averaged reflectance signal could correlated with pigment concentration of each coral nubbin; iii) as the effect of *Symbiodinium* self-shading, light penetration in the tissue and depth-distribution of pigments throughout the tissue are still unknown for soft corals, the use of small *S*. cf. *glaucum* nubbins with a high surface area and relatively small biomass minimized the amount of tissue used to extract Chl *a* that was probably not affecting the reflectance signal. The results obtained for this validation (Fig. 2.2) supported the use of NDVI as a proxy of Chl *a* content. However, it must be noted that NDVI should be used with caution, particularly to detect differences within small Chl *a* ranges.

2.4.2 Coral tissue heterogeneity

A major advantage of using imaging techniques is the possibility to perform a detailed characterization of spatial heterogeneity of the coral tissue. The approach used in this study recorded differences within and between cnidarian species, which would not be possible through conventional Chl *a* fluorescence measurements that only provide a single value for each area analysed. In contrast to *S*. cf. *glaucum* (LL-acclimated) and *S. flexibilis*, a high-degree of surface heterogeneity was observed in *Protopalythoa* sp. (Fig. 2.5), particularly within each polyp. This may be associated with other sources of variability within the polyp area, such as self-shading of symbionts, differential light reception and proximity to polyp mouth and/or tentacles. These potential sources of variability may be further investigated using this method and allow a better understanding of the relationship between the physiological state of the symbionts and the morphological features of the host. This method also allowed the detection of heterogeneity on the surface tissue associated with differential bleaching conditions for HL acclimated *S*. cf. *glaucum*, which may be relevant for seasonal monitoring of symbiotic corals. Furthermore, the spatially detailed investigation of coral tissue heterogeneity may allow a better understanding of the mechanisms that trigger bleaching and the consequent photophysiological responses occurring at the colony level.

The possibility of analysing concurrent images of different photobiological parameters and GFPs fluorescence provides a new application for the study of the functional role of GFPs in symbiotic

corals, a topic that remains controversial (for further information on this topic please see Matz et al. 2006, Oswald et al. 2007, Alieva et al. 2008, Palmer et al. 2009, Kenkel et al. 2011). It is important to note that the current work was designed to explore the potential uses of the concurrent imaging techniques and not to explore the physiological role of GFPs in symbiotic cnidarians. Nonetheless, the results here recorded show that this method allows the investigation of fundamental questions to clarify the functional role of GFPs in symbiotic corals in future studies. For example, it is possible to investigate the direct relationships between these different parameters within a single polyp, as exemplified for *Protopalythoa* sp. (Fig. 2.6). The analysis of the correlation between GFPs and NDVI, as well as with the photophysiological parameters of the symbionts (e.g. electron transport rate, non-photochemical quenching), along with its analysis under different stressors (e.g. light, temperature, salinity), may allow a better understanding of the role of these host-related pigments on the physiology of symbiotic cnidarians. For instance, investigating the association between physiological stress, as monitored by PAM fluorometry (e.g. quantifying photoinhibition through F_v/F_m), bleaching (e.g. quantifying the loss in Chl *a* content) and GFPs content may allow researchers to relate the susceptibility of photoinhibition to GFPs content, thus testing the putative photoprotective role of GFPs (Salih et al. 2000).
It is also important to note that further exploration of intra-polyp photobiological variation should also consider the effect of light shifts associated with coral morphology due to multiple light scattering (Enríquez et al. 2005). The variation in pigment density with tissue expansion/retraction as observed for the GFPs in *Protopalythoa* sp. (Fig. 2.5) is a preliminary finding that should be explored further. Particularly, the suggestion that GFPs are concentrated in the external polyp tissue when polyps are closed (Fig. 2.5 – T1) may be associated with the occurrence of tissue retraction and consequently an apparent increase of GFPs concentration in those regions. This new methodological approach thus allows the simultaneous investigation of the photophysiology of the symbionts and the host's behaviour, and how the relationship between these symbiont and host-related factors, respectively, may change throughout ontogeny.

2.4.3 Image correlation analysis

The use of pixel data from the images of different measurements made in the same coral organism allowed us to overlay images and explore potential relationships between F_v/F_m, NDVI and GFPs. Given the low levels of GFPs recorded for *S.* cf. *glaucum*, it was not possible to investigate its relationships with other parameters in this coral species. Moreover, relationships involving GFPs' were also not possible in *S. flexibilis* due to surface homogeneity, which dramatically reduced the range of the data. If heterogeneity was observed, and low and high relative GFPs content was present in different areas of the surface tissue, the correlation between GFPs and other parameters would probably be detected. Another important use of the acquired images is the ability to explore the in-depth variation of photobiological properties of soft corals at a high-resolution spatial scale, i.e. pixel-by-pixel information (Fig. 2.4). The use of this method to assess within-colony variation has issues associated with statistical assumptions and replicability. Biological replication would imply averaging the data for each colony, which would invalidate the full potential of this method. Further, biological replication would only be useful to assess if similar patterns were observed between different coral colonies. In this study we use independent colonies for each measurement because the main goal of this study was to show different applications of this imaging method and not to investigate ecological and photophysiological patterns. Nevertheless, it is interesting to note the differences observed in the vertical profile of F_v/F_m of *S.* cf. *glaucum* exposed to different light intensities, which may be associated with higher light penetration within the tissue of the coral exposed to HL (Dubinsky et al. 1984, Dubinsky & Falkowski 2011). Another interesting result to explore in future works is the increase of F_v/F_m with tissue depth (Fig. 2.4a). With this imaging

method it is possible to investigate the preferential aggregation of symbionts within the coral tissue and how different light intensities and spectra may affect such arrangements. The effect of *Symbiodinium* self-shading (Wyman et al. 1987) on its photophysiology and concentration of animal pigments (i.e. GFPs) may also be investigated along the vertical profile of soft coral tissue. Future studies using this method may also contribute to understand the irregular decrease of NDVI with depth (Fig. 2.4b) by using contrasting environmental settings and applying different stressors (e.g. light, temperature). Although the use of contrasting light conditions in this study, i.e. HL *versus* LL, was solely aimed to maximize the variability of results associated with the photobiology of the coral species surveyed, our results show that the proposed method can be used to explore in-depth variations of photobiological parameters associated to shifts in ambient light and photoacclimation. For instance, analysis of tissue in-depth variation of photophysiological properties throughout different seasons and depth transects may allow a better understanding of the physiological dynamics of these symbiotic organisms.

In conclusion, the present results support the use of a modified imaging chlorophyll fluorometer to explore the photobiology of symbiotic soft corals and the relationships between photobiological parameters of *Symbiodinium* and GFPs. An important feature of this new experimental approach is the possibility to simultaneously measure and overlay photochemical activity, NDVI and GFPs data from the same coral colony. F_v/F_m was only used to illustrate the possibility of measuring any fluorescence parameter or index possible of being determined by PAM fluorometry. The demonstration of the correlation between Chl *a* and NDVI allows the application of this non-invasive imaging approach to other studies estimating Chl *a* content in symbiotic corals. Being a truly non-invasive technique, captured images can also be used to record and analyse different patterns in coral tissue associated with coral behaviour such as polyp expansion, as illustrated in this study. Moreover, the ability to analyse image information pixel by pixel provides a powerful tool for future investigations on spatial heterogeneity of coral tissues. Although the current study focused on GFPs of the green colour type, it is possible to analyse fluorescent proteins of other colour types through the use of different bandpass filters and excitation wavelengths. This modified imaging system will also facilitate future studies that aim to combine high-resolution spatio-temporal measurements with fine scale sampling of coral tissue to investigate the biology and coral-algal stress physiology.

2.5 Acknowledgments

M.C.L., J.E. and R.J.M.R. were supported by a PhD scholarship (SFRH/BD/63783/2009, SFRH/BD/44860/2008, SFRH/BD/46675/2008, respectively) funded by FCT - Fundação para a Ciência e Tecnologia (QREN-POPH-Type 4.1 – Advanced Training, subsidized by the European Social Fund and national funds MCTES). B.J. was funded by a Post-doctoral contract from the Région Pays de la Loire. This work was also supported by FCT project SeReZoox (PTDC/MAR/113962/2009). We thank two anonymous reviewers for important comments and suggestions.

2.6 References

Alieva NO, Konzen KA, Field SF, Meleshkevitch EA, Hunt ME, Beltran-Ramirez V, Miller DJ, Wiedenmann J, Salih A, Matz MV (2008) Diversity and evolution of coral fluorescent proteins. PLoS One 3:e2680

Baker N, Rosenquist E (2004) Applications of chlorophyll fluorescence can improve crop production strategies: an examination of future possibilities. J Exp Bot 55:1607-1621

Coelho H, Calado R, Olaguer-Feliu AO, Vieira S, Queiroga H, Serodio J (2009) Nondestructive quantification of phytoplankton gut content of brachyuran crab megalopae using *in vivo* chlorophyll *a* fluorescence. J Plankton Res 31:577-581

Collin A, Hench JL, Planes S (2012) A novel spaceborne proxy for mapping coral cover. Proc 12th Int Coral Reef Symp: 5A Remote sensing of reef environments, Cairns, Queensland, Australia

Costa J, Giménez-Casalduero F, Melo R, Jesus B (2012) Colour morphotypes of *Elysia timida* (Sacoglossa, Gastropoda) are determined by light acclimation in food algae. Aquatic Biol 17:81-89

Cox G, Matz M, Salih A (2007) Fluorescence lifetime imaging of coral fluorescent proteins. Microsc Res Tech 70:243-251

Dubinsky Z, Falkowski PG, Porter JW, Muscatine L (1984) Absorption and utilization of radiant energy by light- and shade-adapted colonies of the hermatypic coral *Stylophora pistillata*. Proc R Soc Lond B: Biol Sci 222:203-214

Dubinsky Z, Falkowski P (2011) Light as a source of information and energy in zooxanthellate corals. In: Dubinsky Z, Stambler N (eds) Coral Reefs: An Ecosystem in Transition. Springer Netherlands, Dordrecht, The Netherlands, pp. 107-118

Enríquez S, Méndez ER, Iglesias-Prieto R (2005) Multiple scattering on coral skeletons enhances light absorption by symbiotic algae. Limnol Oceanogr 50:1025-1032

Fabricius-Dyg J, Mistlberger G, Staal M, Borisov SM, Klimant I, Kühl M (2012) Imaging of surface O_2 dynamics in corals with magnetic micro optode particles. Mar Biol 159:1621-1631

Hamilton SC (2012) Applications of coral bio-optics to coral reef management. MSc thesis, Dalhousie University, 80 pp.

Hanley QS, Murray PI, Forde TS (2006) Microspectroscopic fluorescence analysis with prism-based imaging spectrometers: review and current studies. Cytometry A 69:759-766

Helmuth B, Timmerman B, Sebens K (1997) Interplay of host morphology and symbiont microhabitat in coral aggregations. Mar Biol 130:1-10

Hill R, Schreiber U, Gademann R, Larkum AWD, Kuhl M, Ralph PJ (2004) Spatial heterogeneity of photosynthesis and the effect of temperature-induced bleaching conditions in three species of corals. Mar Biol 144:633-640

Hoegh-Guldberg O (1999) Climate change, coral bleaching and the future of the world's coral reefs. Mar Freshwat Res 50:839-866

Honeywill C, Hagerthey S, Paterson DM (2002) Determination of microphytobenthic biomass using pulse-amplitude modulated minimum fluorescence. Eur J Phycol 137:485-492

Joyce KE, Phinn SR (2003) Hyperspectral analysis of chlorophyll content and photosynthetic capacity of coral reef substrates. Limnol Oceanogr 48:489-496

Kenkel CD, Traylor MR, Wiedenmann J, Salih A, Matz MV (2011) Fluorescence of coral larvae predicts their settlement response to crustose coralline algae and reflects stress. Proc R Soc Lond B: Biol Sci 278:2691-2697

Kitajima M, Butler W (1975) Quenching of chlorophyll fluorescence and primary photochemistry in chloroplasts by dibromothymoquinone. Biochim Biophys Acta 376:105-115

Kraay GW, Zapata M, Veldhuis MJW (1992) Separation of chlorophylls c1, c2 and c3 of marine phytoplankton by reverse-phase-c18-high-performance liquid cromatography. J Phycol 28:708-712

Kühl M, Cohen Y, Dalsgaard T, Jorgensen B, Revsbech N (1995) Microenvironment and photosynthesis of zooxanthellae in scleractinian corals studied with microsensors for O_2, pH and light. Mar Ecol Prog Ser 117:159-172

Kühl M, Holst G, Larkum AWD, Ralph PJ (2008) Imaging of oxygen dynamics within the endolithic algal community of the massive coral *Porites lobata*. J Phycol 44:541-550

Kutser T, Miller I, Jupp DLB (2006) Mapping coral reef benthic substrates using hyperspectral space-borne images and spectral libraries. Estuar Coast Shelf Sci 70:449-460

Matz MV, Marshall NJ, Vorobyev M (2006) Are corals colorful? Photochem Photobiol 82:345-350

Maxwell K, Johnson G (2000) Chlorophyll fluorescence - a practical guide. J Exp Bot 51:659-668

Muscatine L, Porter J (1977) Reef Corals - Mutualistic Symbioses Adapted to Nutrient-Poor Environments. BioScience 27:454-460

Muscatine L, Falkowski P, Dubinsky Z, Cook PA, McCloskey L (1989) The effect of external nutrient resources on the population-dynamics of zooxanthellae in a reef coral. Proc R Soc Lond B: Biol Sci 236:311-324

Nebdal L, Trtilek M, Herppich W (2000) Methods and equipment for fluorescence imaging on plant material. Bornimer Agrartechn Ber 25:127-135

Oswald F, Schmitt F, Leutenegger A, Ivanchenko S, D'angelo C, Salih A, Maslakova S, Bulina M, Schirmbeck R, Nienhaus GU, Matz MV, Wiedenmann J (2007) Contributions of host and symbiont pigments to the coloration of reef corals. FEBS Journal 274:1102-1122

Palmer CV, Modi CK, Mydlarz LD (2009) Coral fluorescent proteins as antioxidants. PLoS One 4:e7298

Peñuelas J, Gamon JA, Griffin KL, Field CB (1993) Assessing community type, plant biomass, pigment composition, and photosynthetic efficiency of aquatic vegetation from spectral reflectance. Remote Sens Environ 46:110-118

Perkins R, Kromkamp J, Serôdio J, Lavaud J, Jesus B, Mouget J, Lefebvre S, Forster R (2010) The application of variable chlorophyll fluorescence to micrphytobenthic biofilms. In: Suggett D, Prásil O, Borowitzka M (eds) Chlorophyll *a* fluorescence in aquatic sciences: methods and applications, Developments in Applied Phycology 4. Springer, London, pp. 237-275

Phinn SR, Roelfsema CM, Mumby PJ (2012) Multi-scale, object-based image analysis for mapping geomorphic and ecological zones on coral reefs. Int J Remote Sens 33:3768-3797

R Development Core Team (2012) R: A language and environment for statistical computing. R Foundation for Statistical Computing. R Foundation for Statistical Computing, Vienna, Austria (http://www.R-project.org)

Ralph P, Gademann R, Larkum A, Kühl M (2002) Spatial heterogeneity in active chlorophyll fluorescence and PSII activity of coral tissues. Mar Biol 141:639-646

Ralph PJ, Schreiber U, Gademann R, Kühl M, Larkum AWD (2005) Coral Photobiology Studied with a New Imaging Pulse Amplitude Modulated Fluorometer. J Phycol 41:335-342

Rocha RJM, Calado R, Cartaxana P, Furtado J, Serôdio J (2013a) Photobiology and growth of leather coral *Sarcophyton* cf. *glaucum* fragments stocked under low light in a recirculated system. Aquaculture 414-415:235-242

Rocha RJM, Pimentel T, Serôdio J, Rosa R, Calado R (2013b) Comparative performance of light emitting plastma (LEP) and light emitting diode (LED) in *ex situ* aquaculture of scleractinian corals. Aquaculture 402-403:38-45

Rocha RJM, Serôdio J, Leal MC, Cartaxana P, Calado R (2013c) Effect of light intensity on post-fragmentation photobiological performance of the soft coral *Sinularia flexibilis*. Aquaculture 388-391:24-29

Roff G, Ulstrup KE, Fine M, Ralph PJ, Hoegh-Guldberg O (2008) Spatial heterogeneity of photosynthetic activity within diseased corals from the great barrier reef. J Phycol 44:526-538

Roth MS, Latz MI, Goericke R, Deheyn DD (2010) Green fluorescent protein regulation in the coral *Acropora yongei* during photoacclimation. J Exp Biol 213:3644-3655

Rouse JW, Haas Jr RH, Schell JA, Deering DW (1973) Monitoring vegetation systems in the great plains with ERTS. Proceedings of the Third ERTS Symposium, Vol. 1, pp. 309-317

Salih A, Cox G, Hinde R (1995) Autofluorescence imaging of symbiotic algae in corals using confocal microscopy - a potential tool for environmental monitoring. Zool Stud 34:53-55

Salih A, Larkum A, Cox G, Kühl M, Hoegh-Guldberg O (2000) Fluorescent pigments in corals are photoprotective. Nature 408:850-853

Schlichter D, Meier U, Fricke HW (1994) Improvement of photosynthesis in zooxanthellate corals by autofluorescent chromatophores. Oecologia 99:124-131

Schneider C, Rasband W, Eliceiri K (2012) NIH Image to ImageJ: 25 years of image analysis. Nat Methods 9:671-675

Schreiber U, Schliwa U, Bilger W (1986) Continuous recording of photochemical and nonphotochemical chlorophyll fluorescence quenching with a new type of modulation fluorometer. Photosynthesis Res 10:51-62

Serôdio J, Marques da Silva J, Catarino F (2001) Use of *in vivo* chlorophyll *a* fluorescence to quantify short-term variations in the productive biomass of intertidal microphytobenthos. Mar Ecol Prog Ser 218:45-61

Serôdio J, Cartaxana P, Coelho H, Vieira S (2009) Effects of chlorophyll fluorescence on the estimation of microphytobenthos biomass using spectral reflectance indices. Remote Sens Environ 113:1760-1768

Serôdio J, Pereira S, Furtado J, Silva R, Coelho H, Calado R (2010) *In vivo* quantification of kleptoplastic chlorophyll a content in the “solar-powered” sea slug *Elysia viridis* using optical methods: spectral reflectance analysis and PAM fluorometry. Photochem Photobiol Sci 9:68

Venn A, Loram J, Douglas A (2008) Photosynthetic symbioses in animals. J Exp Bot 59:1069-1080

Wyman K, Dubinsky Z, Porter JW, Falkowski P (1987) Light absorption and utilization among hermatypic corals: a study in Jamaica, West Indies. Mar Biol 96:283-292

Yamaguchi H, Asanuma I, Shimamura H (2008) Negative contribution of groundwater input from subsurface spring to coral reef bleaching. Int Arch Photogramm, Remote Sens Spatial Information Sci 37:719-724

Ziskin D, Aubrecht C, Elvidge C, Tuttle B, Eakin CM, Strong AE, Guild LS (2011) Describing coral reef bleaching using very high spatial resolution satellite imagery: experimental methodology. J Appl Remote Sens 5:053531

Chapter 3 Optimization of monoclonal production of the glass anemone *Aiptasia pallida* (Agassiz in Verrill 1864)

Abstract

Sea anemones within genus *Aiptasia* are commonly used as biological models for biotechnological and molecular research. They are also employed to study the symbiotic interaction between cnidarians and zooxanthellae. In addition, *Aiptasia* is an important prey for the culture of the highly priced ornamental nudibranch *Aeolidiella stephanieae*. The purpose of this study was to determine the best culture conditions for establishing large monoclonal populations of this anemone. This study analysed the effect of the following factors on *Aiptasia pallida* propagation and biomass increase throughout 60 days: initial anemone stocking density, light regime, water temperature and different diet. The best results were achieved at a higher water temperature (26 ºC) and in total darkness. *Artemia* nauplii were a better live prey than *Artemia* metanauplii to maximize biomass production. Lower initial anemone stocking densities maximized propagation ratios. This research provides initial data that enables a large-scale production of monoclonal *A. pallida* to be used as a biological model, for the screening of new natural products or in the aquaculture of ornamental sea slugs.

Keywords

Anemone culture; Biomass; Temperature; Light.

Published: Leal MC, Nunes C, Engrola S, Dinis MT, Calado R (2012) Optimization of monoclonal production of the glass anemone *Aiptasia pallida* (Agassiz in Verrill 1864). Aquaculture 354-355: 91-96 (doi: 10.1016/j.aquaculture.2012.03.035)

3.1 Introduction

Sea anemones within genus *Aiptasia*, commonly known as glass anemones, distribute worldwide from tropical to temperate marine ecosystems (Chen et al. 2008, Sunagawa et al. 2009). *Aiptasia* are known to possess a remarkable trophic plasticity. They are able to accomplish their energetic demands heterotrophically, by preying on zooplankton, and autotrophically, through the photosynthates produced by their endosymbiotic microalgae, popularly known as zooxanthellae (Thorington & Hessinger 1996, Ruppert et al. 2003, Bachar et al. 2007). This symbiotic relationship can supply up to 95% of photosynthetically-fixed carbon to the host (Falkowski et al. 1984, Venn et al. 2008), which may allow some *Aiptasia* species to survive without any external food for long periods (Cook et al. 1988). However, photosynthates provided by the endosymbionts do not meet all the nutritional requirements of their cnidarian host, namely phosphorus and nitrogen, which play a crucial role in anemone growth and reproduction (Bachar et al. 2007).

Aiptasia hardiness in captivity, fast growth rate and asexual reproduction allow researchers to culture monoclonal individuals under controlled laboratorial conditions. Monoclonal individuals are produced when all specimens originate from a single parental organism, thus being genetically identical, which is a useful trait to control morphological and genetic plasticity (Weis et al. 2008). These features have contributed to make *Aiptasia* a successful biological model for research on reproduction (Clayton Jr & Lasker 1985, Chen et al. 2008), physiology (Davy & Cook 2001), stress biology (Goulet et al. 2005), toxicology (Mercier et al. 1997), genetics (Kuo et al. 2004), natural products (Marino et al. 2004) and symbiotic relationships between cnidarians and zooxanthellae (Muller-Parker 1985, Davy & Cook 2001, Mobley & Gleason 2003, Bachar et al. 2007). Furthermore, breeders of marine ornamental species culturing the aeollid nudibranch *Aeolidiella stephanieae* Valdéz 2005 are now targeting the production of large numbers of *Aiptasia*. Although erroneously, *A. stephanieae* is commonly known in the marine aquarium trade as *Berghia verrucicornis*. This small nudibranch feeds exclusively on these sea anemones and is universally employed to control these pests in reef aquariums (Carroll & Kempf 1990, Kristof & Klussmann-Kolb 2010). The efficiency of *A. stephanieae* to control *Aiptasia* is such that these nudibranchs commonly obtain high market prices (average retail price up to 20 € per specimen) in the marine aquarium trade. Curiously, the obstacle impairing the breeding of large numbers of *A. stephanieae*, thus the profitability of this activity, is the absence of a regular and abundant supply of their only prey, i.e. *Aiptasia* (Olivotto et al. 2011). Thus, it is important to determine the best culture conditions for inexpensively establishing large monoclonal populations of glass anemones. The objective of the present study was to investigate the effect of different initial anemone stocking densities, light regimes, water temperatures and diets on the clonal propagation and biomass production of *Aiptasia pallida* (Agassiz in Verrill, 1864). The rationale for this approach was that higher stocking densities may enhance biomass production, but may slow down propagation rates. The supply of artificial light and heat was important to mimic natural sunlight and water temperature conditions, although it increases culture costs. On the other hand, the culture of anemones in dark and at low temperature may have notable drawbacks. While the culture of *A. pallida* in the absence of light prevents autotrophy, lower temperatures may reduce metabolic rates and consequently decrease growth and propagation rates. The effect of live feed leftover diets commonly drained from larviculture tanks was also investigated. *A. pallida* are commonly fed with pricey newly hatched *Artemia* nauplii, and the use of live feed leftovers, particularly *Artemia* metanauplii, reduces the cost of producing live food for *A. pallida*.

3.2 Materials and Methods

3.2.1 Husbandry and preliminary propagation of *A. pallida*

Monoclonal *A. pallida*, originating from a single specimen, were held in a 250 L culture tank (1 m x 0.5 m x 0.5 m) filled with 5 µm filtered and UV irradiated natural seawater. The tank was placed outdoors under natural sunlight and photoperiod. Ceramic tiles (20 mm x 20 mm) were positioned in the tank and lined up against the walls to increase available surface area for the growth of cultured anemones. The use of these ceramic tiles offered two additional advantages: 1) they allowed large numbers of *A. pallida* to be quickly collected from the culture tank; and 2) their smooth surfaces made it possible to easily release the anemones by gently scraping them at the base of their basal disk without inducing significant mechanical damage. Water temperature was kept at 26 ºC. A 300 W electrical heater equipped with a thermostat was used to maintain water temperature. Salinity was kept stable at 35 ± 1 by daily adding freshwater to the culture tank (previously purified using a reverse osmosis unit) and thereby compensating any losses resulting from evaporation. Water circulation was provided by airlifts placed at each corner of the culture tank. Nitrate levels varied between 10 and 20 mg L^{-1}, while ammonia and nitrite remained under detectable levels; pH values recorded were 8.0 ± 0.1. All parameters previously referred were monitored using colorimetric tests (Tropic Marin®, Germany). Anemones were fed every three days with newly hatched *Artemia* nauplii (5 nauplii mL^{-1}; San Francisco Bay Brand Inc., USA) and allowed to freely propagate for six months prior to the start of the experiments. The tank bottom was siphoned once a week together with a 25% partial water change.

3.2.2 Size class determination

In order to determine the best non-destructive method to monitor anemones' biomass, four anemones were randomly sampled from the culture tank, dried on absorbent paper and weighed (Sartorius scale; ± 0.001 g). Samples were freeze-dried for 48 h and weighed again to determine the relationship between wet weight and dry weight. To examine the relationship between dry weight and pedal disk diameter (PDD) (Chomsky et al. 2004a), 70 anemones were randomly collected from the culture tank and their PDD measured. Measurements were performed using callipers (to the nearest 0.05 mm) after the anemone retracted its tentacles and without removing the anemone from the ceramic plate. When necessary, the retraction of the anemone was stimulated with a plastic pipette in order to remove any excess water from inside the gastrovascular cavity. Each specimen was then scrapped off the ceramic plates and its dry weight was determined after freeze-drying for 48 h. Regression analysis supported the use of PDD for measuring the size of anemones, and thus the following size classes were established for PDD: extra small (XS) (PDD <3 mm), small (S) (PDD between 3 and 6 mm), medium (M) (PDD between 6 and 9 mm) and large (L) (PDD >9 mm).

3.2.3 Determination of optimal prey concentration

Anemones from each size class (XS, S, M, L) were placed in separate 300 mL beakers with 5 µm filtered and UV irradiated natural seawater. The beakers were kept in a water bath at 26 °C and a 12 light (Lt): 12 dark (D) photoperiod. The following number of anemones was used in each beaker for each size class: 6 specimens for sizes XS, S and M, and 3 specimens for size L. All experiments were made in triplicate, i.e. 3 different beakers were used for each size class. The anemones were fed with *Artemia* nauplii at the following concentrations: XS) 0.3, 0.6 and 1 nauplii

mL^{-1}; S) 0.6, 1 and 1.3 nauplii mL^{-1}; M) 2, 3 and 4 nauplii mL^{-1}; and L) 5, 6.6 and 8.3 nauplii mL^{-1}. The range of prey concentration to be tested for each anemone size class had been previously determined in a preliminary experiment (unpublished data). After a period of 24 h, classification for prey ingestion was determined through visual observation considering four ingestion levels: partial ingestion, partial ingestion with regurgitation, total ingestion and total ingestion with regurgitation. Partial ingestion occurred when only a portion of all prey provided was ingested by the sea anemone. Partial ingestion with regurgitation was documented when only a portion of all prey provided was ingested together with regurgitated pack(s) of *Artemia* nauplii recorded in the bottom of the container. Total ingestion was defined as the ingestion of all prey provided. Total ingestion with regurgitation was defined when the ingestion of all prey provided was recorded together with the presence of regurgitated pack(s) of *Artemia* nauplii in the bottom of the container. Regurgitated pack(s) of *Artemia* nauplii varied in shape and size, although they were commonly 2-3 mm in diameter and displayed an orange coloration similar to the prey provided to *A. pallida*.

3.2.4 Effect of initial stocking density, light regime, water temperature and diet on clonal propagation and biomass production

Triplicate trials (each performed in 3 L plastic tanks (0.1 m x 0.1 m x 0.3 m)) were performed for each possible combination of the following factors: initial anemone stocking density (90 vs. 180 anemones m^{-2}), light regime (12 h Lt : 12 h D vs. 24 h D), water temperature (22 vs. 26 ºC, regulated through a water heating/cooling device) and diet (*Artemia* nauplii resulting from newly hatched nauplii (hereafter referred to as nauplii) vs. *Artemia* metanauplii resulting from nauplii enriched with *Tetraselmis chui* and *Isochrysis galbana* during 24 h (hereafter referred to as metanauplii)). The experiment lasted 60 days and was performed with XS (PDD <3 mm), S (PDD between 3 and 6 mm) and M (PDD between 6 and 9 mm) anemones. In order to meet the initial anemone stocking densities selected for the present study, the following combination of anemones was selected: 3 XS, 3 S and 3 M anemones (for the 90 anemones m^{-2} treatment) and 6 XS, 6 S and 6 M anemones (for the 180 anemones m^{-2} treatment). We only considered the bottom area (0.1 m^2) of plastic tanks in order to achieve the initial stocking densities. Stocked anemones were fed every 3 days, as preliminary tests verified that this was the average time required for complete food digestion. The number of prey supplied to each tank was calculated in accordance with the results of the experiment described above to determine optimal prey concentration. The following formula was used to calculate the number of prey to provide based on the number of anemones of each size class per tank: (number of XS anemones x 100 prey) + (number of S anemones x 300 prey) + (number of M anemones x 900 prey) + (number of L anemones x 1500). The number of prey was adjusted after counting the number of anemones in each tank. The adjustment was derived from the previous formula, along with results from anemone counts. Anemones were counted and categorized in size classes 15 (t_{15}), 30 (t_{30}), 45 (t_{45}) and 60 (t_{60}) days after the beginning of the experiment (t_0). Every week the bottom of the tanks was siphoned with a pipette to avoid aspiration of small anemones and 50% of the water was replaced. Water quality parameters were monitored as described above for the culture tank. Anemone's clonal propagation was determined by the following ratio: number of anemones at t_x / number of anemones at t_0. Average anemone biomass (wet weight) per replicate was determined using the regression equations referred above for the classification of anemone's size classes (see Fig. 3.1). In order to facilitate the estimation of anemones' biomass in each culture tank, the number of specimens in each size class was counted and multiplied by the average wet weight of each size class. The average wet weights were also calculated using the results obtained from the size class determination essays (XS) 7.37 mg; S) 52.77 mg; M), 213.38 mg; and L 489.21 mg).

3.2.5 Statistical analysis

Simple regression analysis was used to determine the relation between wet weight and dry weight, as well as between dry weight and PDD. Anemone's biomass production and clonal propagation were analysed for the following factors: initial anemone stocking density (2 levels), light regimes (2 levels), water temperature (2 levels), diet (2 levels) and time (4 levels). As measurements were taken from the same tanks at t_{15}, t_{30}, t_{45} and t_{60}, repeated measures 4-way ANOVA (rm-ANOVA) was used. Assumptions of rm-ANOVA were tested and whenever necessary data was transformed (square root) to meet the assumptions (Zar 1998). Tukey's HSD test was used when rm-ANOVAs revealed significant differences ($p<0.05$). All statistical analyses were performed using STATISTICA 8.0 software (StatSoft Inc.).

3.3 Results

3.3.1 Size class determination

A. pallida displayed an average water content of 84.9%. A positive and significant linear association was observed between anemone wet and dry weight (Fig. 3.1A; $F = 1847.435$, $p<0.0001$). A positive and significant logarithmic association was also observed between dry weight and pedal disk diameter (PDD) (Fig. 3.1B; $F = 433.925$, $p<0.0001$). These results supported the use of both wet weight and PDD for all subsequent analysis in the present study to assess *A. pallida* growth.

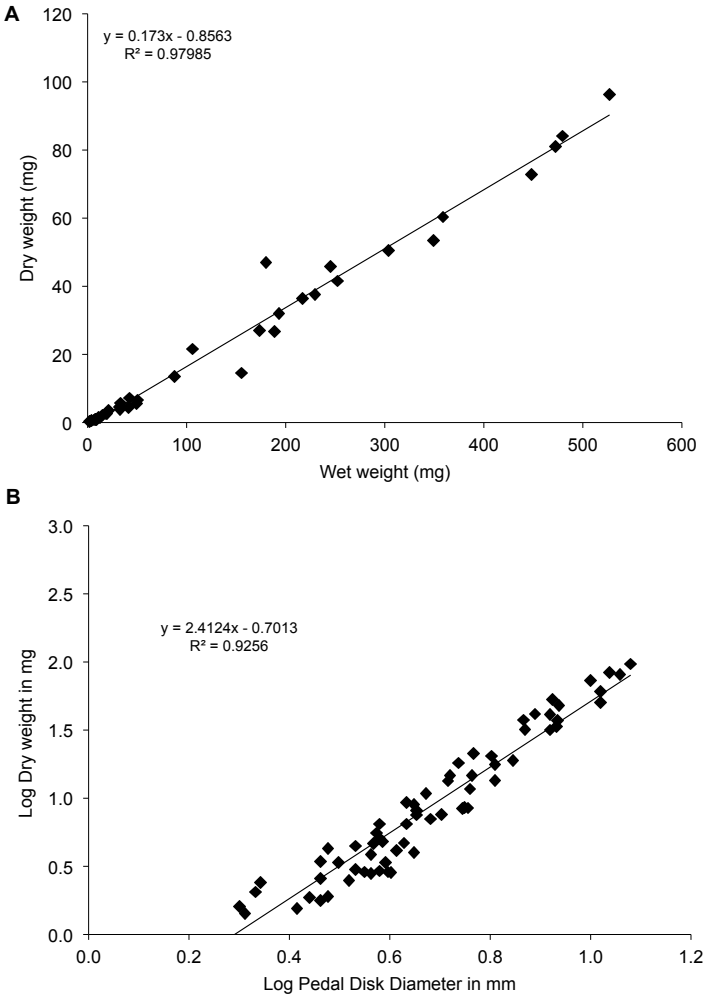

Fig. 3.1 Relationship between dry weight and wet weight (a) and the logarithm of dry weight and the logarithm of the pedal disk diameter (b) of the sea anemone *A. pallida*. Linear (a) and logarithmic (b) regression lines are presented.

3.3.2 Determination of optimal prey concentration

Prey ingestion observed for the different concentrations are summarized in Table 3.1. For XS anemones, the only prey concentration that resulted in feeding behaviours different from partial ingestion with regurgitation was 0.3 nauplii mL^{-1}. For S specimens, regurgitation or total ingestion was only avoided when a prey concentration of 1 nauplii mL^{-1} was provided. For M anemones, 100% of total ingestion and 100% of partial ingestion with regurgitation were observed for concentrations of 2 and 4 nauplii mL^{-1}, respectively. For L anemones, regurgitation was only avoided with a prey concentration of 5 nauplii mL^{-1}.

Table 3.1 Observations of feeding behaviours displayed by different size classes of *Aiptasia pallida* when provided different concentrations of newly hatched *Artemia* nauplii.

A. pallida size class	Prey concentrations (nauplii mL^{-1})	Feeding behaviour (%)
Extra small	0.3	PIR (33.3) TI (33.3) TIR (33.3)
	0.6	PIR (100)
	1	PIR (100)
Small	0.6	TI (100)
	1	PI (100)
	1.3	PI (33.3) PIR (66.6)
Medium	2	TI (100)
	3	TI (66.6) TIR (33.3)
	4	PIR (100)
Large	5	PI (33.3) TI (66.6)
	6.6	PI (33.3) PIR (33.3) TIR (33.3)
	8.3	PIR (66.6) TI (33.3)

Feeding behaviours: partial ingestion (PI), partial ingestion with regurgitation (PIR), total ingestion (TI), total ingestion with regurgitation (TIR).

3.3.3 Effect of initial stocking density, light regime, water temperature and diet on clonal propagation and biomass production

Clonal propagation ratios varied with tested factors throughout the experiment. At t_{60}, significantly higher propagation ratio (p<0.01; 10.1 ± 1.0, average ± SD) was observed in tanks initially stocked with lower anemone density (90 anemones m^{-2}) compared to tanks with higher anemone density (7.9 ± 1.0; 180 anemones m^{-2}). Significantly higher propagation ratios (p<0.01) were also observed with higher water temperature (ratio at 22 ºC = 7.7 ± 0.7; ratio at 26 ºC = 10.3 ± 1.3), as well as in anemones cultured in total darkness (p<0.01; ratio in Lt = 6.9 ± 0.9; ratio in D = 11.1 ± 1.0) and with nauplii as prey (p<0.01; nauplii = 10.5 ± 1.2; metanauplii = 7.5 ± 0.8). When accounting for the interaction of all factors, significant interactions were observed between light regime, temperature and prey. Anemones reared in the dark, at 26 ºC and fed with nauplii recorded propagation ratios significantly higher than other anemones (ratio of 18.9 at t_{60} for 90 anemones m^{-2} and 13.7 at t_{60} for 180 anemones m^{-2}; p<0.01 for both initial stocking densities). In contrast, the lowest propagation ratios at t_{60} were recorded for anemones exposed to light, reared at 22 ºC and fed with metanauplii (4.8 at for 90 anemones m^{-2} and 5.3 at for 180 anemones m^{-2}). No significant differences were observed when considering three or more tested factors (p>0.17), apart from the interaction between water temperature, light and diet (p<0.01).

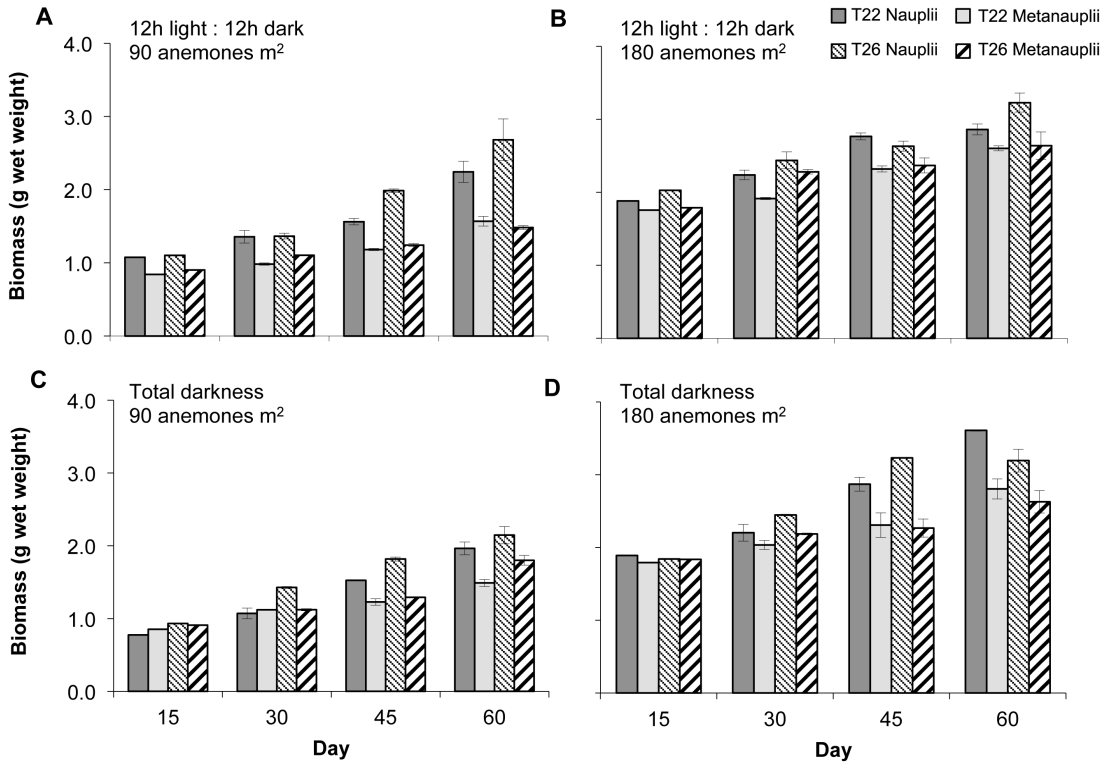

Fig. 3.2 Variation of biomass (g of wet weight) of *A. pallida* per tank throughout the experiment when reared with different conditions (light – a, b; dark – c, d; 90 anemones m^{-2} – a, c; 180 anemones m^{-2} – b, d).

For both light regimes and initial stocking density treatments, the highest biomass recorded at t_{60} was achieved for anemones cultured at 26 ºC and fed with nauplii (Fig. 3.2). The only exception was observed for the treatments in total darkness, higher initial anemone stocking density, fed with nauplii and water temperature of 22 or 26 ºC (Fig. 3.2d). However, no significant differences were observed between these two treatments (Tukey's HSD, p = 0.92). Water temperature induced significant changes on biomass production (df = 1, F = 13.38, p<0.01), in contrast to light regime (df =1, F = 0.02, p = 0.88). Significant interactions between light, diet, water temperature and time were observed for biomass production (df = 3, F = 4.52, p<0.01). At t_{60}, the only significant factors were initial anemone stocking density (df = 1, F = 191.3, p<0.01) and prey (df = 1, F = 68.8, p<0.01). Lower biomass production was observed in tanks with lower initial anemone stocking density and also observed when metanauplii were provided. The highest biomass production for the higher initial anemone stocking density was recorded for the treatment exposed to dark conditions (3.61 mg wet weight, at 22 ºC and fed nauplii; Fig. 3.2d). In contrast, for the lower initial anemone stocking density the highest biomass production was observed for the tank exposed to a 12 h Lt: 12 h D (2.7 mg wet weight; 26 ºC and fed nauplii; Fig. 3.2a).

The average proportion of different anemone size classes per treatment is presented in Fig. 3.3. A noteworthy higher abundance of XS anemones was observed in all tanks (66.7 to 94.7%), while L anemones were the scarcest. Medium and L anemones were almost twice as abundant in light as in dark treatments (average cumulative percentage: Lt – 2.3%, D – 1.3%).

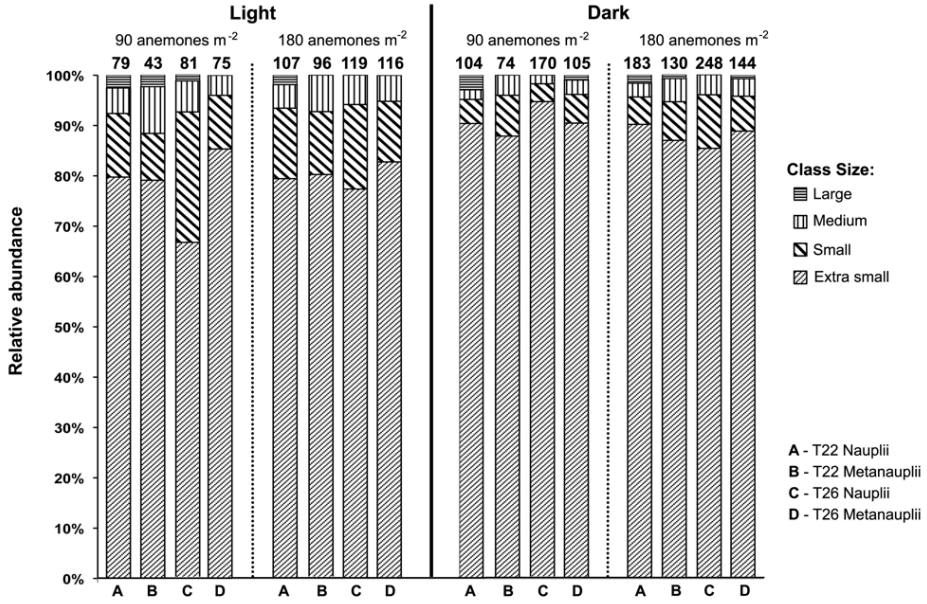

Fig. 3.3 Average proportion of *A. pallida* of different size classes after 60 days (t_{60}) for different light, initial stocking density, water temperature and diet conditions. Total number of anemones is also presented above each bar (a, 22 ºC and nauplii; b, 22 ºC and metanauplii; c, 26 ºC and nauplii; d, 26 ºC and metanauplii).

3.4 Discussion

Anemones are soft-bodied invertebrates that are able to store significant amounts of water in their body cavity. Therefore, the precise measurement of anemones using non-destructive techniques is a challenging task. Different morphological criteria have been used to estimate anemone size. For instance, Clayton Jr and Lasker (1985) used the oral disk diameter for measuring *A. pallida*, while Hand and Uhlinger (1992) used the column length to measure *Nematostella vectensis* Stephenson, 1935. In the case of *Actinia equina*, Chomsky et al. (2004b) used the pedal disk diameter (PDD). Results observed for *A. pallida* are similar to those Chomsky et al. (2004b) observed for *A. equina.* Our results indicate that PDD is a good morphological feature for non-destructive measurement of *A. pallida* biomass. In addition, due to anemone retraction and/or water expulsion from the coelenteron, the measurement of PDD is simpler to accomplish and less prone to variation than other methods commonly used, such as, wet weight, oral disk diameter and column length. The authors recommend that future studies addressing other species of anemones might also evaluate the suitability of using PDD to determine anemone biomass.

Previous studies that maintained live stocks of anemone and/or stimulated anemone growth, either fed the anemones to repletion or omitted any information concerning the amount of prey provided to stocked specimens (Cook et al. 1988, Chomsky et al. 2004a, Chomsky et al. 2004b). Feeding anemones to repletion requires the provision of extra food, which wastes unnecessary food resources and accelerates water quality deterioration. When anemones ingest excess food they often regurgitate, which also contributes to the deterioration of water quality. Therefore, the amount of food provided should be adjusted to the number and size of anemones present in culture tanks, thus avoiding food wastage, regurgitation and deterioration of water quality. A scenario yielding ideal results should be between partial and total ingestion without regurgitation. Total ingestion may suggest that anemones are not fed to repletion while partial ingestion indicates food wastage. In the present study, the most suitable prey concentrations per anemone size class that avoided partial ingestion with regurgitation and/or total ingestion scenarios were 0.3, 1, 3 and 5 nauplii L^{-1} for XS, S, M and L sized anemones, respectively.

The optimization of prey concentration was critical to assure that during the experimental trials enough food was being supplied to *A. pallida*. Higher propagation ratio and biomass production of cultured *A. pallida* were observed when higher water temperature was used (26 ºC) together with total darkness conditions. This was not unexpected as *A. pallida* commonly occurs in tropical regions, to which this species is well adapted. Lower water temperature commonly favours the propagation of temperate species, such as *A. equina* (Chomsky et al. 2004a). The same rationale may be used to explain why the highest water temperature (26 ºC) also favoured the production of *A. pallida* biomass. These results suggest that in order to maximize biomass production one should adjust water temperature to that of the latitudinal distribution of the target anemone species and minimize thermal stress. Higher propagation ratios were also obtained in tanks with lower initial anemone stocking densities, suggesting that space availability is an important factor to consider when targeting the mass culture of anemones. Our results also suggest that initial anemone density can negatively affect the optimization of biomass production. In some particular culture conditions, a decrease in biomass production was observed. This was probably associated with elevated rates of pedal laceration that increased the numbers of small anemones (see Fig. 3.3).

A. pallida commonly have zooxanthellae and thus can benefit from light to survive without heterotrophic feeding (Bachar et al. 2007, Venn et al. 2008). On the other hand, when this species is kept under total darkness it eventually becomes azooxanthellate and loses any energetic income provided by photosynthetic endosymbionts. For this reason, one should expect light to benefit the production of *A. pallida*, both in numbers and biomass. However, previous studies reported no differences on propagation ratios between *Anthopleura elegantissima* exposed to light or kept in total darkness (Sebens 1980), nor between zooxanthellate and azooxanthellate *A. pallida* (Clayton Jr & Lasker 1985). In this study *A. pallida* reared in total darkness generally presented higher propagation ratios and biomass than those reared in light. The higher propagation ratios recorded for anemones in the absence of light may be associated with an enhancement of pedal laceration promoted by anemone displacement within the rearing tank while searching for suitable light conditions (Geller et al. 2005). This behaviour enhances propagation ratios, as peduncle laceration is likely to occur when *A. pallida* moves.

Both nauplii and metanauplii were readily ingested by *A. pallida*, although propagation ratios and biomass increase was favoured by nauplii. These results may be explained by the smaller body size displayed by nauplii, which can make them more vulnerable to predation by *A. pallida*, or by a higher nutritional quality of nauplii than metanauplii. Nevertheless, the present study opens good perspectives for the potential use of live feed leftovers from marine hatcheries.

Large scale production of monoclonal *A. pallida*, as well as other *Aiptasia* species, cultured under optimal and replicable conditions may allow researchers to have a regular supply of high quality and genetically identical specimens to be used as biological models in several research fields, namely for studying cnidarian-dinoflagellate symbiotic relationships (Weis et al. 2008). Additionally, researchers screening for new marine natural products from anemones can eliminate two of the most serious problems commonly faced in this research field: 1) the loss of the source – as anemones will continuously be available under culture; and 2) reproducibility - as monoclonal specimens produced under exactly the same conditions can be used for future trials along the pipeline for the discovery of new drugs (Li & Vederas 2009, Rocha et al. 2011, Leal et al. 2012). The present study provides information that will assist in the development of large scale, monoclonal production of *A. pallida*. However, further research is necessary to understand if the production of these organisms in the absence of light (as suggested by this study) will influence their physiology, gene expression or metabolic pathways once they become infected, or re-infected, by zooxanthellae. Furthermore, the monoclonal production of *A. pallida* using the effluents of industrial hatcheries should also be tested in future studies. Besides the advantage of re-using

live feed leftovers, *A. pallida* may also remove organic nutrients from the effluent. Symbiotic anemones harbour photosynthetic endosymbionts in their tissues, which need nutrients to produce photosynthetates. Eventually, by up taking these nutrients, anemone's endosymbionts will decrease their load in effluents and contribute to improve water quality. This last aspect of effluent bio-remediation will only be possible if light is either naturally available or supplied to the anemones, in order to sustain their photosynthetic endosymbionts.

In conclusion, to optimize the monoclonal production of *A. pallida*, the present results suggest the use of the following conditions: 26 ºC, total darkness and *Artemia* nauplii. Nevertheless, the duration of this study was only 60 days, and the optimal conditions for long-term culture of *A. pallida* remain to be determined. The initial anemone stocking density to be used should be adjusted to the purpose of the monoclonal production: 1) higher stocking densities to enhance anemone asexual reproduction and thus result in higher number of small anemones (of paramount importance for the culture of newly metamorphosed ornamental sea slugs *A. stephanieae*); or 2) lower stocking densities to promote biomass production.

3.5 Acknowledgments

Miguel C. Leal and Sofia Engrola acknowledge financial support by Fundação para a Ciência e Tecnologia, Portugal, through grants SFRH/BD/63783/2009 and SFRH/BPD/49051/2008, respectively. We also thank Nancy Tenenbaum for revising the manuscript and three anonymous reviewers for their comments and suggestions to improve the manuscript.

3.6 References

Bachar A, Achituv Y, Pasternak Z, Dubinsky Z (2007) Autotrophy *versus* heterotrophy: The origin of carbon determines its fate in a symbiotic sea anemone. J Exp Mar Biol Ecol 349:295-298

Carroll D, Kempf S (1990) Laboratory culture of the aeolid nudibranch *Berghia verrucicornis* (Mollusca, Opisthobranchia): some aspects of its development and life history. Biol Bull 179:243-243

Chen C, Soong K, Chen C (2008) The smallest oocytes among broadcast-spawning actiniarians and a unique lunar reproductive cycle in a unisexual population of the sea anemone, *Aiptasia pulchella* (Anthozoa:Actiniaria). Zool Stud 47:37-45

Chomsky O, Kamenir Y, Hyams M, Chadwick-Furman N (2004a) Effects of temperature on growth rate and body size in the Mediterranean sea anemone *Actinia equina*. J Exp Mar Biol Ecol 313:63-73

Chomsky O, Kamenir Y, Hyams M, Dubinsky Z, Chadwick-Furman N (2004b) Effects of feeding regime on growth rate in the Mediterranean sea anemone *Actinia equina* (Linnaeus). J Exp Mar Biol Ecol 299:217-229

Clayton Jr W, Lasker H (1985) Individual and population growth in the asexually reproducing anemone *Aiptasia pallida* Verrill. J Exp Mar Biol Ecol 90:249-258

Cook C, D'Elia C, Muller-Parker G (1988) Host feeding and nutrient sufficiency for zooxanthellae in the sea anemone *Aiptasia pallida*. Mar Biol 98:253-262

Davy S, Cook C (2001) The relationship between nutritional status and carbon flux in the zooxanthellate sea anemone *Aiptasia pallida*. Mar Biol 139:999-1005

Falkowski P, Dubinsky Z, Muscatine L, Porter J (1984) Light and the bioenergetics of a symbiotic coral. BioScience 34:705-709

Geller J, Fitzgerald L, King C (2005) Fission in sea anemones: integrative studies of life cycle evolution. Integr Comp Biol 45:615-622

Goulet T, Cook C, Goulet D (2005) Effect of short-term exposure to elevated temperatures and light levels on photosynthesis of different host-symbiont combinations in the *Aiptasia pallida*/*Symbiodinium* symbiosis. Limnol Oceanogr 50:1490-1498

Hand C, Uhlinger K (1992) The culture, sexual and asexual reproduction, and growth of the sea anemone *Nematostella vectensis*. Biol Bull 182:169-176

Kristof A, Klussmann-Kolb A (2010) Neuromuscular development of *Aeolidiella stephanieae* Valdez, 2005 (Mollusca, Gastropoda, Nudibranchia). Front Zool 7:5

Kuo J, Chen M-C, Lin C-H, Fang LS (2004) Comparative gene expression in the symbiotic and aposymbiotic *Aiptasia pulchella* by expressed sequence tag analysis. Biochem Biophys Res Commun 318:176-186

Leal MC, Puga J, Serôdio J, Gomes NCM, Calado R (2012) Trends in the Discovery of New Marine Natural Products from Invertebrates over the Last Two Decades – Where and What Are We Bioprospecting? PLoS One 7:e30580

Li JW-H, Vederas JC (2009) Drug Discovery and Natural Products: End of an Era or an Endless Frontier? Science 325:161-165

Marino A, Valveri V, Muia C, Crupi R, Rizzo G, Musci G, Laspada G (2004) Cytotoxicity of the nematocyst venom from the sea anemone *Aiptasia mutabilis*. Comp Biochem Physiol C 139:295-301

Mercier A, Pelletier É, Hamel J-F (1997) Effects of butyltins on the symbiotic sea anemone *Aiptasia pallida* (Verrill). J Exp Mar Biol Ecol 215:289-304

Mobley K, Gleason D (2003) The effect of light and heterotrophy on carotenoid concentrations in the Caribbean anemone *Aiptasia pallida* (Verrill). Mar Biol 143:629-637

Muller-Parker G (1985) Effect of feeding regime and irradiance on the photophysiology of the symbiotic sea anemone *Aiptasia pulchella*. Mar Biol 90:65-74

Olivotto I, Planas M, Simões N, Holt G, Avella M, Calado R (2011) Advances in breeding and rearing marine ornamentals. J World Aquacult Soc 42:135-166

Rocha J, Peixe L, Gomes NCM, Calado R (2011) Cnidarians as a Source of New Marine Bioactive Compounds—An Overview of the Last Decade and Future Steps for Bioprospecting. Mar Drugs 9:1860-1886

Ruppert E, Fox R, Barnes R (2003) Invertebrate Zoology: A Functional Approach, Brookes Cole, Belmont, USA, 1008 pp.

Sebens K (1980) The regulation of asexual reproduction and indeterminate body size in the sea anemone *Anthopleura elegantissima* (Brandt). Biol Bull 158:370-382

Sunagawa S, Wilson EC, Thaler M, Smith ML, Caruso C, Pringle JR, Weis VM, Medina M, Schwarz JA (2009) Generation and analysis of transcriptomic resources for a model system on the rise: the sea anemone *Aiptasia pallida* and its dinoflagellate endosymbiont. BMC genomics 10:258

Thorington G, Hessinger D (1996) Efferent mechanisms of discharging cnidae: I. Measurements of intrinsic adherence of cnidae discharged from tentacles of the sea anemone, *Aiptasia pallida*. Biol Bull 190:125-138

Venn A, Loram J, Douglas A (2008) Photosynthetic symbioses in animals. J Exp Bot 59:1069-1080

Weis V, Davy S, Hoegh-Guldberg O, Rodriguez-Lanetty M, Pringle J (2008) Cell biology in model systems as the key to understanding corals. Trends Ecol Evol 23:369-376

Zar J (1998) Biostatistical Analysis, Vol. Prentice Hall International, New Jersey, 663 pp.

Chapter 4 Effect of light, temperature and diet on the fatty acid profile of the tropical sea anemone *Aiptasia pallida*

Abstract

Sea anemones within genus *Aiptasia* are used as biological models for research and as a prey for the culture of the highly priced ornamental nudibranch *Aeolidiella stephanieae*. Symbiotic *Aiptasia* display a remarkable trophic plasticity, being able to fulfil their energetic demands heterotrophically and autotrophically. Consequently, they display a highly variable fatty acid (FA) profile. The objective of the present study was to analyse how light regime (12 h light: 12h dark *versus* 24 h darkness), water temperature (22 *versus* 26 ºC) and diet (*Artemia* nauplii *versus* enriched *Artemia* metanauplii) affect the FA composition of *A. pallida*. The FA profile of wild specimens was also analysed. The dominant FAs of cultured *A. pallida* were 16:0, 18:1*n*-9 and 22:6*n*-3. Higher FA levels were recorded when anemones were exposed to light, with this factor explaining the largest amount of variation in the composition of FA profiles. Cultured *A. pallida* that best mimicked wild anemones were obtained when using a regular light regime, *Artemia* metanauplii and 22 ºC water temperature. Higher FA levels were obtained at a higher temperature and by providing nauplii to cultured anemones. The present study also indicated that *A. pallida* has the potential to recycle nutrients in marine aquacultures.

Keywords

Heterotrophy; Autotrophy; DHA; Anemone production.

Published: Leal MC, Nunes C, Kempf S, Reis A, Silva TL, Serôdio J, Cleary DFR, Calado R (2013) Effect of light, temperature and diet on the fatty acid profile of the tropical sea anemone *Aiptasia pallida*. Aquaculture Nutrition 19: 818-826 (doi: 10.1111/anu.12028)

4.1 Introduction

The tropical sea anemone *Aiptasia pallida* (Agassiz in Verrill, 1864) is commonly used as a model organism in marine biology research, particularly for studying photosynthetic symbiosis, marine venoms and toxins (Marino et al. 2004, Weis et al. 2008). Furthermore, it is used by breeders of marine ornamental species culturing the pricy aeolid nudibranch *Aeolidiella stephanieae* (erroneously referred to in the literature and in the marine aquarium trade as *Berghia verrucicornis*). Curiously, the bottleneck impairing the large-scale production of *A. stephanieae* has not been a zootechnical constraint associated with its life cycle, but rather the absence of a regular and abundant supply of their only prey – *Aiptasia* (Olivotto et al. 2011).

Aiptasia popularity as a biological model is partly associated with the ease of culturing and propagating this species under laboratory conditions. To some extent, this easiness of propagation using very simple protocols and culture systems is a consequence of their remarkable trophic plasticity (Bachar et al. 2007). *A. pallida* is a symbiotic anemone and, as other symbiotic cnidarians, is able to fulfil their energetic demands both heterotrophically, by preying on zooplankton, and autotrophically, through the photosynthates produced and translocated by their endosymbiotic dinoflagellates – the zooxanthellae (Ruppert et al. 2003, Bachar et al. 2007). Some of the most relevant biochemical compounds resulting from this carbon flow are fatty acids (FA), which are known to play important structural roles (e.g. in cell membranes) and act as energy reserves (Richier et al. 2010). In other words, *Aiptasia* can acquire FA heterotrophically through external food sources, as well as autotrophically through the photosynthates produced by their photosynthetic endosymbionts (Bachar et al. 2007, Leal et al. 2012a). This feeding plasticity, also known as mixotrophy, is an important adaptation to unpredictable trophic scenarios. Important FAs, such as 18:2*n*-6 (linoleic acid, LA) and 18:3*n*-3 (alpha-linolenic acid, ALA), cannot be synthesized *de novo* by most marine invertebrates without photosynthetically-active endosymbionts and are important precursors of other *n*-6 and *n*-3 polyunsaturated and highly unsaturated fatty acids (PUFA and HUFA, respectively) (Dalsgaard et al. 2003, Papina et al. 2003, Bachok et al. 2006). These particular FAs (LA and ALA) and their derivatives, such as arachidonic acid (ARA, 20:4*n*-6), eicosapentaenoic acid (EPA, 20:5*n*-3) and docosahexaenoic acid (DHA, 22:6*n*-3), are essential constituents of heterotrophic organisms. Thus, while heterotrophy plays a key role as an important source of these important FAs, so does autotrophy through the production and translocation of photosynthates to cnidarian host tissues.

The objective of the present study was to investigate the effects of light regime, water temperature and diet on the FA profile of *A. pallida*. The FA profile of wild specimens was used as control. The following hypotheses were tested concerning the cnidarian holobiont: (i) the absence of light decreases FA abundance and composition, (ii) higher water temperature shifts the FA profile (e.g. by promoting FA synthesis and/or decreasing FA catabolism) and (iii) food quality affects the FA composition of *A. pallida*. The rationale for this approach was to test if the supply of artificial light and heat to mimic natural sunlight and water temperature are essential to successfully culture *Aiptasia* with a FA profile comparable to that of wild specimens. While this approach will certainly increase production costs, FA profiles displayed by cultured *Aiptasia* can be of paramount importance if they are to be used as prey for culturing highly priced ornamental sea slugs or other academic or commercial applications (Olivotto et al. 2011). The same rationale is also valid to test the effect of depriving cultured anemones from light or exposing them to lower water temperatures, as this approach would decrease production costs. The effect of live feed leftover diets (e.g. live prey daily drained from larviculture tanks) on the FA profile of cultured anemones was also investigated, as *A. pallida* is commonly produced using pricy newly hatched *Artemia* nauplii.

Therefore, by using live feed leftovers, particularly *Artemia* metanauplii, production costs of *A. pallida* will certainly be lower.

4.2 Materials and Methods

4.2.1 Husbandry of *Aiptasia pallida*

Monoclonal specimens of *A. pallida* (originating from a single individual) were held in a 250 L culture tank (1 m x 0.5 m x 0.5 m) filled with 5 µm filtered and UV-irradiated natural seawater and placed outdoors under natural sunlight and photoperiod. Small ceramic tiles (20 mm x 20 mm) were placed in the tank to allow large numbers of *A. pallida* to be quickly collected from the culture tank and to allow them to be easily detached without inducing any mechanical damage. Water temperature was kept at 26 ºC by using a 300 W submersible electrical heater equipped with a thermostat. Salinity was kept stable at 35 ± 1 g L^{-1} by daily adding freshwater to compensate for any losses due to evaporation. Water circulation was provided by airlifts placed at each corner of the culture tank. Ammonia and nitrite were kept under detectable levels, while nitrate was recorded between 10 and 20 mg L^{-1} and pH at 8.0 ± 0.1 (all parameters were determined using colorimetric tests). Anemones were fed every 3 days with newly hatched *Artemia* nauplii (5 nauplii mL^{-1}) and allowed to freely propagate over six months prior to the start of the experiments. The tank bottom was siphoned weekly together with a 25% partial water change.

4.2.2 Experimental design and collection of wild anemones

All experimental trials were performed in quadruplicate using 3 L plastic tanks (0.1 m x 0.1 m x 0.3 m) for each combination of the following factors: light (12 h light: 12 h darkness *versus* continuous darkness), temperature (22 *versus* 26 ºC) and diet (*Artemia* nauplii (nauplii) *versus Artemia* metanauplii enriched with *Tetraselmis chui* and *Isochrysis galbana* (metanauplii)). A total of 32 tanks were used. The anemones cultured under regular light regime, 26 ºC water temperature and fed nauplii were also used as an initial control, as these were the same conditions used for the husbandry of *A. pallida*. Artificial light was supplied by T5 fluorescent light tubes (3 x 30 W). The highest water temperature (26 ºC) was achieved by placing the tanks immersed in a water bath, which had a 300 W submersible electrical heater equipped with a thermostat. The other tanks were at room temperature (22 ºC). All tanks were initially stocked with 9 sea anemones each. Stocked anemones were fed every three days (see Leal et al. (2012b) for details) and prey concentration delivered to each tank was calculated based on the number and size class of anemones observed in each tank and adjusted at day 15, 30 and 45 (see Leal et al. (2012b) for details). Every week the bottom of the tanks was siphoned with a pipette to avoid removal of small anemones and 50% of the water was replaced. Water circulation was provided by airlifts in the corner of the tanks. Water quality parameters were monitored as described above for the communal culture tank.
After 60 days, 10 anemones were randomly collected from each tank for each treatment (n = 40 anemones per treatment), rinsed with distilled water, pooled (total of four composite samples per treatment) and stored in liquid nitrogen for later biochemical analysis. In the last three days prior to the end of the experiment, cultured anemones were not fed, in order to assure that they would display empty gastric cavities at the time of sampling. This was determined in preliminary tests in order to avoid having any undigested prey biasing the biochemical analysis of anemone's tissue. Four samples of each experimental diet (nauplii and metanauplii) were also collected and stored for later biochemical analysis as previously described.

A total of 22 specimens of "wild-type" *A. pallida* were collected from dock pilings and/or reef rock and sponge surfaces in Buttonwood Bay, Key Largo and Crawl Key (Florida Keys, USA) during May 2008. Collected anemones were transported to Auburn University (Alabama, USA) where they were rinsed in distilled water, frozen, lyophilized and shipped to Instituto Nacional de Engenharia, Tecnologia e Inovação (Lisbon, Portugal) for further biochemical analysis (see below).

4.2.3 Fatty acid analysis

FA extraction and preparation of methyl esters were carried out according to Lepage and Roy (1986) and modified by Cohen et al. (1988). Freeze-dried samples (100 mg) were transmethylated with 5 mL of methanol/acetyl chloride (95:5 v/v). The mixture was sealed in a light-protected Teflon-lined vial under nitrogen atmosphere and heated at 80 °C for 1 h. The vial contents were then cooled, diluted with 1 mL of deionised water and extracted with 2 mL of n-heptane. The heptane layer was dried over Na_2SO_4, evaporated until dry under a nitrogen atmosphere and redissolved in heptane, which contained the methyl esters. The methyl esters were then analysed by gas-liquid chromatography on a VARIAN 3800 gas-liquid chromatograph (Varian, Palo Alto, CA, USA), equipped with a flame ionisation detector. Separation was carried out on a 0.32 mm x 30 m fused silica capillary column (film 0.32 µm) Supelcowax 10 (SUPELCO, Bellafonte PA, USA) with helium as carrier gas at a flow rate of 1.3 mL min^{-1}. The column temperature was programmed at an initial temperature of 200°C for 10 min, then increased at 4 °C min^{-1} to 240°C and held there for 16 min. The injector and detector temperatures were 250 and 280°C, respectively, and the split ratio was 1:100. Peak identification was carried out using known standards (Nu-Chek-Prep. Elysian. USA). Peak areas were determined using Varian software, and the fatty acid 17:0 was used as an internal standard. The detection limit for the fatty acids analysed was 0.01 µg mg^{-1} dry weight (dw).

4.2.4 Statistical analysis

FAs of the provided diets (nauplii and metanauplii) were compared using a Students' *t* test after examining assumptions of homogeneity of variances and homoscedasticity. The effect of each treatment (light regime, temperature and diet) and interaction between treatments were tested for significant variation in the FA composition of *A. pallida* using a three-way ANOVA. Tukey's HSD test was used when significant differences were observed ($p<0.05$).

Data matrices of FA abundance were $\log_{10}$ (x + 1) transformed and distance matrices constructed using the Euclidean index with the vegdist function in the vegan package (Oksanen et al. 2009) in R. Variation in FA composition among treatments (temperature, food and light regime) was assessed with Principal Coordinates Ordination (PCO) using the cmdscale function in R with the euclidean distance matrix as input. The PCO was used to describe overall relationship among *A. pallida* from different treatments based on their FA profile. Variation in composition among treatments was tested for significance using the adonis function in vegan. The adonis function is an analysis of variance with distance matrices using permutations that partitions distance matrices among sources of variation; in this case, temperature, food and light regime. It is analogous to PERMANOVA (Anderson 2001) and an alternative to parametric MANOVA when the response variable is multivariate and deviates from multivariate normality, as is often the case for compositional data. In the adonis analysis, the euclidean matrix of FA composition was the response variable with light regime, temperature and diet as independent variables. We also included the interaction terms between light regime, temperature and diet. The number of permutations was set at 999; all other arguments used the default values set in the function. Detailed descriptions of the functions can be found in R and online in the reference manuals (e.g. http://cran.r-project.org/web/packages/vegan/index.html; checked 2012 04 08).

4.3 Results

4.3.1 Fatty acid composition of diets

The total amount of FAs recorded in nauplii (111.51 ± 6.19 µg mg^{-1} dw) was nearly twice that of metanauplii, with most FAs being more abundant in nauplii (Table 4.1). ALA was the dominant FA in both diets (39.4 and 24.6% of the FA pool in nauplii and metanauplii, respectively), though it was significantly higher in nauplii (t = 40.13, df = 6, p<0.05). Other important FAs in both diets were oleic acid (OA, 18:1*n*-9; 17.2 and 17.1% of the FA pool in nauplii and metanauplii, respectively), palmitic acid (PA, 16:0; 12.8 and 12.3% of the FA pool in nauplii and metanauplii, respectively), and LA (6.7 and 6.4% of the FA pool in nauplii and metanauplii, respectively). The only FAs that were present in higher amounts in metanauplii were EPA, ARA and the two *n*-7 FAs (Table 4.1). Higher concentrations of saturated fatty acids (SFA), monounsaturated fatty acids (MUFA) and PUFA were observed in nauplii, while the HUFA and EPA/DHA were higher in metanauplii; however, the sum of EPA and DHA was only equivalent to approximately 1% of total FAs present in each diet.

Table 4.1 Fatty acid composition (µg mg^{-1} dry weight) of diets provided to *Aiptasia pallida* (*Artemia* nauplii (nauplii) and *Artemia* metanauplii enriched with *Tetraselmis chui* and *Isochrysis galbana* (metanauplii); mean ± SD, n = 4)

Fatty acid	Nauplii	Metanauplii
14:0	0.97 ± 0.00*	0.68 ± 0.03
16:0	14.32 ± 0.77*	7.94 ± 0.32
16:1*n*-7	2.21 ± 0.64	3.08 ± 1.66
18:0	7.55 ± 0.52*	6.00 ± 0.33
18:1*n*-7	6.65 ± 0.36*	7.48 ± 0.04
18:1*n*-9	19.15 ± 0.96*	11.01 ± 0.19
18:2*n*-6	7.51 ± 0.29*	4.14 ± 0.02
18:3*n*-3	43.97 ± 1.69*	15.86 ± 0.24
18:3*n*-6	1.21 ± 0.04*	0.46 ± 0.01
20:4*n*-6	0.49 ± 0.07*	1.10 ± 0.03
20:5*n*-3	1.64 ± 0.11*	2.82 ± 0.21
22:6*n*-3	0.32 ± 0.05	0.29 ± 0.02
Σ SFA[1]	23.55 ± 1.49*	15. 39 ± 0.58
Σ MFA[2]	29.84 ± 2.11*	22.71 ± 1.78
Σ PUFA[3]	55.22 ± 2.55*	21.71 ± 0.06
Σ HUFA[4, 5]	2.91 ± 0.05*	4.72 ± 0.28
Σ *n*-3	48.26 ± 2.07*	20.15 ± 0.04
Σ *n*-6	9.87 ± 0.54*	6.28 ± 0.26
n-3 / *n*-6	4.89 ± 0.06*	3.21 ± 0.14
EPA / DHA	5.30 ± 1.22	9.68 ± 1.39
Σ Total	111.51 ± 6.19*	64.53 ± 2.13

With the exception of DHA (22:6*n*-3), only the fatty acids whose content exceeds at least 1% in nauplii and metanauplii are displayed. Significant differences among diets (p<0.05) are marked in the nauplii column (*).

[1] Saturated fatty acids: 12:0, 14:0, 16:0, 18:0, 20:0, 22:0.

[2] Monounsaturated fatty acids: 14:1*n*-5, 16:1*n*-7, 18:1*n*-9, 18:1*n*-7, 20:1*n*-9, 22:1*n*-9, 24:1*n*-9.

[3] Polyunsaturated fatty acids: 18:2*n*-6; 18:3*n*-6; 18:3*n*-3; 20:2*n*-6; 20:3*n*-6; 20:3*n*-3, 22:2*n*-6.

[4] Highly unsaturated fatty acids: 20:4*n*-6; 20:5*n*-3; 22:4*n*-6, 22:5n-3, 22:6*n*-3.

[5] Although PUFA are defined as all fatty acids with ≥2 double bonds, in the present study HUFA (fatty acids with ≥4 double bonds) are not considered within ∑PUFA.

4.3.2 Fatty acid composition of cultured and wild *A. pallida*

The FA composition of cultured *A. pallida* is summarized in Table 4.2. For most of the treatments, HUFA were the dominant FAs, followed by SFA, MUFA and PUFA. In light treatments HUFA content was always 3.5 times greater than PUFA content. In contrast, anemones reared in total darkness and fed nauplii displayed a relatively similar HUFA and PUFA content. HUFA content was approximately twice the PUFA concentration in anemones fed metanauplii and reared in total darkness. PA, OA and DHA were the dominant FAs in *A. pallida* reared under artificial light. Although the content of these particular FA varied among the treatments with artificial light, the range of the contribution to the total FA pool was relatively similar (PA: 21.5 to 25.2%; OA: 10.2 to 13.3%; DHA: 22.9 to 27.8%). The anemones reared under artificial light displayed the highest levels of most FAs detected in this study. These differences were more evident when the FA profiles of light-reared anemones were compared to those of specimens cultured in the dark (the only exceptions being ALA, EPA and docosapentaenoic acid (DPA, 22:5*n*-3)). The EPA/DHA ratio was higher for treatments in the dark, as DHA levels were significantly lower in the absence of light (Table 4.2). Most FAs were present in higher levels when nauplii diet was provided (Table 4.2). The three most abundant FAs, PA (43.93 ± 9.75 µg mg^{-1} dw), OA (27.14 ± 4.37 µg mg^{-1} dw) and DHA (51.02 ± 1.60 µg mg^{-1} dw), displayed their highest concentrations in anemones cultured under light, 26 ºC water temperature and fed nauplii. The contribution of these FA to the total FA pool was 25.0, 21.5 and 13.3%, respectively for DHA, PA and OA. In this treatment, most FAs detected were present in higher levels than those recorded in wild *A. pallida* (Table 4.2).

DHA (15.12 ± 0.54 µg mg^{-1} dw; 22.9% of the total FA pool) and PA (14.08 ± 0.48 µg mg^{-1} dw; 21.3% of the total FA pool) were the two most abundant FAs in wild *A. pallida*. Other relatively important FAs were stearic acid (SA, 18:0; 7.8% of the total FA pool) and ARA (5.0% of the total FA pool). Total HUFA (28.59 ± 2.21 µg mg^{-1} dw) and SFA (22.47 ± 0.59 µg mg^{-1} dw) formed the bulk of total FAs from wild *A. pallida*, while MUFA (7.22 ± 0.29 µg mg^{-1} dw) and PUFA (7.87 ± 0.63 µg mg^{-1} dw) accounted for lower fractions of total FAs.

Ordinations of the first two PCO axes are shown in Fig. 4.1. The first PCO axis in Fig. 4.1a explains 89% of the variation in FA composition and is clearly related to the effect of light. The second axis explained an additional 6% of variation in FA composition and is primarily related to the effect of diet in the FA profiles of anemones. Fig. 4.1b shows the relative contribution of FAs in structuring variation in composition. Most FAs, however, were found in greater concentrations in anemones raised under light conditions, in particular 22:6*n*-3, 18:3*n*-6, 16:1*n*-7, 20:3*n*-6 and 14:0. FA 12:0 were found in every sample raised under light conditions, but were completely absent from samples raised in the dark. Nevertheless, the contribution of 12:0 to the total pool of FAs was always lower than 1%. Fig. 4.1c is a PCO ordination showing the first two PCO axes and explained 94% of the total variance in FA composition. In line with Fig. 4.1a, the first axis (variation explained: 80%) of Fig. 4.1c is primarily related to presence or absence of light. The second axis of Fig. 4.1c is related to variation in the profiles of wild anemones with low concentrations of 14:1*n*-5 and high concentrations of 22:2*n*-6. The treatment combination that most closely resembled wild anemones was a 12 h light photoperiod, temperature of 22 °C and metanauplii.

Table 4.2 Fatty acid composition (μg mg^{-1} dry weight) of *Aiptasia pallida* reared under different light regimes (L: 12 h light photoperiod; D: continuous darkness), water temperature (22 and 26 ºC) and provided with different diets (*Artemia* nauplii – Naup – and *Artemia* metanauplii enriched with *Tetraselmis chui* and *Isochrysis galbana* – Meta) and wild specimens (Wild) (mean ± SD; $n = 4$).

Fatty acid	L 22 Naup	L 26 Naup	L 22 Meta	L 26 Meta	D 22 Naup	D 26 Naup	D 22 Meta	D 26 Meta	Wild
14:0	4.83 ± 0.27^{a}	5.12 ± 1.52^{a}	3.06 ± 1.02^{b}	5.14 ± 0.14^{a}	0.75 ± 0.04^{c}	0.31 ± 0.01^{c}	0.37 ± 0.01^{c}	0.29 ± 0.05^{c}	1.79 ± 0.21
16:0	35.08 ± 1.00^{a}	43.93 ± 9.75^{a}	22.03 ± 7.32^{b}	40.56 ± 0.47^{a}	7.66 ± 0.15^{c}	4.81 ± 0.03^{c}	3.54 ± 0.07^{c}	3.59 ± 0.21^{c}	14.08 ± 0.48
16:1*n*-7	8.53 ± 0.50^{a}	8.71 ± 2.18^{a}	3.88 ± 3.19^{b}	7.70 ± 0.51^{a}	1.63 ± 0.03^{bc}	0.52 ± 0.27^{c}	0.37 ± 0.01^{c}	0.34 ± 0.03^{c}	1.95 ± 0.10
18:0	9.94 ± 0.15^{a}	14.75 ± 2.29^{b}	5.86 ± 1.82^{c}	12.33 ± 0.58^{ab}	3.66 ± 0.08^{cd}	3.61 ± 0.01^{cd}	2.99 ± 0.03^{d}	3.24 ± 0.10^{d}	5.13 ± 0.15
18:1*n*-9	19.94 ± 0.36^{a}	27.14 ± 4.37^{b}	10.44 ± 4.36^{c}	21.24 ± 0.89^{a}	6.89 ± 0.14^{cd}	5.18 ± 0.02^{d}	3.31 ± 0.06^{d}	3.14 ± 0.15^{d}	3.53 ± 0.17
18:1*n*-7	3.61 ± 0.05 ^{abd}	4.11 ± 0.71^{b}	2.26 ± 0.83^{cdefgh}	2.81 ± 0.11^{def}	2.40 ± 0.07^{efgh}	2.05 ± 0.02^{fgh}	1.63 ± 0.02^{gh}	1.55 ± 0.06^{h}	0.67 ± 0.03
18:2*n*-6	3.21 ± 0.02^{a}	5.08 ± 0.85^{b}	2.14 ± 0.84^{c}	4.08 ± 0.34^{ad}	2.83 ± 0.08^{ace}	2.58 ± 0.10^{ace}	1.47 ± 0.05^{f}	1.32 ± 0.07^{f}	2.09 ± 0.16^{a}
18:3*n*-3	6.07 ± 0.34^{a}	6.54 ± 1.05^{a}	1.50 ± 0.54^{b}	2.26 ± 0.09^{b}	9.94 ± 0.18^{c}	9.60 ± 0.15^{c}	4.31 ± 0.17^{d}	4.30 ± 0.28^{d}	0.15 ± 0.12
18:3*n*-6	5.10 ± 0.08^{ab}	5.71 ± 0.91^{b}	3.92 ± 1.42^{a}	5.20 ± 0.29^{ab}	0.97 ± 0.03^{c}	0.39 ± 0.01^{c}	0.33 ± 0.01^{c}	0.26 ± 0.02^{c}	4.92 ± 0.11
20:4*n*-6	3.73 ± 0.07^{abc}	4.49 ± 0.36^{d}	3.32 ± 0.39^{acd}	3.63 ± 0.40^{ad}	1.81 ± 0.06^{bc}	1.54 ± 0.01^{b}	1.54 ± 0.12^{b}	1.50 ± 0.08^{b}	3.17 ± 0.13
20:5*n*-3	3.89 ± 0.09	4.81 ± 0.60	3.15 ± 0.49	3.05 ± 0.33	4.09 ± 0.20	3.23 ± 1.97	3.87 ± 0.28	3.57 ± 0.26	2.66 ± 0.11
22:4*n*-6	7.28 ± 1.87^{abc}	10.85 ± 1.97^{d}	5.70 ± 1.38^{acd}	7.85 ± 1.16^{ad}	3.77 ± 0.40^{bc}	4.74 ± 0.42^{b}	3.85 ± 0.25^{b}	4.81 ± 1.63^{b}	5.25 ± 0.37
22:5*n*-3	2.55 ± 0.41^{abcdefgh}	3.27 ± 0.21^{bdefgh}	2.04 ± 0.55^{cefgh}	2.23 ± 0.35^{defgh}	2.52 ± 0.58^{efgh}	3.15 ± 0.42^{fgh}	2.74 ± 0.12^{gh}	2.83 ± 0.48^{h}	2.39 ± 1.31
22:6*n*-3	40.94 ± 2.94^{a}	51.02 ± 1.60^{b}	28.47 ± 7.91^{c}	36.87 ± 7.91^{ac}	5.66 ± 0.53^{d}	1.47 ± 0.54^{d}	2.13 ± 0.28^{d}	1.54 ± 0.21^{d}	15.12 ± 0.54
Σ SFA[1]	51.94 ± 1.79^{a}	66.11 ± 13.86^{a}	32.48 ± 10.64^{b}	60.06 ± 0.63^{a}	12.75 ± 0.21^{c}	9.43 ± 0.04^{c}	7.61 ± 0.10^{c}	7.80 ± 0.29^{c}	22.47 ± 0.59
Σ MUFA[2]	34.86 ± 0.79^{a}	43.65 ± 7.42^{b}	18.49 ± 6.52^{cd}	34.25 ± 1.56^{a}	12.97 ± 0.58^{de}	9.60 ± 1.14^{e}	6.99 ± 0.36^{e}	6.50 ± 0.37^{e}	7.22 ± 0.29
Σ PUFA[3]	16.35 ± 0.22^{abc}	19.82 ± 2.79^{a}	8.88 ± 2.79^{d}	13.18 ± 0.82^{be}	16.11 ± 0.56^{be}	15.99 ± 1.25^{e}	7.99 ± 0.23^{f}	7.81 ± 0.51^{cdf}	7.87 ± 0.63
Σ HUFA[4, 5]	57.46 ± 5.65^{a}	74.44 ± 2.67^{b}	42.68 ± 10.32^{c}	53.65 ± 9.96^{ac}	17.84 ± 1.61^{d}	14.13 ± 1.35^{d}	14.13 ± 1.36^{d}	14.25 ± 2.60^{d}	28.59 ± 2.21
Σ *n*-3	53.92 ± 3.17 ^{a}	66.26 ± 3.00^{b}	35.28 ± 9.40^{c}	44.72 ± 8.64 ^{ac}	23.60 ± 1.34^{d}	19.82 ± 0.48^{d}	14.18 ± 1.14^{d}	13.48 ± 1.14^{d}	20.32 ± 1.71
Σ *n*-6	19.90 ± 2.64 ^{ab}	27.99 ± 1.97^{c}	16.28 ± 3.57^{a}	22.11 ± 2.19^{b}	10.35 ± 0.82^{d}	10.30 ± 0.60^{d}	7.95 ± 0.44^{d}	8.58 ± 1.87^{d}	16.14 ± 1.12
n-3 / *n*-6	2.72 ± 0.27^{a}	2.37 ± 0.13^{b}	2.16 ± 0.22^{abcd}	2.02 ± 0.25^{bcde}	2.28 ± 0.82^{bc}	1.93 ± 0.14^{cde}	1.78 ± 0.05^{de}	1.58 ± 0.18^{e}	1.26 ± 0.03
EPA/DHA	0.10 ± 0.01^{ab}	0.09 ± 0.01^{ab}	0.11 ± 0.02^{ab}	0.08 ± 0.01^{ab}	0.72 ± 0.05^{abc}	2.16 ± 0.29^{cd}	1.82 ± 0.14^{cd}	2.32 ± 0.22^{d}	0.18 ± 0.01
ARA/EPA	0.95 ± 0.08^{a}	0.94 ± 0.04^{ab}	1.06 ± 0.04^{ab}	1.19 ± 0.02^{ab}	1.65 ± 0.04^{ab}	0.44 ± 0.01^{b}	0.40 ± 0.01^{b}	0.42 ± 0.01^{b}	1.19 ± 0.03
Σ Total	160.61 ± 4.93^{a}	204.01 ± 25.34^{b}	102.54 ± 28.37^{c}	161.13 ± 12.55^{a}	59.67 ± 2.70^{d}	49.15 ± 1.65^{d}	36.72 ± 1.91^{d}	36.36 ± 3.52^{d}	66.15 ± 2.38

Only the fatty acids whose content exceeds at least 1% in any treatment are displayed. Different superscript letters in the same row represent significant differences ($p<0.05$) among treatments (wild specimens excluded).

[1] Saturated fatty acids: 10:0, 12:0, 14:0, 16:0, 18:0, 20:0, 22:0.

[2] Monounsaturated fatty acids: 14:1*n*-5, 16:1*n*-7, 18:1*n*-9, 18:1*n*-7, 20:1*n*-9, 22:1*n*-9, 24:1n-9.

[3] Polyunsaturated fatty acids: 18:2*n*-6; 18:3*n*-6; 18:3*n*-3; 20:2*n*-6; 20:3*n*-6; 20:3*n*-3, 22:2*n*-6

[4] Highly unsaturated fatty acids: 20:4*n*-6; 20:5*n*-3; 22:4*n*-6, 22:5n-3, 22:6*n*-3

[5] Although PUFA are defined as all fatty acids with ≥2 double bonds, in the present study HUFA (fatty acids with ≥4 double bonds) are not considered within ∑PUFA.

Significant differences were observed in the FA composition between levels in the light ($F_{1, 24}$ = 519.16, p<0.001, R^2 = 0.806), temperature ($F_{1, 24}$ = 13.42, p<0.01, R^2 = 0.021) and diet ($F_{1, 24}$ = 54.45, p<0.001, R^2 = 0.085). There were also significant interactions between food and light ($F_{1, 24}$ = 10.09, p<0.01, R^2 = 0.016), food and temperature ($F_{1, 24}$ = 5.97, p<0.05, R^2 = 0.009) and temperature and light ($F_{1, 24}$ = 16.34, p<0.01, R^2 = 0.025) treatments. Most of the variation in composition (>80% out of a total of 84.8% of explained variation), however, was related to differences in the FA composition of anemones raised under different light regimes.

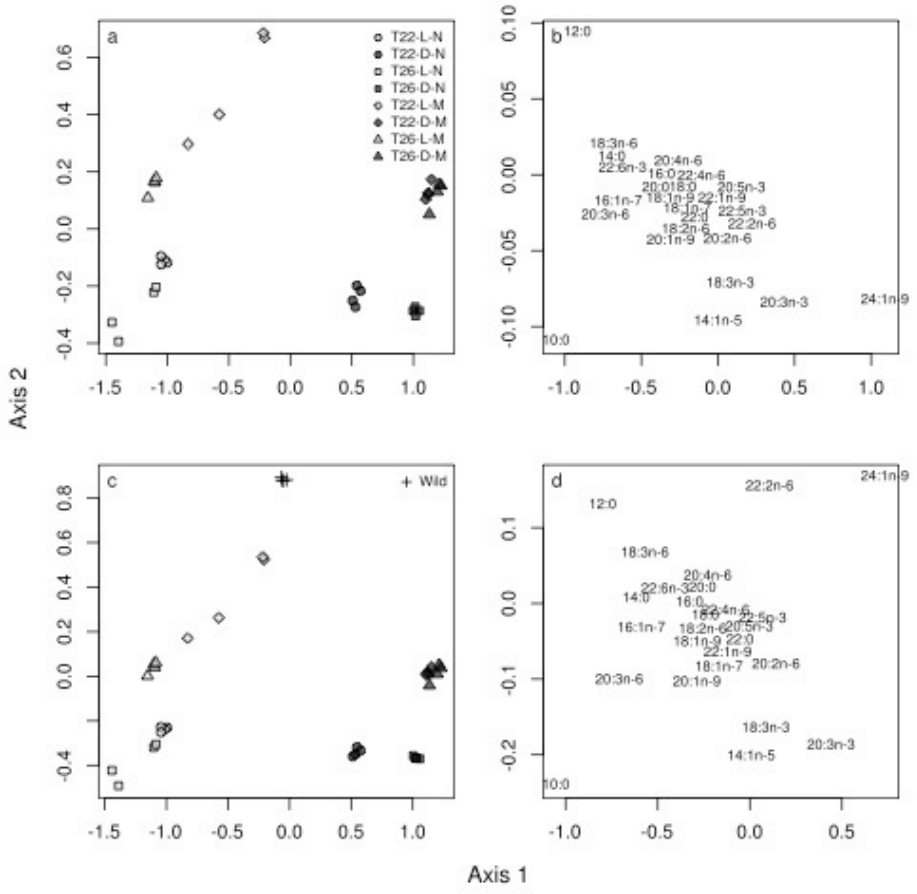

Fig. 4.1 Principal coordinates ordination on fatty acid profiles of *Aiptasia pallida* reared under different water temperatures (22 ºC – T22 – and 26 ºC – T26), light (L: 12 h light and 12 h dark; D: continuous darkness) and provided with different diets (*Artemia* nauplii – N – and *Artemia* metanauplii enriched with *Tetraselmis chui* and *Isochrysis galbana* – M) (a) and cultured and wild *A. pallida* (Wild) (c). Weighted average scores of fatty acid variables are also shown (b, d).

4.4 Discussion

FAs of the symbiotic sea anemone *A. pallida* may be derived from two major sources: heterotrophic feeding and photosynthesis by endosymbiotic dinoflagellates (Bachar et al. 2007). The FA contribution from photosynthesis is very important because unlike the vast majority of marine animals, *A. pallida* can benefit from important FAs, such as LA and ALA, synthesized by their endosymbiotic zooxanthellae (Imbs et al. 2011). These FAs are precursors of the most widely distributed PUFAs of the *n*-6 and *n*-3 series (Dalsgaard et al. 2003, Imbs et al. 2011). In the present study, differences in LA and ALA between treatments were mostly associated with the different live prey provided to sea anemones. Nonetheless, an effect of light was also observed for ALA (Table 4.2; Fig. 4.1). In contrast to other FA that showed higher concentrations in light

treatments (e.g. LA), results indicate that anemones differentially take up ALA from their diet relative to light availability. In other words, when the same diet was provided to *A. pallida*, higher ALA concentrations were observed in anemones reared in total darkness. The nutrient uptake from photosynthates could also be different when anemones were fed different prey. However, this was not observed, as differences in FAs acquired via heterotrophy were not reduced via autotrophy. Anemones reared under light conditions and fed different diets still exhibited the nutritional differences recorded on their prey, as exemplified by recorded levels of PUFA and HUFA (Table 4.2). It is important to note that while PUFA are commonly defined as FA with ≥2 double bonds, in the present study, HUFA (FA with ≥4 double bonds) are not considered within PUFA (Kelly & Scheibling 2012).

A. pallida exposed to artificial light displayed 2–5 times higher levels of total FAs than monoclonal conspecifics cultured in the dark (Table 4.2). The role played by zooxanthellae on the pool of FAs, with emphasis on DHA, is further highlighted if we consider that this essential FA only accounted for less than 1% of the FAs recorded for the live prey provided (Table 4.1). The high concentration of DHA observed for anemones exposed to light was not associated with initial stocking conditions, as results for anemones reared in total darkness showed significantly lower levels of DHA (Table 4.2). Variation of DHA with light regime is likely to be associated with zooxanthellae, as this FA is mainly synthesized by the photosynthetic endosymbionts (Imbs et al. 2011). Temperature also contributed to some differences on the FA profiles recorded for cultured *Aiptasia*, and it may have a positive or negative incidence on FA concentration depending on other parameters (Table 4.2). FA variation associated with temperature may be related to shifts in their biosynthesis, as some FAs (e.g. SFA and PUFA) are known to be temperature-regulated in order to adjust cell membrane fluidity and lipid viscosity (Papina et al. 2007).

The experimental treatment that produced the most similar FA profile to that recorded for wild anemones was the one using a 12 h light photoperiod, 22 ºC water temperature and metanauplii as prey (Fig. 4.1). Nevertheless, higher FA concentrations were achieved when water was heated to 26 ºC and nauplii were provided. Although FA concentrations varied substantially between these two treatments and wild organisms, EPA/DHA and ARA/EPA ratios were relatively similar (Table 4.2). This outcome indicates that both treatments generate *A. pallida* with higher FA concentrations than wild specimens but with comparable FA proportions.

The present study demonstrated that it is important to provide light to cultured anemones, in order to allow zooxanthellae to thrive and synthetize important FAs (namely DHA and PA). These findings may provide valuable information for the production in captivity of the ornamental nudibranch *Aeolidiella stephanieae* (displaying a retail value in the marine aquarium trade up to 20 € per specimen), as DHA and PA have already been shown to be important FA in parental diets of *A. stephanieae* (Leal et al. 2012a). It is possible that a deficiency in these two FA in the diet of these ornamental sea slugs may negatively affect larval hatching, metamorphosis and juvenile growth. *Aiptasia* is known to be the only food source for this stenophagous nudibranch (Carroll & Kempf 1990), which is commonly employed by marine aquarists to control outbreaks of these anemones in reef aquaria (Borneman & Lowrie 2001). As previously stated, the most significant bottleneck impairing the culture of *A. stephanieae* at a commercial scale is the lack of a constant supply of *Aiptasia* (Banger 2011, Olivotto et al. 2011). Our results indicate that by manipulating light, water temperature and diet, it is possible to shift the FA profile of *A. pallida* and simultaneously reduce its culture costs. Although the use of artificial light is an important factor that should not be discarded (whenever employing sunlight is not a feasible option), the fact that *A. pallida* can be cultured at lower temperatures without compromising the FA profile of *A. pallida* (using wild specimens as standards) will certainly reduce production costs. The use of live-feed

leftovers (metanauplii rather than nauplii) can also be used to decrease culture costs and still produce *A. pallida* with FA proportions similar to those displayed by wild specimens.
Another important aspect that is worth mentioning is related to the potential use of *A. pallida* in integrated aquaculture. This symbiotic tropical anemone may facilitate the recycling of nutrients present in the wastewater of culture facilities (e.g. outflow water enriched in nutrients and/or containing discarded uneaten live or pelleted feeds). Bischoff et al. (2009) already suggested the use of the polychaete *Nereis diversicolor* to recycle and even enhance the levels of some nutrients that would otherwise be lost. A similar rationale can be used to employ *Aiptasia* to recycle nutrients, namely FAs, from effluents. The present work demonstrated how *Aiptasia* harbouring healthy colonies of zooxanthellae may be used to recycle live-feed leftovers. The metanauplii used in our study exhibited sub-optimal levels of DHA and thus were not suitable to be used as live food for marine larviculture. However, DHA levels in *A. pallida* reared with a regular light regime and fed metanauplii were higher than organisms captured in the wild, where prey concentration is expected to be lower than concentrations used in this study (varying between 300 and 5000 prey L^{-1}). As long as either sunlight or artificial light is provided to *Aiptasia*, nutrient recycling from effluent culture water may be possible. Additionally, it has already been shown that growth of symbiotic zooxanthellae is favoured when they are hosted in anemones colonising marine environments with high levels of particulate food and/or cnidarians hosts able to feed heterotrophically (Steen 1986, Cook et al. 1988). In this way, *Aiptasia* produced in fish farm effluents and harbouring photosynthetic endosymbionts may be employed as an alternative source for DHA and other FAs. In future studies it should be investigated if FAs (with emphasis to DHA) from cultured *Aiptasia* may eventually contribute to the current effort to decrease the incorporation of fish derived products within compound animal feeds commonly employed in aquaculture (Tacon & Meitian 2009).

4.5 Acknowledgments

Miguel C. Leal was supported by a PhD scholarship (SFRH/BD/63783/2009) funded by Fundação para a Ciência e Tecnologia, Portugal (QREN-POPH-Type 4.1 – Advanced Training, subsidised by the European Social Fund and national funds MCTES). We also thank Sofia Engrola for her support during the culture of *Aiptasia*, Maria M. Mays and Shanna D. Hanes for their assistance in the collection of wild *A. pallida* in the Florida Keys, and three anonymous reviewers for their helpful comments and suggestions.

4.6 References

Anderson M (2001) A new method for non-parametric multivariate analysis of variance. Austral Ecol 26:32-46

Bachar A, Achituv Y, Pasternak Z, Dubinsky Z (2007) Autotrophy *versus* heterotrophy: The origin of carbon determines its fate in a symbiotic sea anemone. J Exp Mar Biol Ecol 349:295-298

Bachok Z, Mfilinge P, Tsuchiya M (2006) Characterization of fatty acid composition in healthy and bleached corals from Okinawa, Japan. Coral Reefs 25:545-554

Banger D (2011) Breeding *Berguia* nudibranches: the best kept secret, CreateSpace, USA, 140 pp.

Bischoff AA, Fink P, Waller U (2009) The fatty acid composition of *Nereis diversicolor* cultured in an integrated recirculated system: Possible implications for aquaculture. Aquaculture 296:271-276

Borneman E, Lowrie J (2001) Advances in captive husbandry and propagation: an easily utilized reef replenishment means from the private sector? Bull Mar Sci 69:897-913

Carroll D, Kempf S (1990) Laboratory culture of the aeolid nudibranch *Berghia verrucicornis* (Mollusca, Opisthobranchia): some aspects of its development and life history. Biol Bull 179:243-253

Cohen Z, Vonshak A, Richmond A (1988) Effect of environmental conditions on fatty acid composition of the red alga *Porphyridium cruentum*: correlation to growth rate. J Phycol 24:328-332

Cook C, D'Elia C, Muller-Parker G (1988) Host feeding and nutrient sufficiency for zooxanthellae in the sea anemone *Aiptasia pallida*. Mar Biol 98:253-262

Dalsgaard J, St John M, Kattner G, Müller-Navarra D, Hagen W (2003) Fatty acid trophic markers in the pelagic marine environment. Adv Mar Biol 46:225-340

Imbs AB, Yakovleva IM, Latyshev NA, Pham LQ (2011) Biosynthesis of polyunsaturated fatty acids in zooxanthellae and polyps of corals. Russ J Mar Biol 36:452-457

Kelly J, Scheibling R (2012) Fatty acids as dietary tracers in benthic food webs. Mar Ecol Prog Ser 446:1-22

Leal MC, Nunes C, Alexandre D, Silva TL, Reis A, Dinis MT, Calado R (2012a) Parental diets determine the embryonic fatty acid profile of the tropical nudibranch *Aeolidiella stephanieae*: the effect of eating bleached anemones. Mar Biol 159:1745-1751

Leal MC, Nunes C, Engrola S, Dinis M, Calado R (2012b) Optimization of monoclonal production of the glass anemone *Aiptasia pallida* (Agassiz in Verrill, 1864). Aquaculture 354-355:91-96

Lepage G, Roy C (1986) Direct transesterification of all classes of lipids in a one-step reaction. J Lipid Res 27:114-120

Marino A, Valveri V, Muia C, Crupi R, Rizzo G, Musci G, Laspada G (2004) Cytotoxicity of the nematocyst venom from the sea anemone *Aiptasia mutabilis*. Comp Biochem Phys C 139:295-301

Oksanen J, Kindt R, Legendre P, O'Hara B, Simpson G, Solymos P, Stevens M, Wagner H (2009) vegan: Community Ecology Package. R Package verion 1.15-4 http://CRANR-projectorg/package=vegan

Olivotto I, Planas M, Simões N, Holt G, Avella M, Calado R (2011) Advances in breeding and rearing marine ornamentals. J World Aquacult Soc 42:135-166

Papina M, Meziane T, Van Woesik R (2003) Symbiotic zooxanthellae provide the host-coral *Montipora digitata* with polyunsaturated fatty acids. Comp Biochem Phys B 135:533-537

Papina M, Meziane T, Van Woesik R (2007) Acclimation effect on fatty acids of the coral *Montipora digitata* and its symbiotic algae. Comp Biochem Phys B 147:583-589

Richier S, Sabourault C, Ferrier-Pagès C, Merle P-F, Furla P, Allemand D (2010) Cnidarian-dinoflagellate symbiosis-mediated adaptation to environmental perturbations. In: Seckbach J, Grube M (eds) Symbiosis and Stress, Cellular Origin, Life in Extreme Habitats and Astrobiology. Springer, New York, 651 p.

Ruppert E, Fox R, Barnes R (2003) Invertebrate Zoology: A Functional Approach, Brookes Cole, Belmont, USA, 1008 p.

Steen R (1986) Evidence for heterotrophy by zooxanthellae in symbiosis with *Aiptasia pulchella*. Biol Bull 170:267-278

Tacon A, Meitian M (2009) Fishing for deed or fishing for food: increasing global competition for small pelagic forage fish. Ambio 38:294-302

Weis V, Davy S, Hoegh-Guldberg O, Rodriguez-Lanetty M, Pringle J (2008) Cell biology in model systems as the key to understanding corals. Trends Ecol Evol 23:369-376

Chapter 5 Molecular assessment of heterotrophy and prey digestion in zooxanthellate cnidarians

Abstract

Zooxanthellate cnidarians are trophically complex, relying on both autotrophy and heterotrophy. Although several aspects of heterotrophy have been studied in these organisms, information linking prey capture with digestion is still missing. We used prey-specific PCR-based tools to assess feeding and prey digestion of two zooxanthellate cnidarians - the tropical sea anemone *Aiptasia* sp. and the scleractinian coral *Oculina arbuscula*. Prey DNA disappeared rapidly over the initial 1–3 days, whereas complete digestion of prey DNA required up to 10 days in *O. arbuscula* and 5 or 6 days in *Aiptasia* sp. depending on prey species. These digestion times are considerably longer than previously reported from microscopy-based examination of zooxanthellate cnidarians and prey DNA breakdown in other marine invertebrates, but similar to prey DNA breakdown reported from terrestrial invertebrates such as heteroptera and spiders. Deprivation of external prey induced increased digestion rates during the first days after feeding in *O. arbuscula*, but after 6 days of digestion there were no differences in the remaining prey levels in fed and unfed corals. This study indicates that prey digestion by symbiotic corals may be slower than previously reported and varies with the type of prey, the cnidarian species and its feeding history. These observations have important implications for bioenergetic and trophodynamic studies on zooxanthellate cnidarians.

Keywords

Predator-prey interactions; Digestion; qPCR; dla-qPCR; Scleractinian corals; *Aiptasia*.

Published: Leal MC, Nejstgaard JC, Calado R, Thompson ME, Frischer ME (2014) Molecular assessment of heterotrophy and prey digestion in zooxanthellate cnidarians. Molecular Ecology 23: 3838-3848 (doi:10.1111/mec.12496)

5.1 Introduction

The association between cnidarians and photosynthetic endosymbiotic dinoflagellates (genus *Symbiodinium*; commonly termed zooxanthellae) is among the most investigated ecological associations (e.g. see reviews by Venn et al. 2008, Davy et al. 2012). This relationship provides the cnidarian with translocated photosynthates from zooxanthellae, and the host provides a sheltered light-rich environment with inorganic nutrients (Porter 1976, Falkowski et al. 1984). Besides autotrophy through endosymbionts, zooxanthellate cnidarians are also able to feed heterotrophically, particularly by preying on zooplankton. This form of heterotrophy may account for a significant portion of the nutrition of zooxanthellate cnidarians, particularly when photosynthetic products are unavailable, such as when light is limiting or during bleaching events (Anthony & Fabricius 2000, Grottoli et al. 2006, Palardy et al. 2008).

Heterotrophy in zooxanthellate cnidarians has been thoroughly investigated, at least in terms of prey capture and ingestion (see Houlbrèque & Ferrier-Pagès 2009 for a review). However, lack of quantitative data on prey digestion processes presently limits the understanding of trophic ecology of these organisms. It is also important to understand digestion dynamics in deprivation of external food since heterotrophic starvation affects the bioenergetics and bleaching susceptibility of zooxanthellate cnidarians (Titlyanov et al. 2000, Borell et al. 2008).

Investigations on prey ingestion and digestion in zooxanthellate cnidarians have been challenged by inherent limitations in available methods. Feeding studies on these organisms have largely been based on clearance rates during incubations in experimental chambers and visual observations of polyp dissections (e.g. Sebens 1981, Sebens & Johnson 1991, Houlbrèque et al. 2004, Palardy et al. 2005, Grottoli et al. 2006). The first method, clearance rate, is an indirect estimate of prey capture as it builds on the assumption that all prey that disappears during incubation have been ingested. The second method, visual identification of prey content, is prone to error as it relies on the visual recognition of partially digested prey, likely causing a substantial underestimation of digestion times, especially for small prey types (see Nejstgaard et al. 2008 for thorough discussion on limitations in bottle incubation and microscopical gut analyses in feeding studies).

During the last decade, there has been a dramatic increase in the development and use of molecular methods to study trophic interactions, both in marine and terrestrial environments (Symondson 2002, Sheppard & Harwood 2005, King et al. 2008). PCR-based methods have enabled direct assessment of feeding dynamics through the analysis of prey DNA sequences and provide qualitative and quantitative assessments of prey capture and digestion (e.g. Deagle et al. 2006, Troedsson et al. 2009, Durbin et al. 2012, Roura et al. 2012). While these molecular tools have been successfully used to study marine invertebrate trophic interactions (Troedsson et al. 2007, Simonelli et al. 2009, O'Rorke et al. 2012a, Roura et al. 2012), to our knowledge they have only been applied once to zooxanthellate cnidarians to investigate the presence/absence of prey ingested by corals (Leal et al. 2014). The use of PCR-based methods to investigate heterotrophy in these organisms may provide a more accurate and reliable estimate of prey ingestion and digestion, which may have implications for bioenergetic estimates of zooxanthellate cnidarians. Ultimately, by using a molecular approach to study the nutrition of these organisms, researchers may achieve a better understanding of the cnidarian-dinoflagellate symbiosis.

In this study, we investigated heterotrophy and prey digestion of zooxanthellate cnidarians fed different prey under laboratory settings using three PCR-based approaches. Standard endpoint PCR was used to develop a qualitative assessment of heterotrophic feeding (Leal et al. 2014). Prey DNA breakdown was assessed by the development and use of differential amplification length quantitative PCR (dla-qPCR) (Deagle et al. 2006, Troedsson et al. 2009). Quantitative PCR (qPCR) was used to estimate digestion time (Durbin et al. 2012). As experimental organisms we used the

brine shrimp *Artemia* sp. nauplii and the rotifer *Brachionus plicatilis* as prey for the symbiotic tropical sea anemone *Aiptasia* sp. and the scleractinian symbiotic coral *Oculina arbuscula*. *Aiptasia* sp. is acknowledged as a model organism for the study of the cnidarian-dinoflagellate symbiosis (Weis et al. 2008) and *O. arbuscula* is a facultative symbiotic species that is able to survive when deprived of its photosynthetic endosymbionts and thus represents a coral capable of a high degree of nutritional plasticity (Miller 1995). These prey species (*Artemia* sp. and *B. plicatilis*) were chosen as they are robust prey model organisms for coral feeding studies (e.g. Titlyanov et al. 2001, Houlbrèque & Ferrier-Pagès 2009, van Os et al. 2012, Leal et al. 2013).
In this study, we address the following hypotheses: (i) prey DNA breakdown of zooxanthellate cnidarians is identical for different prey species, and (ii) different zooxanthellate cnidarian species have similar digestion rates regardless of prey species and starvation conditions.

5.2 Materials and Methods

5.2.1 Zooplankton cultures

Artemia sp. nauplii were hatched from cysts (San Francisco Bay strain; Brine Shrimp Direct suppliers, Ogden UT, USA) by immersion in aerated water (26 ºC, 25 ppt salinity). Nauplii were captured after 20–24 hours incubation and rinsed with filtered seawater (Whatman GF/F filter, nominal pore size 0.7 µm). Live cultures of *B. plicatilis* ('L' type; Reef Nutrition, Campbell CA, USA) were maintained in aerated tanks (Hoff & Snell 2008) and fed a mixture of microalgae (RGcomplete APBreed, Reed Mariculture, Campbell CA, USA). *B. plicatilis* were captured using a sieve (100 µm mesh) and rinsed with filtered seawater (GF/F). Species identification was confirmed by amplification of nearly the complete 18S rRNA gene using the primers Univ18S-15F and Univ18S-1765R (Gruebl et al. 2002) and sequencing approximately 900 bp from the 5'-end of the amplified fragments (Table 5.1). The recovered 18S rRNA gene sequence of *Artemia* sp. (876 bp) and *B. plicatilis* (893 bp) were identical to the sequences reported by Weekers et al. (2002) (GenBank #AJ238061) and by Giribet et al. (2004) (GenBank #AY218118), respectively.

Table 5.1 Primers used in this study

Primer[a]	Primer sequence (5' to 3')
Univ18S-15F	CTC CCA GTA GTC ATA TGC[b]
Univ18S-1765R	ACC TTG TTA CGA CTT[b#]
Bp18S-202F	GGT CGC AAG ATC CCT TTG TA
Bp18S-255R	CAT GCG ATC AGC ACA AAG TT
Bp18S-304R	CGA AAG TTG ATA GGG CAG ACA
Bp18S-345R	CCG TTA CCC GTT ACA ACC AT
Bp18S-385R	CGT TTC TCA TGC TCC CTC TC
Bp18S-440R	CCC GTT CTA GGA GTG GGT AA
Bp18S-626R	ACC CGA GAT CCA ACT ACG AG
Af18S-1298F	GTT GGT GGA GCG ATT TGT CT[c]
Af18S-1373R	GGA TCC ATC GTC TAT TTA GCA G
Af18S-1387R	AGA GCC ATC CAC CAC TAG GA[c]
Af18S-1422R	TCT CAT ATG GCT AGA CGC CAC T
Af18S-1496R	GCG CTG ATT CTT CCA GTG TA
Af18S-1547R	CAA CCA CGG AAG AGG TTC AG
Af18S-1589R	TAG GGA TTC CTG GTT CAT GG

[a] Primer name includes organism, direction and target location
[b] Gruebl et al. (2002).
[c] Mackie & Geller (2010).
[#] This primer is 3 bp shorter than the one originally described as preleminary investigations showed improved results for this "universal" primer set.

5.2.2 Zooxanthellate cnidarians collection and husbandry

O. arbuscula was collected at Gray's Reef National Marine Sanctuary (Georgia, USA, 30.3939 ºN 80.8885 ºW, 20 m depth, May 2012) under the manager's permit and fragmented into replicate coral nubbins (Highsmith 1982). Corals were kept unfed in a recirculating tank maintained at 24 ºC and 35 ppt salinity. The aquarium system was composed of a 200 L tank connected to a 100 L filter tank equipped with a protein skimmer and a biological filter (Sheridan et al. 2013). Partial water changes (10% of total system volume) with fresh filtered seawater were performed weekly. The coral tank was illuminated from above (two 21 W T5 bulbs: actinic blue and natural daylight; Coralife, Franklin WI, USA) in a 12 h light: 12 h dark cycle.

Aiptasia sp. were supplied by a local marine ornamentals wholesaler and stocked in a recirculating tank (40 L) with an external trickle filter. The tank was illuminated from above (6 W T5 bulb natural daylight; Coralife, Franklin WI, USA) in a 12 h light: 12 h dark cycle. Water changes were performed as previously described. Apart from light, all other culture conditions followed the protocol to produce monoclonal *Aiptasia* by Leal et al. (2012). The anemones were starved one week prior to conducting the experiments.

O. arbuscula was visually identified to the species level, and its identity was supported by sequencing a fragment of its 18S rRNA gene as described above (GenBank #JX983594). The resulting sequence was submitted to GenBank (accession JX983594). It was not possible to identify *Aiptasia* specimens used in this study to the species level based on morphology or the 849 bp 18S rRNA gene sequence. Sequencing results indicated a high degree of similarity (>98%) to *Aiptasia mutabilis* (GenBank #FJ489438), *Aiptasia insignis* (GenBank #AY046885) and *Aiptasia pulchella* (GenBank #EU190846, AY297437). Therefore we used clones stemming from one individual in all experiments and refer to them as *Aiptasia* sp.

5.2.3 Feeding experiments

Experiments for each cnidarian species fed *Artemia* sp. or *B. plicatilis* were performed in Plexiglass chambers (Vogel & LaBarbera 1978) with a water volume of 1200 mL (30 x 4 x 12 cm) and water

flow (0.1 m s^{-1}) provided by an internal pump (TOM Aquarium & Pet Products, Inc., Shawnee KS, USA). Each replicate consisted of a separate feeding chamber with a single coral fragment (~25 polyps) or small anemone (~3 to 6 mm). *Aiptasia* sp. was fed either *Artemia* or *B. plicatilis* at a concentration of 2000 L^{-1} that were added once all polyps were expanded. *Aiptasia* sp. was fed for 15 min and *O. arbuscula* for 30 min. Feeding times were different between species because prey capture rates were higher in *Aiptasia* sp. than *O. arbuscula*, and overfeeding the first could lead to prey regurgitation and potentially bias feeding results. After feeding, organisms were sampled and thoroughly rinsed three times in GF/F-filtered seawater.

For the qualitative assessment of heterotrophy, *Aiptasia* sp. and *O. arbuscula* were rinsed and sampled immediately after feeding. For prey digestion assessment, *Aiptasia* sp. and *O. arbuscula* were rinsed and either sampled immediately after feeding (day 0) or transferred to a prey-free chamber and kept in continuous heterotrophic starvation until being sampled after 24 h (day 1), 48 h (day 2), 72 h (day 3), 96 h (day 4), 144 h (day 6), 192 h (day 8), and 240 h (day 10). Unfed *O. arbuscula* and *Aiptasia* sp. were also sampled as negative controls.

To investigate whether continuous starvation after feeding affected the relatively long prey digestion times observed for *O. arbuscula* (see Results section) a subset of experiments was conducted where corals were fed either *B. plicatilis* or *Artemia* sp. and transferred to a prey-free chamber after feeding (day 0). After the first day, the prey type was switched so that corals remained fed but that post experimental feeding did not interfere with the specific detection of the prey that were provided on day 0. Samples were collected after 2, 3 and 6 days of incubation.

For all experiments involving *O. arbuscula*, individual polyps were sampled (Kemp et al. 2008). For all experiments involving *Aiptasia* sp., whole individuals were used for total genomic DNA (gDNA) extraction. For each digestion time point of each experiment with *O. arbuscula*, nine samples were taken: three polyps sampled per coral nubbin and a total of three nubbins from different colonies (n = 3 x 3). For *Aipasia* sp. experiments, a total of three single organisms were sampled.

5.2.4 Genomic DNA extraction and purification

gDNA from zooplankton cultures, corals and anemones were extracted using the DNeasy Blood & Tissue kit (Qiagen, Valencia, CA, USA). DNA quantity was estimated using the Quant-iT PicoGreen dsDNA assay kit (Invitrogen) on a Nanodrop ND3300 fluorospectrometer (NanoDrop products, Wilmington, DE). Each time a feeding experiment was performed, the gDNA of a known number of the zooplankton prey used in the experiment was also extracted for later use as standards in qPCR assessments. This information allowed the estimation of gDNA content per individual prey, which was used to estimate ingested prey numbers based on prey DNA content at ingestion (day 0).

5.2.5 Assessment of prey DNA breakdown

Prey DNA breakdown was assessed through the dla-qPCR assay (Deagle et al. 2006, Troedsson et al. 2009). This assay utilizes multiple primer sets that amplify different sized fragments in a single specific area of the prey 18S rRNA gene. Prey DNA breakdown is defined as a decline in amplifiable target DNA strand length over time.

5.2.6 Primers

Primer pairs targeting *Artemia* sp. 18S rRNA were designed using previously referenced nucleotide sequences (Weekers et al. 2002) (GeneBank #AJ238061), apart from the forward (Af18S-1298F) and the reverse (Af18S-1387R) primers (Mackie & Geller 2010). All *B. plicatilis* primer pairs were designed using an alignment of nucleotide sequences (GeneBank #AY218118, #U29235,

#U49911). Using a single forward primer, sets of reverse primers were designed to amplify fragments of increasing size from 50 to 500 bp. Primer design was facilitated using Primer 3 software (Rozen & Skaletsky 2000). All oligonucleotides were synthesized by Integrated DNA Technologies (www.idtdna.com).

Ten candidate reverse primers targeting *Artemia* 18S rRNA gene were tested with Af18S-1298F, and ten candidate reverse primers targeting *B. plicatilis* 18S rRNA gene were tested with a forward primer (Bp18S-202F). Six reverse primers were ultimately selected for each prey species (Table 5.2) based on: (i) similar annealing temperature with forward primer, (ii) specificity and (iii) reaction efficiency. Primer specificity was confirmed *in silico* in the NCBI database by BLAST searching (http://ncbi.nlm.nih.gov/BLAST/) and empirically in PCR assays against gDNA purified from each predator and prey species. However, these primer sets were not specifically validated for use beyond this study and therefore should be used cautiously in any future studies. Amplification efficiency for each primer set was calculated using the slope of the log standard curve (Heid et al. 1996) over a target gDNA template concentration range of 0.02 – 100 ng mL^{-1}. Minimum detection sensitivity was 4 and 3 pg of gDNA from *Artemia* sp. and *B. plicatillis*, respectively. PCR reactions were performed in 20 µL reaction volumes using the prey-specific primers. qPCR reactions were performed using a Bio-Rad CFX96™ C1000™ real-time thermal cycler (Bio-Rad Laboratories, Hercules, CA, USA) in 96-well plates with each reaction containing 10 µL of SsoFast™ EvaGreen® Supermix, 400 nM of primers and template gDNA ranging between 200 and 600 ng mL^{-1}. Amplification conditions included an initial denaturation step (2 min, 98 ºC) followed by 40 amplification cycles (5 s, 98 ºC; 5 s annealing/extension temperature; Table 5.2). All reactions were run in triplicate and PCR grade water was used as template for negative controls. PCR products were visualized by gel electrophoresis on a 1% agarose gel buffered in 1X TAE (0.04M Tris-Acetate, 0.001M EDTA, pH 8.0).

Table 5.2 PCR product length, assay annealing temperatures and PCR performance characteristics used in this study.

Forward primer	Reverse primer	Length (bp)	Annealing temperature (ºC)	PCR efficiency (%)	Correlation efficiency
Bp18S-202F	Bp18S-255R	53	60	99.8	0.996
Bp18S-202F	Bp18S-304R	102	60	100.2	0.996
Bp18S-202F	Bp18S-345R	143	60	100.7	0.996
Bp18S-202F	Bp18S-385R	183	60	99.7	0.989
Bp18S-202F	Bp18S-440R	238	60	99.9	0.981
Bp18S-202F	Bp18S-626R	424	60	95.4	0.972
Af18S-1298F	Af18S-1373R	73	61	100.8	0.997
Af18S-1298F	Af18S-1387R	90	60	98.8	0.996
Af18S-1298F	Af18S-1422R	112	60	95.0	0.994
Af18S-1298F	Af18S-1496R	198	58	98.1	0.996
Af18S-1298F	Af18S-1547R	249	61	98.7	0.994
Af18S-1298F	Af18S-1589R	291	58	100.1	0.992

5.2.7 PCR/ qPCR amplification of zooplankton prey

All endpoint PCRs were performed using the reaction details and the same equipment as previously described. Only one primer set per prey species was used for PCR (*B. plicatilis*: Bp18S-202F and Bp18S-626R; *Artemia*: Af18S-1298F and Af18S-1547R), whereas all the species-specific primer sets were used for qPCR assays (Table 5.1). The appropriate amount of template DNA in all assays was achieved using 1 µL of either undiluted, five-fold or ten-fold dilution of gDNA extract. For each qPCR, a dilution series of extracted gDNA from each zooplankton culture was run as a

quantitative standard. All reactions were run in triplicate and PCR-grade water used as template for negative control. PCR products were visualized by gel electrophoresis as described above.
The number of prey ingested by each *Aiptasia* sp. and *O. arbuscula* polyp on day 0 was estimated using gDNA quantification from culture extracts and qPCR results based on the smallest fragments amplified for each prey.

5.2.8 Statistical analysis

The significance of differences in the prey DNA content obtained using each primer set (i.e. different fragment sizes) was tested for each experimental day using a one-way ANOVA. One-way ANOVA was also used to assess the significance of differences in prey DNA content between digestion times. Tukey's HSD test was used when ANOVA results revealed significant differences ($p<0.05$). Student's *t*-test was used to compare prey DNA contents for the same digestion time of *O. arbuscula* fed only once or continuously. Assumptions of homogeneity of variances and homoscedasticity were tested before all statistical analyses. When the assumptions were not met, square root transformations were performed. All statistical analyses and plots were facilitated using R (R Development Core Team 2012).

5.3 Results

5.3.1 Qualitative detection of prey in the predators

PCR was used to detect the presence of prey 18S rRNA in DNA extracted from the zooxanthellate cnidarians fed the respective prey species: *Artemia* sp. and *B. plicatilis*. These results, although not quantitative, indicated that both *Aiptasia* sp. and *O. arbuscula* ingested both prey species.

5.3.2 Assessment of the quantitative breakdown of prey DNA by dla-qPCR

Immediately after ingestion (day 0) there was no indication of prey breakdown, that is, there was no statistically significant difference in amplified DNA concentration between the dla-qPCR amplicons for any of the prey and predators (Fig. 5.1a, d and Fig. 5.2a, d, one way-ANOVA, $p = 0.87$, 0.91, 0 57 and 0.84, respectively). This indicates that in all predator-prey combinations, the full length of the target region of the prey DNA was intact and amplifiable immediately after ingestion. However, the dla-qPCR assessment of *Artemia* sp. DNA ingested by *Aiptasia* sp. 1 day after ingestion (Fig. 5.1a) demonstrated that DNA breakdown had occurred, that is, the shorter fragments displayed a higher concentration compared with the longer fragments, although the trend was not significant ($p = 0.24$; Fig. 5.2a). Over the next 6 days the quantity of prey DNA declined (Fig. 5.1b-c; Tukey's HSD test, $p<0.05$) and was not detectable by day 8 (data not shown).
Degradation of *B. plicatilis* DNA was also evaluated in *Aiptasia* sp. (Fig. 5.1d-f). Similar to *Artemia* sp., by day 1 significant *B. plicatilis* DNA breakdown was apparent and DNA degradation continued through day 4 ($p<0.05$), decreasing consistently over time (Tukey's HSD test, $p<0.05$). *B. plicatilis* DNA was undetectable in the experimental animals after 6 days (data not shown).

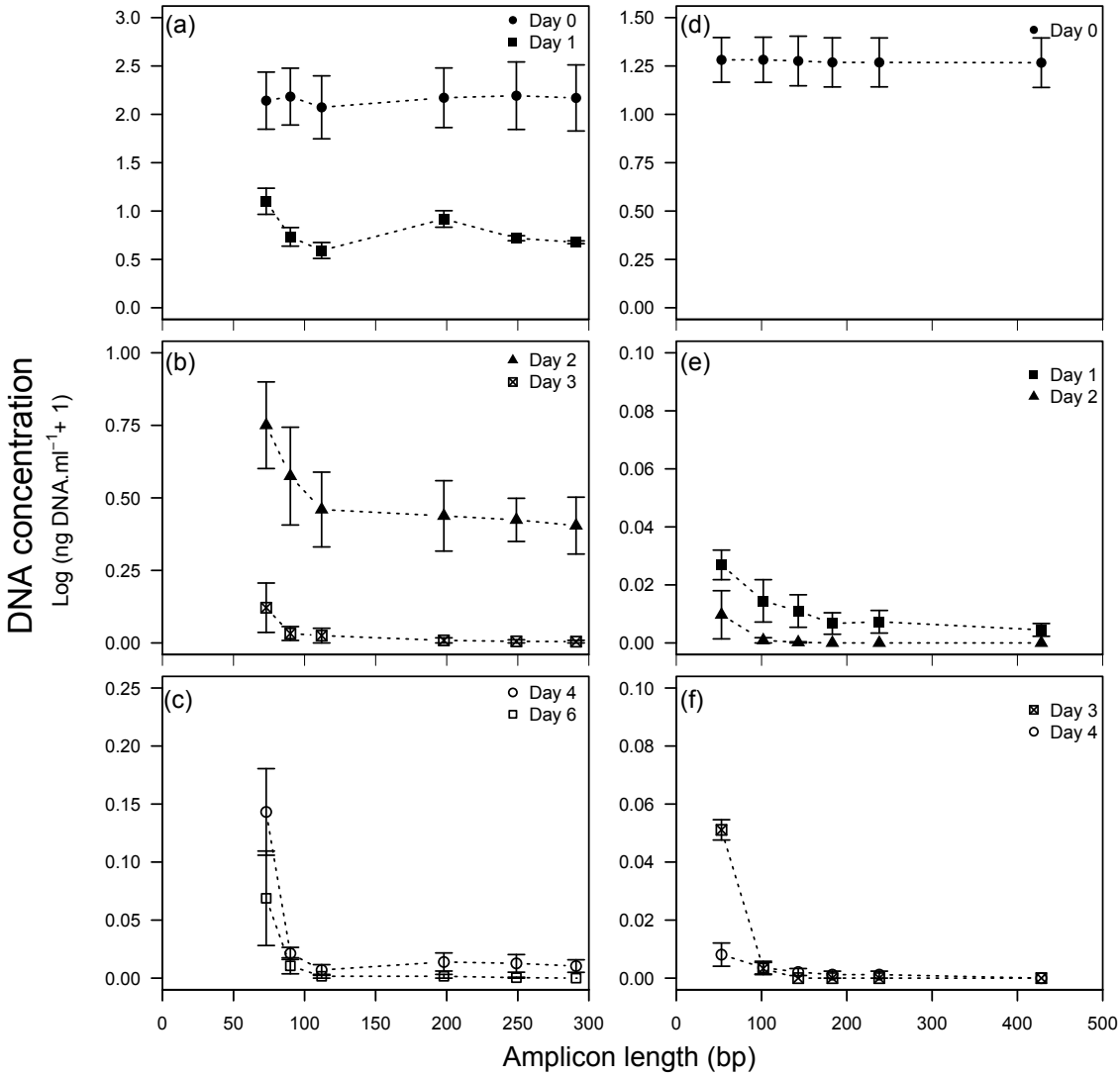

Fig. 5.1 Prey DNA breakdown based on the amplification of different sizes of DNA fragments of *Artemia* sp. (a, b, c) and *Brachionus plicatilis* (d, e, f) ingested by *Aiptasia* sp. 0, 1, 2, 3, 4 and 6 days after feeding (error bars denote standard error).

Similar to *Aiptasia* sp., prey DNA breakdown was also observed for *O. arbuscula* fed *B. plicatilis* (Fig. 5.2e-h). Compared to the first observation shortly after ingestion (day 0; Fig. 5.2e), the breakdown of *B. plicatilis* DNA was significant at day 1 ($p<0.01$) and breakdown increased with time (Tukey's HSD test, $p<0.05$). In contrast to *Aiptasia* sp., however, even after 10 days, prey DNA was still detectable (Fig. 5.2h). Furthermore, when the coral ingested *Artemia* sp., no differential DNA breakdown between the shortest and longest fragments could be detected over the observation period of 10 days (Fig. 5.2a-d; $p \geq 0.17$).

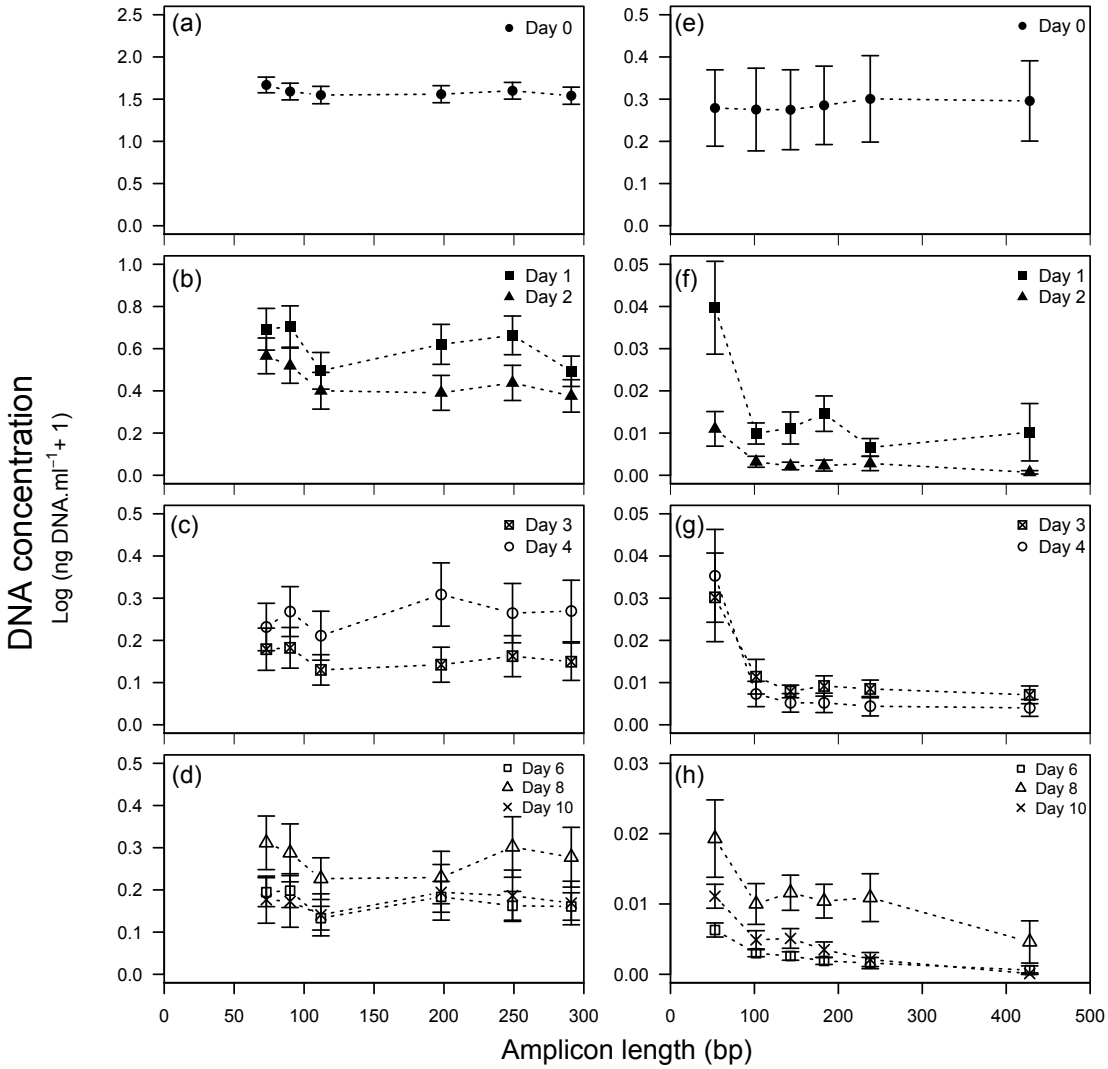

Fig. 5.2 Prey DNA breakdown based on the amplification of different sized DNA fragments of *Artemia* sp. (a, b, c, d) and *Brachionus plicatilis* (e, f, g, h) ingested by *Oculina arbuscula* 0, 1, 2, 3, 4, 6, 8 and 10 days after feeding (error bars denote standard error).

5.3.3 Estimation of prey digestion time

Prey digestion by *Aiptasia* sp. (Fig. 5.3) and *O. arbuscula* (Fig. 5.4) over time was assessed by quantifying the amount of the PCR amplicon using the prey-specific dla-qPCR primer sets that produced the smallest amplified fragments. Significant differences in prey DNA content over the digestion time were observed for both zooxanthellate cnidarians fed either prey ($p<0.05$). *Aiptasia* sp. fed *Artemia* sp. (Fig. 5.3a) exhibited significant differences in prey DNA content between day 0 and all other days, between day 1 and days 3, 4 and 6 (Tukey's HSD test, $p<0.01$), and between day 2 and days 3, 4 and 6 (Tukey's HSD test, $p<0.1$). *Artemia* sp. DNA was digested more slowly by *O. arbuscula*, but its DNA content in the coral was significantly higher on day 0 than in all other days (Fig. 5.4, Tukey's HSD test, $p<0.01$). Compared to *Artemia* sp., *B. plicatilis* digestion was faster. *B. plicatilis* DNA content in both *Aiptasia* sp. (Fig. 5.3b) and *O. arbuscula* (Fig. 5.4b) was significantly higher on day 0 compared with all other days (Tukey's HSD test, $p<0.01$). No significant difference in *B. plicatilis* DNA content was observed among all other days for both zooxanthellate cnidarians (Tukey's HSD test, $p \geq 0.65$).

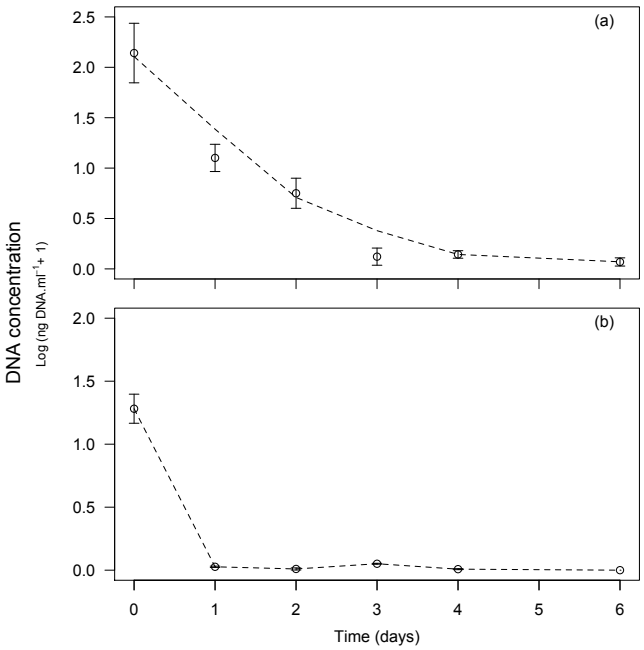

Fig. 5.3 Digestion time of *Aiptasia* sp. fed either *Artemia* sp. (a) and *Brachionus plicatilis* (b) based on the prey DNA content estimated by qPCR amplifying a 73-bp (*Artemia* sp.) and 53-bp (*B. plicatilis*) fragments of the 18S rRNA. Error bars denote standard errors.

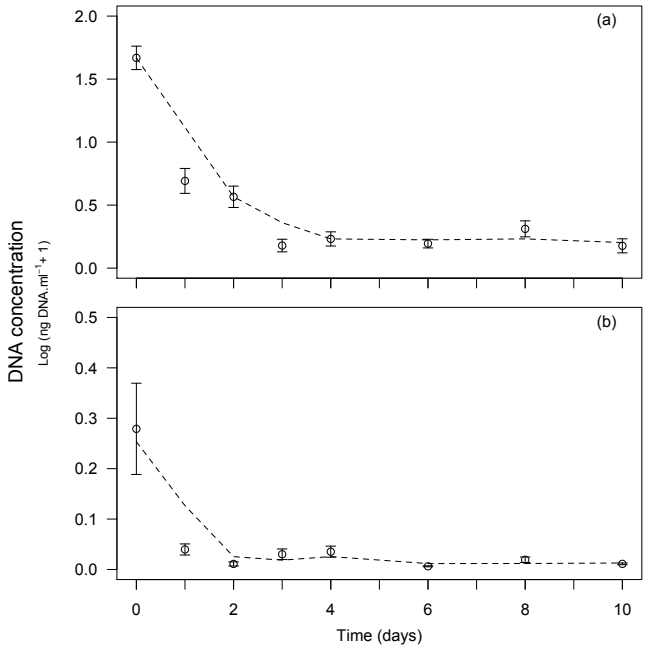

Fig. 5.4 Digestion time of *Oculina arbuscula* fed either *Artemia* sp. (a) and *Brachionus plicatilis* (b) based on the prey DNA content estimated by qPCR amplifying a 73-bp (*Artemia* sp.) and 53-bp (*B. plicatilis*) fragments of the 18S rRNA. Error bars denote standard errors.

Prey digestion time may also change with the number of prey initially captured and ingested. The estimation of prey numbers ingested by each *Aiptasia* sp. individual during feeding experiments (sampled on day 0) indicated that the number of ingested *Artemia* was higher (ca. 36) than for *B. plicatilis* (ca. 11). *O. arbuscula* individual polyps showed similar rates (ca. 21 and 22 for *Artemia* sp. and *B. plicatilis*, respectively).

5.3.4 Effect of starvation conditions

The patterns of prey DNA breakdown for *O. arbuscula* fed once and then starved (Fig. 5.2) did not differ from when the corals were fed continuously with an alternative prey (data not shown). In contrast, prey digestion time differed for *O. arbuscula* starved after initial ingestion compared to individuals fed continuously with alternative prey (Fig. 5.5). Starved corals exhibited lower prey DNA content on day 3 when initially fed *Artemia* sp. (t = 3.163, df = 6.895, p<0.05; Fig. 5.5a) and on day 2 when initially fed *B. plicatilis* (t = 3.71, df = 5.158, p<0.05; Fig. 5.5b). However, no differences were observed between feeding regimes by day 6. Thus, starvation significantly increased the digestion rate of the investigated coral at least during the first 2/3 days after feeding.

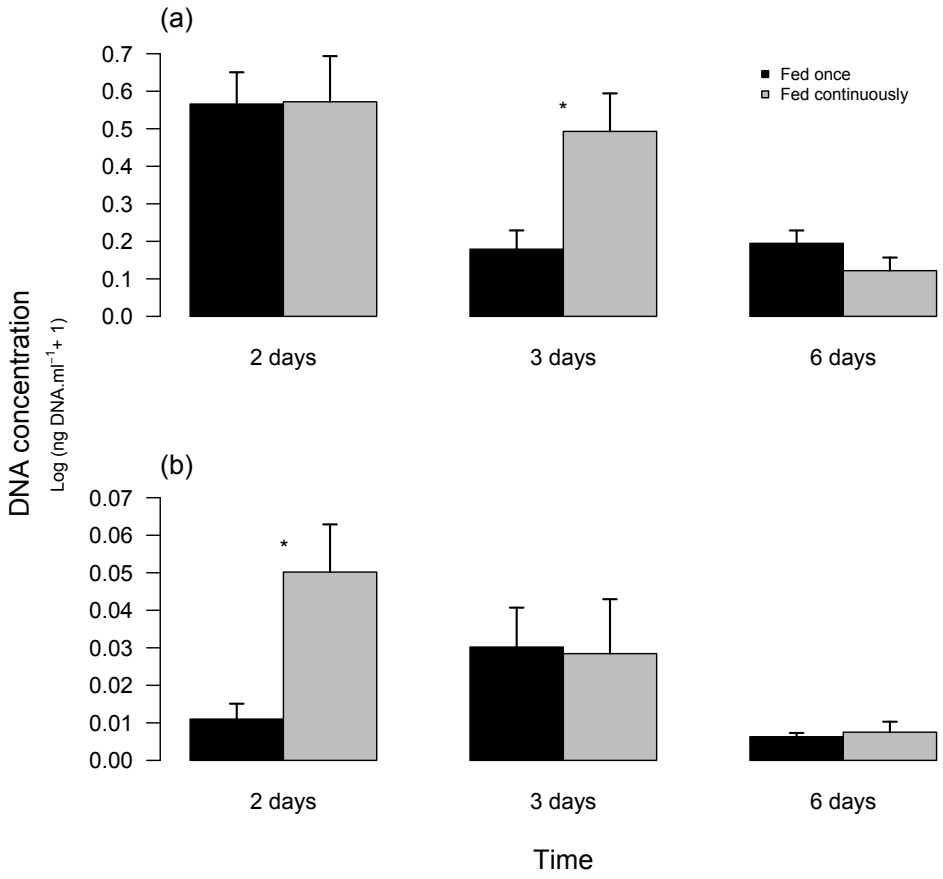

Fig. 5.5 Prey DNA content of *Oculina arbuscula* fed once and continuously. *O. arbuscula* fed once was fed either *Artemia* sp. (a) or *Brachionus plicatilis* (b) on day 0. *O. arbuscula* continuously fed were fed *B. plicatilis* or *Artemia* sp. every day depending whether they were fed *Artemia* or *B. plicatilis* on day 0, respectively. Error bars denote standard errors, and significant differences (p<0.05) between prey DNA content for the same day are marked (*).

5.4 Discussion

Development of molecular tools has transformed our ability to study zooxanthellate cnidarians, in particular the puzzling relationship between the cnidarian host and the endosymbiotic zooxanthellae (Davy et al. 2012, Meyer & Weis 2012). Molecular-based approaches can also be used to investigate heterotrophy of zooxanthellate cnidarians, particularly PCR-based methods that are already widely used to examine trophic relationships in terrestrial and marine invertebrates (e.g. Hoogendoorn & Heimpel 2001, Nejstgaard et al. 2003, Weber & Lundgren 2009, Lundgren & Fergen 2011). In this study, we applied for the first time these PCR-based approaches to

investigate heterotrophic feeding and digestion in zooxanthellate cnidarians, demonstrate the utility of these methods and provide new insights into the trophic ecology of these organisms.

Artemia sp. ingested by *O. arbuscula* did not exhibit the differential length prey breakdown pattern observed for the three other predator and prey combinations (Fig. 5.2a-d). The slow overall decrease of *Artemia* sp. DNA in the coral could indicate a reduced digestion and/or assimilation of *Artemia* sp. or, alternatively, a gradual egestion of undigested prey DNA. In contrast to the coral, *Aiptasia* sp. exhibited differential prey DNA breakdown when feeding on *Artemia* sp. (Fig. 5.1a-c), suggesting that different zooxanthellate cnidarian species may use different mechanisms to digest their prey. Further, differential DNA breakdown was observed for *B. plicatilis* in both predator species. This suggests species-specific prey DNA degradation or digestion, and/or an unequal assimilation of prey DNA as a source of nutrition. Exploration of this hypothesis will require further study.

The dla-qPCR assay also provides information regarding the optimal amplicon size to use in qPCR estimations of prey DNA and, consequently, prey digestion time. Prey DNA may be quickly degraded and affect quantification of ingested prey by leading to an underestimation of DNA levels (Deagle et al. 2006, Troedsson et al. 2009). In contrast to data available for other marine invertebrates, including copepods and pelagic tunicates that display prey digestion times up to a couple of hours (Durbin et al. 2012; ME Frischer, unpub. data), prey digestion in zooxanthellate cnidarians is significantly slower. This suggests that prey DNA can successfully be used to detect ingested prey in both laboratory and field studies, as long prey DNA digestion times are likely to maximize prey detectability. The laboratory assessment of the dla-qPCR profile of a particular predator-prey species combination thus provides important information for the *in situ* quantification of feeding rates using qPCR, as gut content estimates can be corrected based on prey DNA digestion (Troedsson et al. 2009). However, this species-specific approach may only be useful in the field when certain prey species are known to occur in the sampling site. Future studies using qPCR to quantify feeding in the field and laboratory should use specific primer sets for the target prey that amplify short sequences to minimize potential underestimation, as has been shown for many other organisms (Zaidi et al. 1999, Chen et al. 2000, Hoogendoorn & Heimpel 2001, Agustí et al. 2003). For purposes other than the assessment of specific-prey ingestion and digestion, for example the general identification of diet components, it is important that the information contained in the region between the primers also exhibits sufficient variability to distinguish the potential prey species in the system. The use of this approach in the field would require sequencing techniques with group-specific primers (see reviews by O'Rorke et al. 2012b, Pompanon et al. 2012).

Digestion time has been largely overlooked as a parameter in trophic studies of zooxanthellate cnidarians. Based on visual observation, it has been suggested that digestion of zooplankton in zooxanthellate cnidarians can take up to 6 h, although prey may remain in coelenterons for up to 12 h (Lewis 1982, Clayton Jr 1986, Fabricius et al. 1995, Sebens et al. 1996). In this study, prey DNA content in both *Aiptasia* sp. (Fig. 5.3) and *O. arbuscula* (Fig. 5.4) continues to decrease substantially for up to 1 or 3 days when fed *B. plcatilis* or *Artemia* sp., respectively. The discrepancy between early studies (Fabricius et al. 1995, Sebens et al. 1996) and our work are most likely associated with the use of the highly sensitive and specific molecular approaches. We suggest that digestion times of 1–3 days more likely represents the time of complete digestion compared to the shorter digestion times reported in previous studies. However, the extended periods up to 6 or 10 days (Fig. 5.4-Fig. 5.5) for which trace amounts of prey DNA was detected may reflect incomplete gastric evacuation of residual prey material rather than active digestion. This slower digestion strategy may also be associated with the presence of symbiotic microorganisms colonizing the cnidarians gut that maximize nutrient assimilation through a slow digestion, as observed in some terrestrial invertebrates (Douglas 2009). Similarly, as the gastric

cavity of corals has a high load of endosymbiotic bacteria (Agostini et al. 2011), prey digestion in zooxanthellate cnidarians may also be supported by a relatively slow endosymbiotic process similar to what have been observed in true bugs and spiders (Sheppard et al. 2005, Douglas 2009). Moreover, high nutrient concentrations were recorded in the coral gastric cavity, particularly phosphorus (Agostini et al. 2011). DNA is a phosphorous-rich nutrient source and it is possible that the long detection times of prey DNA may be associated with a strategy of these zooxanthellate cnidarians to store prey DNA as an energy/nutrient source. Although extracellular DNA is known to be an important nutrient source for bacteria (Finkel & Kolter 2001), further investigation is needed to assess the role of prey DNA in the nutrition of zooxanthellate cnidarians.

A second set of experiments with continuous feeding were performed in order to investigate if the long digestion times observed in this study were associated with post feeding starvation. The results show similar DNA contents on day 6 regardless of the heterotrophic starvation condition of the coral (Fig. 5.5; approximately 8% and 1%, respectively, of *Artemia* sp. and *B. plicatilis* DNA content recorded at day 0). These results suggest that prey DNA presence in coral polyps after 6 days (Fig. 5.4 andFig. 5.5) is not associated with a slower digestion of prey caused by the absence of other heterotrophic sources of food. However, differences in prey DNA content on days 2 and 3 between *O. arbuscula* starved after initial feeding and fed continuously (Fig. 5.5) may suggest a differential prey digestion associated with heterotrophic starvation.

This study provides new insights on the feeding and digestion mechanisms of zooxanthellate cnidarians. It also provides data of relevance for designing molecular approaches to study cnidarian heterotrophy in the laboratory and field. The long digestion times observed for zooxanthellate cnidarians have important implications for the definition of heterotrophic starvation in these organisms. We therefore suggest that future investigations addressing the effect of heterotrophic starvation in the ecophysiology of zooxanthellate cnidarians carefully consider the full time span of the starvation period when designing experiments. On the other hand, the long residence time of prey DNA may facilitate detection of prey DNA from field-collected specimens. Finally, sensitive and selective PCR-based approaches, such as shown here, opens new possibilities to study nutritional plasticity in the cnidarian-algal symbiosis and its response to stress events.

5.5 Acknowledgments

M.C.L. was supported by a PhD scholarship (SFRH/BD/63783/2009) funded by the Fundação para a Ciência e Tecnologia (QREN-POPH-Type 4.1 – Advanced Training, subsidized by the European Social Fund and national funds MCTES). Partial support was also provided by the US National Science Foundation to M.E.F. (awards OCE 0825999 and OCE 1031263) and J.C.N. (award OCE 0824499). The authors thank Christine Ferrier-Pagès for the discussion on coral heterotrophy and valuable input to this research and Devin Dumont and Karin Paquin from the University of Georgia Marine Extension Service Marine Education Center and Aquarium (MECA) for maintaining the corals. We are also grateful to Greg McFall and NOAA's Gray's Reef National Marine Sanctuary for access to and help collecting the corals used in this study, and to the editor and five anonymous reviewers for their helpful comments and suggestions to improve the manuscript.

5.6 References

Agostini S, Suzuki Y, Higuchi T, Casareto BE, Yoshinaga K, Nakano Y, Fujimura H (2011) Biological and chemical characteristics of the coral gastric cavity. Coral Reefs 31:147-156

Agustí N, Unruh TR, Welter SC (2003) Detecting *Cacopsylla pyricola* (Hemiptera: Psyllidae) in predator guts using COI mitochondrial markers. Bull Entomol Res 93:179-185

Anthony KRN, Fabricius KE (2000) Shifting roles of heterotrophy and autotrophy in coral energetics under varying turbidity. J Exp Mar Biol Ecol 252:221-253

Borell E, Yuliantri A, Bischof K, Richter C (2008) The effect of heterotrophy on photosynthesis and tissue composition of two scleractinian corals under elevated temperature. J Exp Mar Biol Ecol 364:116-123

Chen Y, Giles KL, Payton ME, Greenstone MH (2000) Identifying key cereal aphid predators by molecular gut analysis. Mol Ecol 9:1887-1898

Clayton Jr W (1986) Ingestion, digestion and assimilation efficiency of the sea-anemone *Aiptasia pallida* fed zooplankton prey. Int Rev Gesamt Hydrobiol 71:709-717

Davy SK, Allemand D, Weis VM (2012) Cell biology of cnidarian-dinoflagellate symbiosis. Microbiol Mol Biol Rev 76:229-261

Deagle BE, Eveson JP, Jarman SN (2006) Quantification of damage in DNA recovered from highly degraded samples - a case study on DNA in faeces. Front Zool 3:11

Douglas AE (2009) The microbial dimension in insect nutritional ecology. Funct Ecol 23:38-47

Durbin EG, Casas MC, Rynearson TA (2012) Copepod feeding and digestion rates using prey DNA and qPCR. J Plankton Res 34:72-82

Fabricius KE, Genin A, Benayahu Y (1995) Flow-dependent herbivory and growth in zooxanthellae-free soft corals. Limnol Oceanogr 40:1290-1301

Falkowski P, Dubinsky Z, Muscatine L, Porter J (1984) Light and the bioenergetics of a symbiotic coral. BioScience 34:705-709

Finkel SE, Kolter R (2001) DNA as a nutrient: novel role for bacterial competence gene homologs. J Bacteriol 183:6288-6293

Giribet G, Soernsen M, Funch P, Kristensen R, Sterrer W (2004) Investigations into the phylogenetic position of Micrognathozoa using four molecular loci. Cladistics 20:1-13

Grottoli AG, Rodrigues LJ, Palardy JE (2006) Heterotrophic plasticity and resilience in bleached corals. Nature 440:1186-1189

Gruebl T, Frischer M, Sheppard M, Neumann M, Maurer A, Lee R (2002) Development of an 18S rRNA gene-targeted PCR-based diagnostic for the blue crab parasite *Hematodinium* sp. Dis Aquat Org 49:61-70

Heid CA, Stevens J, Livak KJ, Williams PM (1996) Real time quantitative PCR. Genome Res 6:986-994

Highsmith R (1982) Reproduction by fragmentation in corals. Mar Ecol Prog Ser 7:207-226

Hoff F, Snell T (2008) Plankton culture manual, Florida Aqua Farms, Inc., Dade City, Florida, USA, 186 pp.

Hoogendoorn M, Heimpel G (2001) PCR-based gut content analysis of insect predators: using ribosomal ITS-1 fragments from prey to estimate predation frequency. Mol Ecol 10:2059-2067

Houlbrèque F, Tambutte E, Richard C, Ferrier-Pages C (2004) Importance of a micro-diet for scleractinian corals. Mar Ecol Prog Ser 282:151-160

Houlbrèque F, Ferrier-Pagès C (2009) Heterotrophy in Tropical Scleractinian Corals. Biol Rev 84:1-17

Kemp DW, Fitt WK, Schmidt GW (2008) A microsampling method for genotyping coral symbionts. Coral Reefs 27:289-293

King RA, Read DS, Traugott M, Symondson WO (2008) Molecular analysis of predation: a review of best practice for DNA-based approaches. Mol Ecol 17:947-963

Leal MC, Nunes C, Engrola S, Dinis M, Calado R (2012) Optimization of monoclonal production of the glass anemone *Aiptasia pallida* (Agassiz in Verrill, 1864). Aquaculture 354-355:91-96

Leal MC, Nunes C, Kempf SC, Reis A, Silva TL, Serôdio J, Cleary DFR, Calado R (2013) Effect of light, temperature and diet on the fatty acid profile of the tropical sea anemone *Aiptasia pallida*. Aquac Nutr 19:818-826

Leal MC, Ferrier-Pagès C, Calado R, Thompson ME, Frischer ME, Nejstgaard JC (2014) Coral feeding on microalgae assessed with molecular trophic markers. Mol Ecol 23:3870-3876

Lewis J (1982) Feeding behaviour and feeding ecology of the Octocorallia (Coelenterate: Anthozoa). J Zool 196:371-384

Lundgren JG, Fergen JK (2011) Enhancing predation of a subterranean insect pest: a conservation benefit of winter vegetation in agroecosystems. Appl Soil Ecol 51:9-16

Mackie JA, Geller J (2010) Experimental parameters affecting quantitative PCR of *Artemia franciscana*: a model for a marine zooplanktonic target in natural plankton samples. Limnol Oceanogr Methods 8:337-347

Meyer E, Weis VM (2012) Study of cnidarian-algal symbiosis in the "omics" age. Biol Bull 223:44-65

Miller M (1995) Growth of a temperate coral - Effects of temperature, light, depth, and heterotrophy. Mar Ecol Prog Ser 122:217-225

Nejstgaard JC, Frischer ME, Raule CL, Gruebel R, Kohlberg KE, Verity PG (2003) Molecular detection of algal prey in copepod guts and fecal pellets. Limnol Oceanogr Methods 1:29-38

Nejstgaard JC, Frischer ME, Simonelli P, Troedsson C, Brakel M, Adiyaman F, Sazhin AF, Artigas LF (2008) Quantitative PCR to estimate copepod feeding. Mar Biol 153:565-577

O'Rorke R, Lavery S, Chow S, Takeyama H, Tsai P, Beckley LE, Thompson PA, Waite AM, Jeffs AG (2012a) Determining the diet of larvae of western rock lobster (*Panulirus cygnus*) using high-throughput DNA sequencing tachniques. PLoS One 7:e42757

O'Rorke R, Lavery S, Jeffs A (2012b) PCR enrichment techniques to identify the diet of predators. Mol Ecol Resour 12:5-17

Palardy JE, Grottoli AG, Matthews KA (2005) Effects of upwelling, depth, morphology and polyp size on feeding in three species of Panamanian corals. Mar Ecol Prog Ser 300:79-89

Palardy JE, Rodrigues LJ, Grottoli AG (2008) The importance of zooplankton to the daily metabolic carbon requirements of healthy and bleached corals at two depths. J Exp Mar Biol Ecol 367:180-188

Pompanon F, Deagle BE, Symondson WOC, Brown DS, Jarman SN, Taberlet P (2012) Who is eating what: diet assessment using next generation sequencing. Mol Ecol 21:1931-1950

Porter JW (1976) Autotrophy, heterotrophy, and resource partitioning in Caribbean reef-building corals. Am Nat 110:731-742

R Development Core Team (2012) R: A language and environment for statistical computing. R Foundation for Statistical Computing. R Foundation for Statistical Computing, Vienna, Austria (http://www.R-project.org)

Roura Á, González ÁF, Redd K, Guerra Á (2012) Molecular prey identification in wild *Octopus vulgaris* paralarvae. Mar Biol 159:1335-1345

Rozen S, Skaletsky H (2000) Primer 3 on the WWW for general users and for biologist programmers. Methods Mol Biol 132:365-386

Sebens KP (1981) The allometry of feeding, energetics, and body size in three sea anemone species. Biol Bull 161:152-171

Sebens KP, Johnson AS (1991) Effects of water movement on prey capture and distribution of reef corals. Hydrobiologia 226:91-101

Sebens KP, Vandersall KS, Savina LA, Graham KR (1996) Zooplankton capture by two scleractinian corals, *Madracis mirabilis* and *Montastrea cavernosa*, in a field enclosure. Mar Biol 127:303-317

Sheppard SK, Bell J, Sunderland KD, Fenlon J, Skervin D, Symondson WO (2005) Detection of secondary predation by PCR analyses of the gut contents of invertebrate generalist predators. Mol Ecol 14:4461-4468

Sheppard SK, Harwood JD (2005) Advances in molecular ecology: tracking trophic links through predator-prey food-webs. Funct Ecol 19:751-762

Sheridan C, Kramarsky-Winter E, Sweet M, Kushmaro A, Leal MC (2013) Diseases in coral aquaculture: causes, implications and preventions. Aquaculture 396-399:124-135

Simonelli P, Troedsson C, Nejstgaard JC, Zech K, Larsen JB, Frischer ME (2009) Evaluation of DNA extraction and handling procedures for PCR-based copepod feeding studies. J Plankton Res 31:1465-1474

Symondson WOC (2002) Molecular identification of prey in predator diets. Mol Ecol 11:627-641

Titlyanov EA, Tsukahara J, Titlyanova TV, Leletkin VA, Van Woesik R, Yamazato K (2000) Zooxnthellae population density and physiological state of the coral *Stylophora pistillata* during starvation and osmotic shock. Symbiosis 28:303-322

Titlyanov EA, Titlyanova T, Yamazato K, Van Woesik R (2001) Photo-acclimation of the hermatypic coral *Stylophora pistillata* while subjected to either starvation or food provisioning. J Exp Mar Biol Ecol 257:163-181

Troedsson C, Frischer ME, Nejstgaard JC, Thompson EM (2007) Molecular quantification of differential ingestion and particle trapping rates by the appendicularian *Oikopleura dioica* as a function of prey size and shape. Limnol Oceanogr 52:416-427

Troedsson C, Simonelli P, Nägele V, Nejstgaard JC, Frischer ME (2009) Quantification of copepod gut content by differential length amplification quantitative PCR (dla-qPCR). Mar Biol 156:253-259

van Os N, Massé LM, Séré MG, Sara JR, Schoeman DS, Smit AJ (2012) Influence of heterotrophic feeding on the survival and tissue growth rates of *Galaxea fascicularis* (Octocorralia: Occulinidae) in aquaria. Aquaculture 330-333:156-161

Venn A, Loram J, Douglas A (2008) Photosynthetic symbioses in animals. J Exp Bot 59:1069-1080

Vogel S, LaBarbera M (1978) Simple flow tanks for research and teaching. BioScience 28:638-643

Weber DC, Lundgren JG (2009) Detection of predation using qPCR: effect of prey quantity, elapsed time, chaser diet, and sample preservation on detectable quantity of prey DNA. J Insect Sci 9:41

Weekers PHH, Murugan G, Vanfleteren JR, Belk D, Dumont HJ (2002) Phylogenetic analysis of anostracans (Branchiopoda: Anostraca) inferred from nuclear 18S ribosomal DNA (18S rDNA) sequences. Mol Phylogen Evol 25:535-544

Weis V, Davy S, Hoegh-Guldberg O, Rodriguez-Lanetty M, Pringle J (2008) Cell biology in model systems as the key to understanding corals. Trends Ecol Evol 23:369-376

Zaidi R, Jaal Z, Hawkes N, Hemingway J, Symondson WO (1999) Can multiple-copy sequences of prey DNA be detected amongst the gut contents of invertebrate predators? Mol Ecol 8:2081-2087

Chapter 6 Coral feeding on microalgae assessed with molecular trophic markers

Abstract

Herbivory in corals, especially for symbiotic species, remains controversial. To investigate the capacity of scleractinian and soft corals to capture microalgae, we conducted controlled laboratory experiments offering five algal species: the cryptophyte *Rhodomonas marina*, the haptophytes *Isochrysis galbana* and *Phaeocystis globosa*, and the diatoms *Conticribra weissflogii* and *Thalassiosira pseudonana*. Coral species included the symbiotic soft corals *Heteroxenia fuscescens* and *Sinularia flexibilis*, the asymbiotic scleractinian coral *Tubastrea coccinea*, and the symbiotic scleractinian corals *Stylophora pistillata, Pavona cactus* and *Oculina arbuscula.* Herbivory was assessed by endpoint PCR amplification of algae-specific 18S rRNA gene fragments purified from coral tissue genomic DNA extracts. The ability to capture microalgae varied with coral and algal species and could not be explained by prey size or taxonomy. Herbivory was not detected in *S. flexibilis* and S. *pistillata*. *P. globosa* was the only algal prey that was never captured by any coral. Although predation defence mechanisms have been shown for *Phaeocystis* spp. against many potential predators, this study is the first to suggest this for corals. This study provides new insights on herbivory in symbiotic corals and suggests that corals may be selective herbivorous feeders.

Keywords

Heterotrophy; Phytoplankton; PCR; Coral feeding; Specific primers.

Published: Leal MC, Ferrier-Pagès C, Calado R, Thompson ME, Frischer ME, Nejstgaard JC (2014) Coral feeding on microalgae assessed with molecular trophic markers. Molecular Ecology 23: 3870-3876 (doi:10.1111/mec.12486)

6.1 Introduction

Symbiotic and asymbiotic corals are able to ingest a wide range of prey, from pico- and nanoplankton to mesozooplankton (see review by Houlbrèque & Ferrier-Pagès 2009). For symbiotic corals that harbour photosynthetic dinoflagellates (zooxanthellae), ingested prey provides essential nutrients that cannot be supplied by zooxanthellae. However, heterotrophic feeding may also account for a significant fraction of the fixed carbon, especially during bleaching events, or in deep and/or turbid areas when photosynthetic products are unavailable (Anthony & Fabricius 2000, Grottoli et al. 2006).

Most studies addressing coral heterotrophy have focused on the ingestion of zooplankton prey and have documented significant ingestion rates (e.g. Sebens et al. 1996, Sebens et al. 1998, Palardy et al. 2008). In contrast, the ability of corals (sub-class Hexacorallia) to ingest phytoplankton has been overlooked and, therefore, the importance of herbivory in coral nutrition remains unclear for most species. Although the capacity of asymbiotic soft corals (order Alcyonacea) to feed on phytoplankton has been relatively well investigated (e.g. Fabricius et al. 1995a,b, Widdig & Schlichter 2001, Migne & Davoult 2002, Orejas et al. 2003, Lira et al. 2008), only a few studies have investigated herbivory in symbiotic corals (Sorokin 1973, Ribes et al. 1998, Tremblay et al. 2012, Seemann et al. 2013). Further, it is not known if selectivity occurs when feeding on microalgae and, if so, what are the mechanisms involved. This knowledge gap may be associated with methodological limitations. Current techniques to assess coral feeding include microscopy of dissected polyps and prey removal rates in feeding chambers. The first method is expected to be inaccurate for microalgae because such small prey items are difficult to detect quantitatively in the relatively large polyps, and microalgae may rapidly loose recognizable features such as fluorescence, flagella and cell shape after ingestion. The prey removal approach does not allow its detection in high prey concentrations when microalgae ingestion may be high, and may be prone to several containment effects including trophic cascades as discussed in Nejstgaard et al. (2008).

In this study, we performed a qualitative assessment of the potential for symbiotic and asymbiotic corals to capture microalgae using molecular trophic markers. While these molecular tools have been successfully used to study marine invertebrate trophic interactions (e.g. Troedsson et al. 2007, Simonelli et al. 2009, O'Rorke et al. 2012a, Roura et al. 2012), they have only been used once to investigate coral feeding on zooplankton (Leal et al. 2014).

In order to assess the potential for coral herbivory, laboratory feeding studies were conducted with two symbiotic soft corals, three symbiotic and one asymbiotic scleractinian corals. Corals were offered five different microalgae separately as monospecific prey concentrations typical of bloom conditions. Prey capture was assessed using endpoint PCR and prey species-specific primers targeted to the 18S rRNA gene of the different microalgae prey in order to address the following two initial hypotheses: (i) tested coral species are able to capture microalgae and (ii) prey size and/or taxonomy determines coral success in capturing microalgae.

6.2 Materials and Methods

6.2.1 Corals

Two soft and four scleractinian coral species were investigated in this study: the tropical corals *Tubastrea coccinea*, *Heteroxenia fuscescens, Pavona cactus, Stylophora pistillata and Sinularia flexibilis* and the temperate coral *Oculina arbuscula* (Table 6.1). Coral species selection was based on the range of different coral types (scleractinian/soft corals and presence/absence of

zooxanthellae) that was available either in laboratory cultures or by field access. With the exception of *O. arbuscula*, all corals were cultured at 26 °C in open flow-through aquaria supplied with natural seawater continuously pumped from a 50-m depth well (renewal rate of 50% h^{-1}). The four tropical symbiotic species were maintained at an irradiance of 200 µmol photons m^{-2} s^{-1} (12 h light: 12 h dark cycle). The asymbiotic species, *T. coccinea,* was maintained in the dark. Feeding trials using these species were conducted at Centre Scientifique de Monaco. The temperate symbiotic species *O. arbuscula* was maintained under an irradiance of 100 µmol photons m^{-2} s^{-1} (12 h light: 12 h dark cycle) at 24 °C in a recirculating system composed of a 200 L aquarium connected with a 100 L reservoir equipped with a protein skimmer and a biological filter. Partial water changes (20%) were performed weekly using freshly pumped filtered seawater. Experiments with *O. arbuscula* were conducted at the Skidaway Institute of Oceanography (Savannah, Georgia, USA).
Coral nubbins were prepared from three different colonies from each coral species by cutting their apical branches or, for soft corals, portions of several polyps. Coral nubbins were allowed to heal until tissue recovery was observed at the sites of fracture. The five symbiotic corals were not fed until the experimental feeding trials were performed (at least 2 weeks before the trials). The asymbiotic *T. coccinea* was fed twice a week with newly hatched *Artemia* sp. nauplii.

Table 6.1 Coral species used in this study. All corals are tropical, except for the temperate *Oculina arbuscula*.

Species	Family	Coral type	Distribution[#] (collection site)	Symbiotic status	Polyp size (diameter in mm)
Tubastrea coccinea	Dendrophylliidae	Scleractinian	Coral reefs worldwide (southeast Asia)	Asymbiotic	10-12
Heteroxenia fuscescens	Xeniidae	Soft	Red Sea and Eastern Africa (Red Sea)	Symbiotic	8-10 (1 mm mouth)
Oculina arbuscula	Oculinidae	Scleractinian	Mid and South Atlantic Bight (Georgia coast, USA)	Symbiotic	2-3
Pavona cactus	Agariciidae	Scleractinian	Indo-Pacific, Red-Sea and Western Indian Ocean (Red Sea)	Symbiotic	0.2-0.3
Stylophora pistillata	Pocilloporidae	Scleractinian	Indo-Pacific, Red-Sea and Western Indian Ocean (Red Sea)	Symbiotic	0.5-1
Sinularia flexibilis	Alcyoniidae	Soft	Indo-Pacific (Indo-Pacific)	Symbiotic	0.5

[#] Distribution according with Veron (2000)

6.2.2 Microalgae

Five microalgal species from three phyla were utilized as prey during this study: the diatoms *Conticribra weissflogii* and *Thalassiosira pseudonana*, the cryptophyte *Rhodomonas marina,* and the haptophytes *Isochrysis galbana* and *Phaeocystis globosa* (see Table 6.2 for strain, source and cell size). Microalgae species selection was based on availability in cultures and what has been commonly used as model phytoplankton prey species. All algae were grown in semi-continuous batches, in *f*/2 media, 14:10 h light cycle and at 20 °C. All microalgae used in the experiments were single-cell form in exponential growth phase.

Table 6.2 Microalgae used as prey in this study. All algae were grown in single cell (solitary) form.

Species	Algae group	Distribution[#]	Cell size (μm)	Source / Strain
Conticribra weissflogii	Diatom	Coastal waters in the Atlantic and Pacific Oceans	5-12	CCMP 1050
Thalassiosira pseudonana	Diatom	World's oceans	4-6	CCMP 1335
Rhodomonas marina	Cryptophyte	Northeast Atlantic	5-8	IFREMER (Brest, France)
Isochrysis galbana	Haptophyte	Northeast Atlantic	4-6	CCMP 1611
Phaeocystis globosa	Haptophyte	World's oceans	4-6	CCMP 628

According with www.algaebase.org and www.marinespecies.org

6.2.3 Feeding experiments

Feeding experiments were performed in triplicate with each of the six coral species and each of the five microalgae prey species, respectively (6 coral species x 5 microalgae species x 3 replicates = 90 feeding trials). Each coral nubbin was individually incubated in 200 mL cylindrical feeding chambers. Preliminary feeding experiments conducted with newly hatched *Artemia* sp. nauplii confirmed that feeding behaviour was not affected by the gentle semi-circular mixing generated by a magnetic stirring plate (130 rpm) in the experimental feeding chambers. After the polyps were completely expanded, a single microalgae species was added at a final concentration of approximately 10^4 cells mL^{-1}. Corals were allowed to feed for 60 min, and after this period, each coral fragment was harvested and thoroughly rinsed three times in consecutive baths of freshly filtered seawater (Whatman GF/F filter, nominal pore size 0.7 μm) to remove any algae remaining on the coral surface layer (Sebens et al. 1996, Ribes et al. 1998, Anthony 2000). Negative experimental feeding controls consisted of corals placed in feeding chambers without algal prey and processed exactly as fed animals. Positive experimental controls consisted of analysis of feeding chamber water after algal prey had been added. Water was collected and filtered onto 0.8 μm Supor (Pall Corp) filters and genomic DNA (gDNA) extracted. All experimental controls were conducted in triplicate. Coral tissue from scleractinian species was harvested using an air pick, while the polyps of soft corals were cut into small pieces. The air pick consisted of a 0.8 mm opening plastic pipette tip attached to a flexible tubing, collection bottle and a vacuum pump, as successfully used by Ferrier-Pagès et al. (2011) and others to harvest tissue from scleractinian corals.

6.2.4 DNA extraction, primer design and PCR

The gDNA was purified from coral tissues and microalgae using the DNeasy Blood & Tissue kit (Qiagen, Valencia, CA, USA), following the manufacturer's specifications. To maximize DNA yield, DNA was eluted twice from the DNeasy spin columns with 100 μL of elution buffer supplied by the manufacturer.

Prey-specific PCR primers used in this study are shown in Table 6.3. Unless otherwise noted, 18S rRNA gene targeted PCR primers used in this study were designed using the software package Primer3 (Rozen & Skaletsky 2000). Algal species sequence alignments were constructed using the BioEdit sequence alignment editor (Hall 1999). Regions conserved in target organisms but divergent from other diatoms, cryptophytes and haptophytes were targeted for primer design. The specificity of each primer pair in detecting algal DNA was confirmed empirically in PCR assays

against gDNA purified from all coral and algal species used in this study, and against *Artemia* sp. that was used to feed the asymbiotic corals. However, these primer sets were not specifically validated for use beyond this study and therefore should be used cautiously in any future studies. All oligonucleotides were synthesized and purified (standard desalting) by Integrated DNA Technologies (www.IDT.com).

Table 6.3 Primers used in this study and its product length and optimal annealing for each microalgae species.

Microalgae	Forward primer (5' to 3')	Reverse primer (5' to 3')	Product length (bp)	Annealing temperature (ºC)
Conticribra weissflogii	CTA TGC CGA CTC AGG ATT GG	ATG CAC CAC CAC CCA TAG AA	244	60
Thalassiosira pseudonana	CTA TGC CGA CTC AGG ATT GG	ATG CAC CAC CAC CCA TAG AA	244	50
Rhodomonas marina	GCG ACT CCA TTG GCA CCT TGT[a]	CAA TGT CTG GAC CTG GTA AGT	175	57
Isochrysis galbana	CCG ACT AGG GAT TGG AGG AT	ATT TAG CAG GCT GCG GTC TC	295	55
Phaeocystis globosa	GGC TAC TTC TAG TCT TGT AAT TGG A[b]	AAA GAA GGC CGC GCC[b]	194	56

[a] From Troedsson et al. (2009)
[b] From Nejstgaard et al. (2008)

All PCRs were performed in 25 µL reaction volumes using prey-specific primers (Table 6.3). PCR was performed using an Applied Biosystems GeneAmp PCR System 9700 and the Qiagen Taq PCR Master Mix reagents (Qiagen, Valencia, CA, USA). Each reaction contained 12.5 µL of Qiagen Taq PCR Master Mix, 120 nM of each primer and template gDNA ranging from 200 to 600 ng mL^{-1}. This concentration was achieved using 2 µL of either undiluted or ten-fold dilution (in water) of the gDNA purifications. Amplification conditions consisted of an initial denaturation step (10 min, 94 ºC) followed by 35 3-step amplification cycles (denaturation: 30 s, 94 ºC; annealing: 30 s, temperature described in Table 3; extension: 60 s, 72 ºC) and by a final extension step (72 ºC, 7 min). PCR grade water was used as template for negative control. PCR products were visualized by gel electrophoresis on a 2% agarose gel buffered in 1X TAE (0.04M Tris-Acetate, 1mM EDTA, pH 8.0).

6.3 Results and Discussion

Endpoint PCR was successfully used to detect microalgal small subunit (18S) rRNA gene fragments in total gDNA extracts collected from corals immediately after exposure to single species microalgae suspensions. Herbivory was detected in four of the six corals for at least one type of microalgae prey. *T. coccinea*, the only asymbiotic coral examined in this study, captured the largest range of prey types (three of five microalgae species). Herbivory was not detected in *S. flexibilis* and *S. pistillata* (Table 6.4). The haptophyte *I. galbana* was the microalgae detected in most corals (three of six coral species). In contrast, the closely taxonomically related and similar sized (4-6 µm) microalgae *P. globosa* was not detected in any of the six tested corals. Although only three of the five symbiotic corals captured some microalgae, these results support the hypothesis that corals are able to capture microalgae but indicate that herbivory can be variable across coral species and algal prey types. There was not a clear relationship between prey selection and algae prey size or prey taxonomy in the relatively small-sized phytoplankton tested here.

Table 6.4 Number of times algal prey was detected per a total of three feeding experiments performed for each coral species and prey microalgae combination.

Coral species	*Conticribra weissflogii*	*Thalassiosira pseudonana*	*Rhodomonas marina*	*Isochrysis galbana*	*Phaeocystis globosa*
Tubastrea coccinea	3	3	0	1	0
Heteroxenia fuscescens	0	0	3	0	0
Oculina arbuscula	2	0	0	2	0
Pavona cactus	0	0	3	2	0
Stylophora pistillata	0	0	0	0	0
Sinularia flexibilis	0	0	0	0	0

The question of whether zooxanthellate scleractinian corals are capable of feeding heterotrophically and specifically whether they may feed on microalgae has been a matter of speculation for some time. Three decades ago, Sorokin (1973) addressed this question reporting herbivory in *Pavona* sp. In a more recent study, Tremblay *et al.* (2012) reported that *S. pistillata* was able to graze on natural mixtures of pico- and nanoplankton. However, *S. pistillata* did not capture any of the microalgae in the present study. A possible explanation for these differences may be that this coral species is a selective feeder.

The results from this study support the possibility of selective microalgae grazing by zooxanthellate corals although the basis for such selectivity is unknown. For example, *P. cactus* and *O. arbuscula* were only able to capture some of the microalgae species tested (Table 6.4). A hypothesis that could explain selective feeding is a relationship between coral polyp and prey size. However, in this study, all microalgae were similarly sized (4-12 µm) and orders of magnitude smaller than the polyp width (0.2-12 mm) (Table 6.1). For example, *O. arbuscula*, a species with relatively large polyps (2-3 mm in diameter) and *P. cactus*, a species with smaller polyps (0.2-0.3 mm in diameter), were both able to capture the small (4 – 6 µm) microalgae *I. galbana*. Further, *R. marina*, *I. galbana* and *T. pseudonana* have very similar sizes (4-8 µm, Table 6.2), but contrasting results were observed among the different coral species provided with these prey (Table 6.4). Similarly, others have reported that polyp size does not limit zooplankton feeding or influence feeding rates (Sebens et al. 1996, Palardy et al. 2005, 2006). These observations suggest that coral grazing on microalgae and zooplankton is not simply a matter of physical capacity and that other factors are likely to be involved. An alternative hypothesis to size-based selectivity is prey mobility-based selectivity. However, this would not likely explain the striking difference between the two very similar sized haptophyte species *I. galbana* and *P. globosa* (Table 6.4).

Another possibility may be a differential feeding preference by each coral species based on algal palatability. However, if this is the case, selectivity will likely be difficult to predict based on algal taxonomy alone. For example, *O. arbuscula* fed differently on two closely related diatom species (*T. pseudonana* and *C. weissflogii*) (Table 6.4). Similarly, the results from this study with the asymbiotic coral *T. coccinea* highlight the difficulty of predicting prey preference. As an asymbiotic coral species, *T. coccinea* is generally thought to be able to feed on phytoplankton (Fabricius et al. 1995a,b). However, in this study, we were not able to detect feeding by *T. coccinea* on *P. globosa* or *R. marina*. Selectivity based on algal palatability could explain negative results, as it is unknown whether these microalgae species are present in coral reefs and therefore may be considered artificial prey. On the other hand, besides *P. globosa*, all other algae selected for the experiments

are widely used food algae that have never been found toxic. Thus, they would represent good model algae for generic tests of potential feeding. In addition, although these microalgae are mainly recorded in temperate environments, most of them have a relatively broad distribution (Table 6.2). However, the use of prey species that may be absent from tropical ecosystems is not likely to cause any bias, as corals are capable to feed on prey that are known to be absent from their natural habitat, such as *Artemia* cysts and nauplii (e.g. Helmuth & Sebens 1993, Sebens et al. 1998, Piniak 2002).

One possible mechanism for feeding selectivity could also be entrapment of algae cells in coral mucus, that is, false positives due to an incomplete wash process before extraction. However, our results do not support this, as we would expect the majority of tested algae species to be trapped by the most mucus-producing species if microalgae would passively be entrapped in the mucus. Further, while the highly mucus producing *S. pistillata* and *S. flexibilis* did not show any positives for the microalgae, the much less mucous producing *P. cactus* showed positive PCR products for two of the tested algae.

Consistent in this study was the avoidance of *P. globosa* as a prey item. Feeding-deterring mechanisms have been reported for *Phaeocystis* spp. for a wide range of potential predators (Nejstgaard et al. 2007). We therefore speculate that this may be due to feeding deterring mechanism(s) as has previously been reported also for strains of single-celled *P. globosa* fed to copepod nauplii (Dutz & Koski 2006). To our knowledge, this is the first time potential feeding-deterring effects in *Phaeocystis* spp. have been suggested for corals.

In conclusion, this study contributes to the growing understanding that both symbiotic and asymbiotic corals have the capacity to capture phytoplankton. This finding has ecological consequences to coral reef ecology, as phytoplankton has been largely overlooked as a potential food source of symbiotic corals. Furthermore, symbiotic corals may now be considered in carbon budgets assessing phytoplankton grazing and benthic-pelagic coupling in coral reefs (Yahel et al. 1998), which may contribute to the understanding of the complex food web dynamics of coral reef ecosystems. We further provide new insights on prey selectivity; specifically that prey selectivity may not be predictable based on prey size or taxonomy alone. However, future feeding selectivity studies should expand the range of microalgae and corals species, which should encompass a wider range of prey and polyp sizes. Ultimately, coral herbivory may be investigated *in situ*, where the range of prey and predators are much larger. Therefore, the methodological approach using species-specific primers may only be useful when certain prey species are known to occur in the sampling site. An alternative approach to investigate coral herbivory in nature would be to use sequencing techniques with group-specific primers (O'Rorke et al. 2012b, Pompanon et al. 2012).

6.4 Acknowledgments

M.C.L. was supported by a Ph.D scholarship (SFRH/BD/63783/2009) funded by the Fundação para a Ciência e Tecnologia (QREN-POPH-Type 4.1 – Advanced Training, subsidized by the European Social Fund and national funds MCTES). M.E.F., M.E.T. and an undergraduate assistant Christy Pavel were supported by the US National Science Foundation (OCE 082599 and 1031263). J.C.N. was supported by the US National Science Foundation (OCE 0824499) and C.F.-P. by the government of the Principality of Monaco. The authors thank Cécile Rottier and Séverine Sikorski for help with coral maintenance, feeding experiments and DNA extractions, Laura Birsa for culture maintenance, Christy Pavel for help with developing primer sets, and University of Georgia Marine Extension Service for tank maintenance, particularly Devin Dumont and Karin Paquin. We are also grateful to three anonymous reviewers and to NOAA Gray's Reef, particularly Greg McFall and Sarah Fangman. *Oculina arbuscula* corals were collected at Gray's Reef National Marine Sanctuary under the manager's permit.

6.5 References

Anthony K (2000) Enhanced particle-feeding capacity of corals on turbid reefs (Great Barrier Reef, Australia). Coral Reefs 19:59-67

Anthony KRN, Fabricius KE (2000) Shifting roles of heterotrophy and autotrophy in coral energetics under varying turbidity. J Exp Mar Biol Ecol 252:221-253

Dutz J, Koski M (2006) Trophic significance of solitary cells of the prymnesiophyte *Phaeocystis globosa* depends on cell type. Limnol Oceanogr 51:1230-1238

Fabricius KE, Benayahu Y, Genin A (1995a) Herbivory in asymbiotic soft corals. Science 268:90-92

Fabricius KE, Genin A, Benayahu Y (1995b) Flow-dependent herbivory and growth in zooxanthellae-free soft corals. Limnol Oceanogr 40:1290-1301

Ferrier-Pagès C, Peirano A, Abbate M, Cocito S, Negri A, Rottier C, Riera P, Rodolfo-Metalpa R, Reynaud S (2011) Summer autotrophy and winter heterotrophy in the temperate symbiotic coral *Cladocora caespitosa*. Limnol Oceanogr 56:1429-1438

Grottoli AG, Rodrigues LJ, Palardy JE (2006) Heterotrophic plasticity and resilience in bleached corals. Nature 440:1186-1189

Hall TA (1999) BioEdit: a user-friendly biological sequence alignment editor and analysis program for Windows 95/98/NT. Nucleic Acids Symposium Series 41:95-98

Helmuth B, Sebens K (1993) The influence of colony morphology and orientation to flow on particule capture by the scleractinian coral *Agaricia agaricites* (Linnaeus). J Exp Mar Biol Ecol 165:251-278

Houlbrèque F, Ferrier-Pagès C (2009) Heterotrophy in tropical scleractinian corals. Biol Rev 84:1-17

Leal MC, Nejstgaard JC, Calado R, Thompson ME, Frischer ME (2014) Molecular assessment of heterotrophy and prey digestion in zooxanthellate cnidarians. Mol Ecol 23:3838-3848

Lira AKF, Naud J-P, Gomes PB, Santos AM, Perez CD (2008) Trophic ecology of the octocoral *Carijoa riisei* from littoral of Pernambuco, Brazil. I. Composition and spatio-temporal variation of the diet. J Mar Biol Assoc UK 89:89-99

Migne A, Davoult D (2002) Experimental nutrition in the soft coral *Alcyonium digitatum* (Cnidaria: Octocorallia): removal rate of phytoplankton and zooplankton. Cah Biol Mar 43:9-16

Nejstgaard JC, Tang KW, Steinke M, Dutz J, Koski M, Antajan E, Long JD (2007) Zooplankton grazing on *Phaeocystis*: a quantitative review and future challenges. Biogeochemistry 83:147-172

Nejstgaard JC, Frischer ME, Simonelli P, Troedsson C, Brakel M, Adiyaman F, Sazhin AF, Artigas LF (2008) Quantitative PCR to estimate copepod feeding. Mar Biol 153:565-577

O'Rorke R, Lavery S, Chow S, Takeyama H, Tsai P, Beckley LE, Thompson PA, Waite AM, Jeffs AG (2012a) Determining the diet of larvae of western rock lobster (*Panulirus cygnus*) using high-throughput DNA sequencing tachniques. PLoS One 7:e42757

O'Rorke R, Lavery S, Jeffs A (2012b) PCR enrichment techniques to identify the diet of predators. Mol Ecol Resour 12:5-17

Orejas C, Gili J-M, Arntz W (2003) Role of small-plankton communities in the diet of two Antarctic octocorals (*Primnoisis antarctica* and *Primnoella* sp.). Mar Ecol Prog Ser 250:105-116

Palardy JE, Grottoli AG, Matthews KA (2005) Effects of upwelling, depth, morphology and polyp size on feeding in three species of Panamanian corals. Mar Ecol Prog Ser 300:79-89

Palardy JE, Grottoli AG, Matthews KA (2006) Effect of naturally changing zooplankton concentrations on feeding rates of two coral species in the Eastern Pacific. J Exp Mar Biol Ecol 331:99-107

Palardy JE, Rodrigues LJ, Grottoli AG (2008) The importance of zooplankton to the daily metabolic carbon requirements of healthy and bleached corals at two depths. J Exp Mar Biol Ecol 367:180-188

Piniak G (2002) Effects of symbiotic status, flow speed, and prey type on prey capture by the facultatively symbiotic temperate coral *Oculina arbuscula*. Mar Biol 141:449-455

Pompanon F, Deagle BE, Symondson WOC, Brown DS, Jarman SN, Taberlet P (2012) Who is eating what: diet assessment using next generation sequencing. Mol Ecol 21:1931-1950

Ribes M, Coma R, Gili J (1998) Heterotrophic feeding by gorgonian corals with symbiotic zooxanthella. Limnol Oceanogr 43:1170-1179

Roura Á, González ÁF, Redd K, Guerra Á (2012) Molecular prey identification in wild *Octopus vulgaris* paralarvae. Mar Biol 159:1335-1345

Rozen S, Skaletsky H (2000) Primer 3 on the WWW for general users and for biologist programmers. Methods Mol Biol 132:365-386

Sebens KP, Vandersall KS, Savina LA, Graham KR (1996) Zooplankton capture by two scleractinian corals, *Madracis mirabilis* and *Montastrea cavernosa*, in a field enclosure. Mar Biol 127:303-317

Sebens KP, Grace SP, Helmuth B, Maney Jr EJ, Miles JS (1998) Water flow and prey capture by three scleractinian corals, *Madracis mirabilis*, *Montastrea cavernosa* and *Porites porites*, in a field enclosure. Mar Biol 131:347-360

Seemann J, Berry KL, Carballo-Bolaños R, Struck U, Leinfelder RR (2013) The use of ^{13}C and ^{15}N isotope labeling techniques to assess heterotrophy of corals. J Exp Mar Biol Ecol 442:88-95

Simonelli P, Troedsson C, Nejstgaard JC, Zech K, Larsen JB, Frischer ME (2009) Evaluation of DNA extraction and handling procedures for PCR-based copepod feeding studies. J Plankton Res 31:1465-1474

Sorokin YI (1973) On the feeding of some scleractinian corals with bacteria and dissolved organic matter. Limnol Oceanogr 18:380-385

Tremblay P, Naumann MS, Sikorski S, Grover R, Ferrier-Pagès C (2012) Experimental assessment of organic carbon fluxes in the scleractinian coral *Stylophora pistillata* during a thermal and photo stress event. Mar Ecol Prog Ser 453:63-77

Troedsson C, Frischer ME, Nejstgaard JC, Thompson EM (2007) Molecular quantification of differential ingestion and particle trapping rates by the appendicularian *Oikopleura dioica* as a function of prey size and shape. Limnol Oceanogr 52:416-427

Troedsson C, Simonelli P, Nägele V, Nejstgaard JC, Frischer ME (2009) Quantification of copepod gut content by differential length amplification quantitative PCR (dla-qPCR). Mar Biol 156:253-259

Veron JEN (2000) Corals of the World, Australian Institute of Marine Science, Townsville, Qld, Australia. 1382 pp.

Widdig A, Schlichter D (2001) Phytoplankton: a significant trophic source for soft corals? Helgol Mar Res 55:198-211

Yahel G, Post A, Fabricius K, Marie D, Vaulot D, Genin A (1998) Phytoplankton distribution and grazing near coral reefs. Limnol Oceanogr 43:551-563

Chapter 7 Trophic ecology of the facultative symbiotic coral *Oculina arbuscula*

Abstract

Symbiotic corals are trophically complex, relying on both auto- and heterotrophy. Here, the nutrition of the temperate facultative symbiotic scleractinian coral *Oculina arbuscula* was investigated under natural conditions. Nutrition of symbiotic and aposymbiotic colonies during spring and fall was assessed by determining the carbon and nitrogen isotope signature of its tissues, photosynthetic endosymbionts and potential food sources (plankton and particulate organic matter) in seawater and sediment. The nutrition of symbiotic colonies was primarily derived from their endosymbionts, regardless of the season. However, aposymbiotic colonies of *O. arbuscula* relied preferentially on sediment organic matter as well as pico- and nanoplankton (<10 µm). As this small planktonic fraction that includes phytoplankton has been overlooked as a potential food source for symbiotic scleractinian corals, this study provides new insights into this feeding mode in these reef-building organisms.

Keywords

Heterotrophy; Autotrophy; Symbiosis; Aposymbiotic; Stable Isotopes.

Published: Leal MC, Ferrier-Pagès C, Calado R, Brandes JA, Frischer ME, Nejstgaard JC (2014) Trophic ecology of the facultative symbiotic coral *Oculina arbuscula*. Marine Ecology Progress Series 504: 171-179 (doi: 10.3354/meps.10750)

7.1 Introduction

Nutrition of symbiotic corals relies largely on organic compounds supplied by endosymbiotic dinoflagellates from genus *Symbiodinium* (hereafter referred to as symbionts) (Porter 1976, Falkowski et al. 1984). Up to 100% of the metabolic requirements of the coral host is supplied by photosynthetically-fixed carbon translocated from its symbionts under optimal light conditions (Muscatine et al. 1981). Besides autotrophy, corals are also able to feed heterotrophically, particularly by capturing zooplankton and other planktonic organisms (Houlbrèque & Ferrier-Pagès 2009, Leal et al. 2014a). Experimental studies have shown that feeding increases photosynthesis, respiration and calcification rates in several coral species (e.g. Ferrier-Pagès et al. 2003, Houlbrèque et al. 2003, 2004a, Rodrigues & Grottoli 2007). Heterotrophy is also known to play an important role in coral metabolism particularly under stressful conditions, for example when light is limiting or during bleaching events (Anthony & Fabricius 2000, Grottoli et al. 2006, Palardy et al. 2008, Leal et al. 2013).

There is ample literature on experimental studies of coral nutrition (see review by Houlbrèque & Ferrier-Pagès 2009). In contrast, field studies assessing the importance of heterotrophy for coral metabolism are limited. This knowledge gap is likely associated with constraints in tracing nutrient fluxes between corals and their constantly changing food environment. Thus, only a few studies have assessed so far the grazing impact of whole coral communities by measuring the plankton abundance upstream and downstream of waters flowing above the reef (Glynn 1973, Ribes et al. 2003, Yahel et al. 2005, Houlbrèque et al. 2006), while others performed coral gut content dissections (e.g. Sebens et al. 1996, Palardy et al. 2006).

Stable carbon and nitrogen isotope ratios ($\delta^{13}C$ and $\delta^{15}N$) have been used in laboratory experiments to assess the relative importance of auto- and heterotrophy in coral nutrition. A review of the literature indicates that $\delta^{13}C$ signatures of corals and their symbionts are generally similar as it reflects a high degree of nutrient exchange between the two partners (e.g. Muscatine et al. 1989, Reynaud et al. 2002), with a slightly more negative value for the coral host that further decreases if heterotrophy becomes the main nutrition mode (Muscatine et al. 2005). The isotopic $\delta^{13}C$ signature of tropical corals usually varies between -12 and -16‰, but it may reach -18‰ (e.g. *Madracis mirabilis*) or -28‰ (e.g. *Cladocora caespitosa*) in temperate corals. The $\delta^{15}N$ signature of the coral host is usually correlated with the heterotrophic food source and more enriched than the symbionts because of nutrient-recycling in the symbiosis (Reynaud et al. 2009). Although isotopes provide information on the trophic level and potential nutritional sources of the coral host, this method has rarely been used *in situ* to estimate the contribution of auto- and heterotrophy to coral nutrition and compared with potential food sources (e.g. Muscatine et al. 1989, Muscatine et al. 2005, Alamaru et al. 2009). Moreover, to our knowledge, this approach has never been applied to assess the preferential prey of symbiotic and aposymbiotic corals *in situ*. As the nutrition of bleached corals may significantly rely on heterotrophy (Grottoli et al. 2006, Hughes & Grottoli 2013), it is important to know the natural food sources that support corals *in situ*, especially as corals face increasing challenges in the future ocean.

The present study focuses on the temperate scleractinian coral *Oculina arbuscula*. This species is endemic to the temperate waters of the northwestern Atlantic Ocean. *O. arbuscula* is a facultatively symbiotic species that naturally occurs with and without zooxanthellae and therefore exhibits considerable nutritional plasticity (Miller 1995, Piniak 2002, Leal et al. in 2014b). The aim of this study is to investigate the contribution of auto- and heterotrophy in *O. arbuscula* living under different natural conditions and to determine its potential food sources. We hypothesize that the contribution of auto- and heterotrophy to *O. arbuscula* nutrition varies with symbiotic status of the colony and with season. To address the proposed hypothesis, symbiotic and aposymbiotic coral

colonies were sampled, and the isotopic signature of the coral tissue compared with that of potential autotrophic (symbionts) and heterotrophic (organic matter in the water column and sediment) food sources.

7.2 Materials and Methods

7.2.1 Sampling

Corals were collected from Gray's Reef National Marine Sanctuary (GRNMS). GRNMS is located off the Georgia coast (USA) between the inner- and mid- continental shelf portion of the South Atlantic Bight (SAB). Coral specimens for this study were collected at 20 m depth (30.3939 N, 80.8853 W) under the manager's permit. GRNMS is structured as a ledge system with vertical relief hard-bottom levelling off into a sandy plateau habitat (Hunt 1974). The reef is tidally influenced and seasonally dynamic with respect to temperature, light, turbidity, and nutrients. In addition, because it is relatively shallow, it is regularly affected by large storms that often resuspend the benthos (Hyland et al. 2006).
Coral samples were collected during the spring (May 2012) and fall (October 2012). In each season, a branching portion of five symbiotic and five aposymbiotic coral colonies were randomly collected by SCUBA. Aposymbiotic colonies were usually found in shaded areas close to the ledge. Collected corals were enclosed underwater in a plastic bag containing the surrounding seawater and brought to the laboratory where they were cleaned of epiphytes and sediment. Coral samples were subdivided in two and frozen at -80 ºC. To characterize the isotopic signature of the particulate organic matter (POM) suspended in seawater, five 2 L bottles of seawater were sampled near the corals in each season using a Niskin bottle and transported to the laboratory for filtration. A concentrated sample of large plankton organisms was collected at the sampling site during daytime with a vertical plankton tow (63 µm mesh size) close to the benthic environment. Samples for sediment organic matter (SOM) analysis were taken at each season by SCUBA divers near the corals by scraping the upper 1 cm of the surface sediment into a plastic bag containing surrounding seawater (Riera 1998). The sampling effort of the POM and SOM fractions in each season was performed to provide an overall characterization of the isotopic signature of the potential food sources of *O. arbuscula* and to frame this coral within the food chain, as performed by similar studies with benthic organisms (e.g. Riera et al. 1996, 1999, Ferrier-Pagès et al. 2011, Cocito et al. 2013).

7.2.2 Laboratory procedures

No more than a week after sampling the coral samples were thawed and individually placed in 100 mL beakers (pre-combusted at 480 ºC for at least 4 h) containing 20 mL of filtered seawater (0.7 µm). The coral tissue of each colony was completely removed from the skeleton with an air pick and homogenized with a Potter tissue grinder (precombusted at 480 ºC). Half of the homogenate was freeze-dried and used to estimate the mean signal of the holobiont (host tissue with its symbionts). The other half of the homogenate was separated into a coral host and a symbiont fraction. For the coral host fraction, the homogenate was centrifuged at 3000 g for 10 min at 4 ºC to pellet most of the symbionts. The supernatant was re-centrifuged twice to eliminate the remaining symbionts, transferred to Pyrex petri dishes and freeze-dried. The absence of symbionts in this fraction was confirmed by microscopic examination. For the symbiont fraction, the pellet obtained by centrifugation was washed several times with filtered seawater until no contamination by host cells was visible upon microscopic examination and freeze-dried. Holobiont, host and symbiont

fractions were fumigated with HCl in a closed chamber for 18 h to remove carbonates and dried at 70 ºC for 24 h, ground to a fine powder and kept dried until subsequent analysis. Isotopic analyses were performed on these three sets of samples, with each colony treated individually. The other half of the coral samples were analysed for chlorophyll *a* (Chl *a*) content and symbiont density. For this purpose, coral tissue was detached as previously described and homogenized in 12 mL of filtered seawater. A 2 mL sub-sample was taken for symbiont density as in Rocha et al. (2013). The remaining 10 mL subsamples were centrifuged (5000 g, 10 min, 4 ºC) and the pellet containing the symbionts was re-suspended in 10 mL of 90% acetone. Pigments were extracted at 4 ºC during 24 h. Chl *a* content was determined with and without acidification according to Parsons et al. (1984) using a 10-AU Turner fluorometer (Turner Designs, Sunnyvale, CA). Symbiont density and Chl *a* data were normalized to coral surface area using the single wax dipping method (Veal et al. 2010).
Water samples for POM analysis were size fractionated through inverse filtration to avoid cell breakage. The size fractions were: particles smaller than 10 µm (pico- and nanoplankton) and particles between 10 and 63 µm (large nanoplankton and small microplankton). Particles larger than 63 µm (zooplankton) resulted from the plankton tow collection. Each fraction was then filtered onto pre-combusted 25 mm Whatman GF/F filters, and the filters dried at 70 ºC for 24 h. A fraction of zooplankton samples was collected on filters and treated as above for stable isotope analysis.
For the measurement of stable isotopic ratios of SOM, particles larger than 63 µm were removed by sieving. A sub-sample of approximately 5 g of the fraction smaller than 63 µm was dried at 70 ºC and ground using a mortar and pestle. Afterwards, a sub-sample of approximately 200 mg was acidified as described for coral samples. Once acidified and dried (70 ºC), the sediment was mixed with Milli-Q water and again dried, ground to a fine pounder and dried.
Dried samples of coral, POM and SOM fractions were analysed for $\delta^{13}C$ and $\delta^{15}N$ using a Thermo-Fisher Delta V plus isotope ration mass spectrometer coupled to an Thermo Flash elemental analyser (Fry et al. 1992). Internal chitin standards (Sigma) cross-standardized to internal isotopic reference materials were run at the beginning of each run, and for every 10 samples. Average precision of standards and replicate samples for $\delta^{13}C$ and $\delta^{15}N$ was 0.1‰ and 0.2‰, respectively.

7.2.3 Statistical analysis

Chl *a* content per coral surface area, symbiont density and Chl *a* content per cell were compared using a two-way ANOVA, with the categorical factors being symbiotic status (two levels: symbiotic and aposymbiotic colonies) and season (two levels: spring and fall). The isotopic signatures of the different samples (holobiont, coral host tissue, symbiont) collected from both seasons (spring and fall) from coral colonies with different symbiotic status (symbiotic and aposymbiotic) were compared using a three-way ANOVA. Whenever assumptions of normality and homoscedasticity were violated, ANOVA were performed on square-root transformed data. Tukey's HSD test was used when ANOVA revealed significant differences ($p<0.05$). Isotopic signatures of SOM and different POM size classes were compared separately between seasons using a Student's *t*-test. The theoretical food source of the coral host was calculated taking into account a trophic enrichment of 1‰ and 3.5‰ for $\delta^{13}C$ and $\delta^{15}N$ following Ferrier-Pagès et al. (2011). All statistical analysis and plots were performed using R software (R Development Core Team 2013).

7.3 Results

The density and concentration of symbiotic *O. arbuscula* symbionts and Chl *a*, respectively, were similar between spring and fall (Fig. 7.1). Symbiont density and Chl *a* concentration were significantly lower in aposymbiotic colonies compared to symbiotic colonies (2-way ANOVA, $p<0.01$). The amount of Chl *a* per symbiont cell was significantly different between symbiotic and

aposymbiotic corals (p<0.05; symbiotic: 1.33 ± 0.39 pg cell^{-1}; aposymbiotic: 0.54 ± 0.21 pg cell^{-1}; average ± SD).

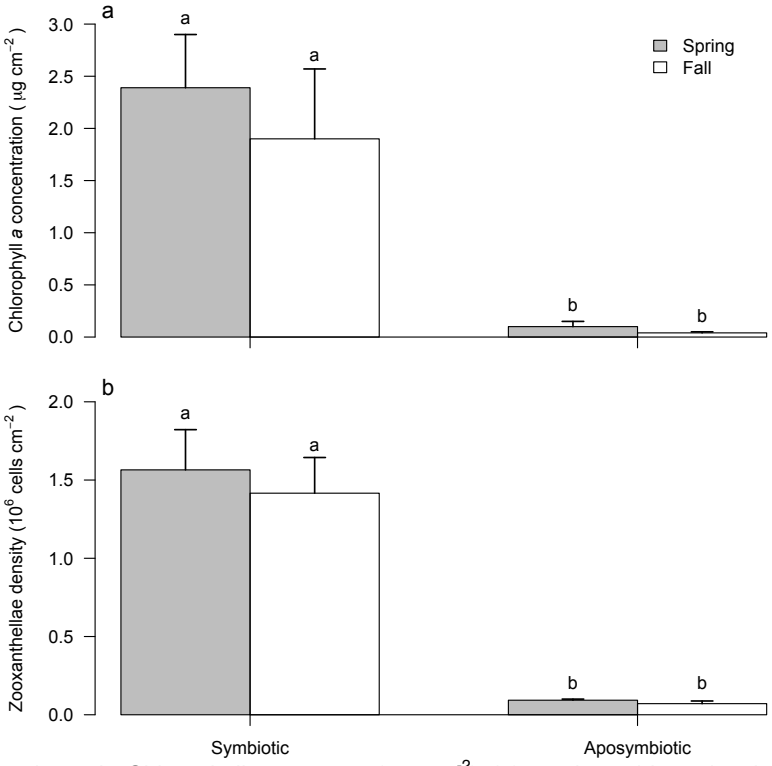

Fig. 7.1 *Oculina arbuscula* Chlorophyll *a* content (µg cm^{-2}) (a), and symbiont density (cells cm^{-2}) (b) in symbiotic and aposymbiotic colonies of *O. arbuscula* during spring and fall (mean ± SD, n = 5). Significant differences (p<0.05) are denoted with different letters.

Carbon ($\delta^{13}C$) and nitrogen ($\delta^{15}N$) isotopic signatures are shown in Fig. 7.2 and Table 7.1. A significant effect of season, symbiotic status and coral fraction (holobiont, coral host, symbionts) was observed in the $\delta^{13}C$ isotopic signature (Table 7.2). The $\delta^{13}C$ was always similar between the holobiont and coral host regardless of symbiotic status (Fig. 7.2), and similar between the coral host and zooxanthellae in symbiotic colonies for each season. Season had no effect on $\delta^{13}C$ of the symbionts (Fig. 7.2), but significantly changed the $\delta^{13}C$ signature of the holobiont and coral host. This signature was ca. +1‰ and +5‰ higher in fall than in spring for symbiotic and aposymbiotic corals, respectively (Tukey's HSD, p<0.05). The $\delta^{13}C$ signature of the holobiont and coral host was significantly more negative in aposymbiotic than in symbiotic colonies in spring (Tukey's HSD, p<0.05). This same signature for the symbionts was similar between symbiotic conditions during both seasons.

Table 7.1 $\delta^{13}C$ and $\delta^{15}N$ values (mean ± SD) for the sediment organic matter (SOM) and different size fractions of particulate organic matter (POM) in spring and fall. Significant differences between seasons for each isotopic signature are marked with different letters.

Potential food sources	$\delta^{13}C$ (‰)		$\delta^{15}N$ (‰)	
	Spring	Fall	Spring	Fall
SOM <63 µm	-20.6 ± 0.2^a	-21.2 ± 0.3^b	5.5 ± 0.5	6.1 ± 0.4
POM <10 µm	-24.6 ± 0.2^a	-22.4 ± 0.3^b	4.9 ± 0.2^a	6.2 ± 0.3^b
POM 10 – 63 µm	-24.5 ± 0.2^a	-19.6 ± 0.6^b	6.6 ± 0.1^a	7.3 ± 0.2^b
POM >63 µm	-22.3 ± 0.1^a	-17.7 ± 0.6^b	5.8 ± 0.4^a	7.5 ± 0.3^b

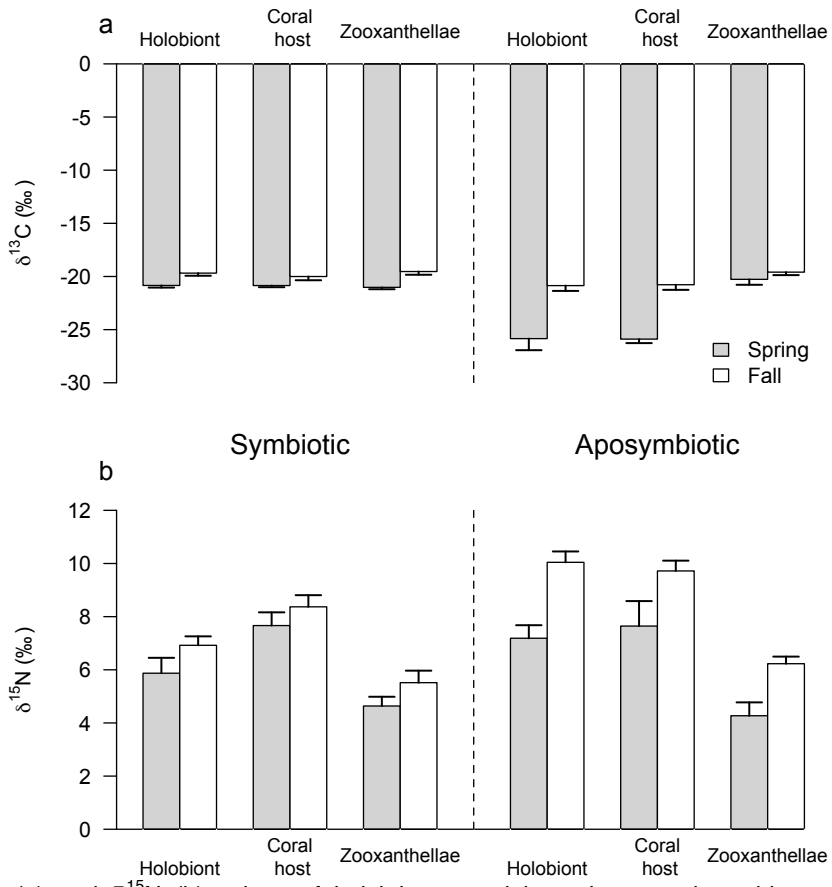

Fig. 7.2 $\delta^{13}C$ (a) and $\delta^{15}N$ (b) values of holobtiont, coral host tissue and symbionts of symbiotic and aposymbiotic *Oculina arbuscula* colonies sampled during spring and fall (mean ± SD, $n = 5$).

A significant effect of season, symbiotic status and holobiont fraction was observed for the $\delta^{15}N$ isotopic signature (Table 7.2). In symbiotic corals, the $\delta^{15}N$ isotopic signature was significantly lower in the holobiont than in the coral host during both seasons (Tukey's HSD, $p<0.05$; Fig. 7.2). In contrast, there were no significant seasonal differences in $\delta^{15}N$ signatures of the holobtiont and coral host fractions from aposymbiotic colonies (Tukey's HSD, $p = 0.76$ and 0.88, respectively). Overall, the $\delta^{15}N$ isotopic signature was always higher in the fall than in the spring for all fractions of the coral holobiont (Fig. 7.2). Significant differences between symbiotic and aposymbiotic colonies were observed in the fall for the $\delta^{15}N$ isotopic signature of coral host (Tukey's HSD, $p<0.05$). The $\delta^{15}N$ signature was significantly higher in the coral host than in the symbionts during both seasons, for both symbiotic and aposymbiotic colonies (Fig. 7.2b).

The $\delta^{13}C$ and $\delta^{15}N$ isotopic signatures of SOM were generally lower than POM, and an overall increase on the signature of both isotopes was observed with increasing POM size classes (Table 7.1). While the $\delta^{13}C$ isotopic signature of SOM was lower in spring, all POM fractions displayed higher $\delta^{13}C$ values in this season (Student's *t*-test, $p<0.05$). The $\delta^{15}N$ isotopic signatures of all POM fractions were significantly higher in the fall (Table 7.1).

Carbon and nitrogen signatures of the different samples are plotted simultaneously in Fig. 7.3. In order to identify the preferential nutrition mode of *O. arbuscula* in each season, the theoretical food source is also indicated in Fig. 7.3. A similar pattern in the functioning of symbiotic colonies was observed in both seasons (Fig. 7.3a, b), with the isotopic signature of the theoretical food source being relatively close to the signature of the symbionts. In aposymbiotic colonies (Fig. 7.3c, d), the theoretical food source during spring and fall was similar to the smallest POM fraction (<10 µm), and also to SOM during the fall.

Table 7.2 Three-way ANOVA comparing the $\delta^{13}C$ and $\delta^{15}N$ isotopic signatures between holobiont fraction (holobiont, coral host tissue and symbiont), symbiotic status of the coral colonies (symbiotic and aposymbiotic), and seasons (spring and fall).

Factor	df	$\delta^{13}C$		$\delta^{15}N$	
		F	*p*	F	*p*
Fraction	2	108.19	<0.01	251.91	<0.01
Season	1	426.27	<0.01	197.68	<0.01
Symbiotic status	1	261.63	<0.01	91.36	<0.01
Fraction * Season	2	30.43	<0.01	4.96	<0.05
Fraction * Symbiotic status	2	93.14	<0.01	30.63	<0.01
Fraction * Symbiotic status	1	119.39	<0.01	43.48	<0.01
Fraction * Season * Symbiotic status	2	53.84	<0.01	1.33	0.27

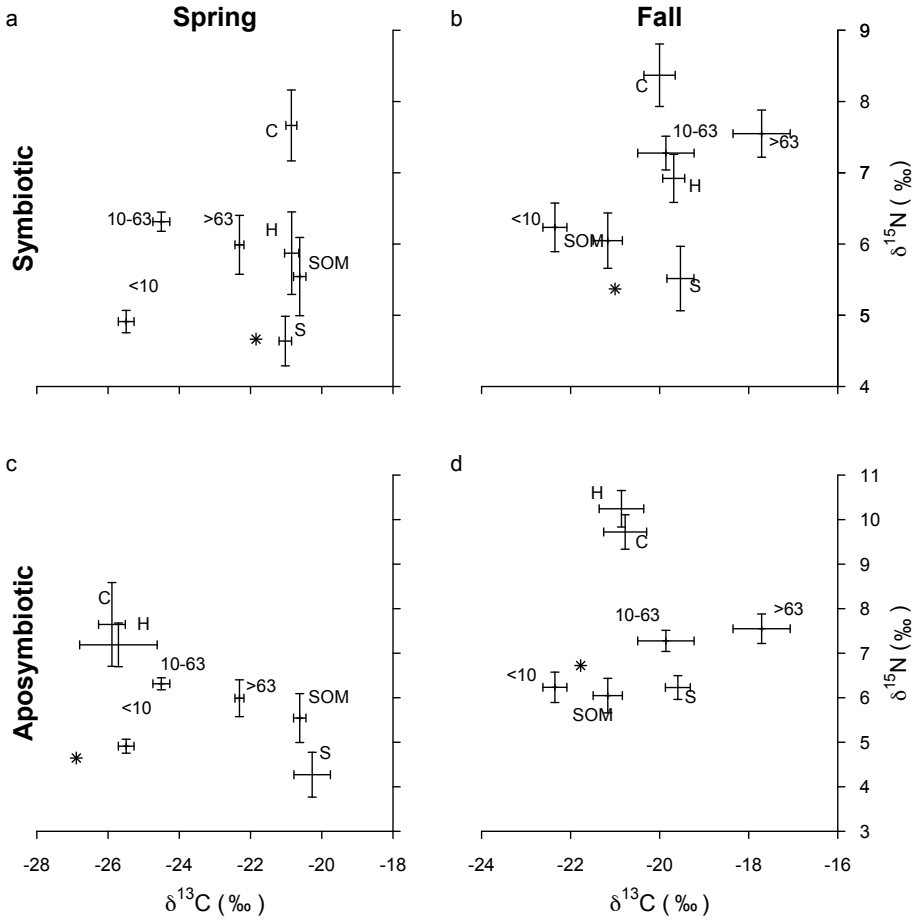

Fig. 7.3 $\delta^{13}C$ *versus* $\delta^{15}N$ (mean ± SD) for symbiotic (a, c) and aposymbiotic (b, d) *Oculina arbuscula*, sediment and seawater sampled during spring (a, b) and fall (c, d). Asterisks correspond to the theoretical food source of the coral host, taking into account the trophic enrichment of 1‰ and 3.5‰ for $\delta^{13}C$ and $\delta^{15}N$, respectively (H, holobiont; C, coral host; S, symbiont; SOM, sediment organic matter; <10, seawater organic matter smaller than 10 µm; 10-63, seawater organic matter between 10 and 63 µm; >63, seawater organic matter larger than 63 µm).

7.4 Discussion

This study examined the contribution of algal symbionts and external food sources to the carbon and nitrogen balance of the temperate scleractinian coral *O. arbuscula*. The isotopic signatures observed for the different coral fractions and potential food sources confirm that pico- and nanoplankton (<10 µm) and SOM largely contribute to the nutrition of *O. arbuscula in situ*. The results of this study also confirmed our two hypotheses, as auto- and heterotrophic contributions to *O. arbuscula* nutrition varied with the symbiotic status of the colony and with the season.

The similar $\delta^{13}C$ isotopic signature of the different fractions (holobiont, coral host and symbiont) in symbiotic colonies suggests high nutrient exchange between the symbionts and the host. However, the isotopic signature for the host and particularly for the symbionts (approximately -20‰) was more negative than is typically reported in tropical symbiotic corals, which display higher $\delta^{13}C$ closer to -12‰ (e.g. Muscatine et al. 1989, Swart et al. 2005). This is probably associated with the highly productive temperate and often turbid waters where *O. arbuscula* occurs (Miller 1995). Low light levels influence the $\delta^{13}C$ signature, as well as the heterotrophic status of the colony (Muscatine et al. 1989, Seemann et al. 2013). Larger heterotrophic contribution may be associated with lower autotrophic inputs due to the relatively low zooxanthellae density present in symbiotic colonies (Fig. 7.1a) as compared to other tropical and temperate symbiotic corals (e.g. Fitt et al. 2000, Rodolfo-Metalpa et al. 2006, Ferrier-Pagès et al. 2011).

The $\delta^{15}N$ isotopic signature of the coral host also indicates a high degree of heterotrophy. Regardless of symbiotic status, the theoretical food source of the coral host had a similar $\delta^{15}N$ signature to that of <10 µm POM fraction in both seasons and also to SOM in fall (Fig. 7.3). Further, the seasonal changes observed for the isotopic signature of the coral host are likely associated with the seasonality of heterotrophic food sources (Table 7.1), as the variation of $\delta^{15}N$ isotopic signature between spring and fall for the symbiotic (+0.8‰) and asymbiotic (+2.1‰) coral host followed the same pattern of the <10 µm POM fraction (+1.3‰). This also supports the hypothesis that the primary nitrogen source for both symbiotic and aposymbiotic colonies derives from heterotrophy (Ferrier-Pagès et al. 2003, Piniak et al. 2003). Moreover, the difference observed for the $\delta^{15}N$ isotopic signature among the holobiont fractions (Fig. 7.2b) is probably due to a higher retention of heavy nitrogen by the host (after prey ingestion), and excretion (and subsequent re-uptake by the zooxanthellae) of light nitrogen from waste products (Reynaud et al. 2009). This nutrient recycling in the symbiosis contributes to the $\delta^{15}N$ enrichment of 3‰ observed between the coral host and the symbionts observed during both seasons (Fig. 7.2).

Heterotrophy was the expected nutrition mode of aposymbiotic colonies (Miller 1995). The large difference between symbionts and coral host and holobiont fractions supports the low contribution of autotrophy (Fig. 7.3c,d). In contrast to the results observed for symbiotic colonies, the $\delta^{13}C$ isotopic signature of the coral host was significantly lower than the symbionts (Fig. 7.2a). However, this was not detected in asymbiotic colonies during fall. The $\delta^{13}C$ isotopic signature of asymbiotic *O. arbuscula* in fall was similar among all coral fractions and to the results observed for symbiotic corals (Fig. 7.2a). One possibility is that aposymbiotic colonies sampled in the fall were originally symbiotic and recently bleached. The results could therefore reflect the isotopic signature of the coral in its former symbiotic condition, where both auto- and heterotrophy occur (mixotrophy) together with high nutrient exchange between the host and symbionts. It has been speculated that corals rely on energy reserves from autotrophy when bleached (Grottoli et al. 2004), and that both photoautotrophic and heterotrophic acquired carbon play a crucial role in the recovery from bleaching (Hughes et al. 2010, Hughes & Grottoli 2013). As autotrophy in *O. arbuscula* has not been considered to be as important as in tropical corals (Muscatine et al. 1989, Muscatine et al. 2005), it is important to determine to what extent this holds true for this coral in its natural environment. Here we address this question through calculation of the isotopic signature of the

theoretical food source (Fig. 7.3). Although the exact number for isotopic fractionation for this coral species is unknown, results for symbiotic *O. arbuscula* show that the isotopic signature of the theoretical food source is similar to the symbionts in symbiotic corals and to certain fractions of organic matter available in the environment (Fig. 7.3a,b). While it is not clear which of these fractions is the preferential food source for the symbiotic colonies due to the contribution of autotrophy to the coral's nutrition, the theoretical food source of these colonies in fall was also similar to the isotopic signature of SOM. Aposymbiotic *O. arbuscula* was notably similar to the <10 µm POM fraction in spring (Fig. 7.3c) and also to SOM in fall (Fig. 7.3d). This reliance on pico- and nanoplankton during both seasons has only been reported in few studies, as this small planktonic fraction has been overlooked as a potential food source for scleractinian corals (e.g. Houlbrèque et al. 2006, Naumann et al. 2009, Ferrier-Pagès et al. 2011). While the analysis performed in this study do not allow us to perform an accurate characterization of the organisms present in the <10 µm POM, it is known that this fraction is mainly composed by bacteria, phototrophic and heterotrophic flagellates, diatoms and cyanobacteria (Lalli & Parsons 1997). In the SAB region, phototrophs account for 60-90% of the carbon biomass of pico- and nanoplankton, particularly diatoms that compose 30-70% of the phototrophic community (Verity et al. 1993, 1996). In recent laboratory experiments, Leal et al. (2014a) demonstrated that symbiotic *O. arbuscula* is able to feed on microalgae from 4 to 12 µm. Herbivory is a poorly documented feature of symbiotic corals (Houlbrèque & Ferrier-Pagès 2009) that has already been reported for several asymbiotic soft corals (Fabricius et al. 1995, Fabricius et al. 1998) and only more recently has been described for a reduced number of symbiotic corals (Tremblay et al. 2012, Seemann et al. 2013). While the molecular trophic markers used by Leal et al. (2014a) provide information on prey capture, the present study provides information on the coral food sources that were assimilated over time. This supports the hypothesis that small planktonic organisms, including phytoplankton, may play a relevant contribution to the nutrition of scleractinian corals such as *O. arbuscula.*

In conclusion, this study suggests that SOM and the planktonic fraction <10 µm, which is abundant and constantly available in reef waters (e.g. Furnas et al. 1990, Ferrier-Pagès & Gattuso 1998, Tada et al. 2003), are important nutrient sources for *O. arbuscula*. The use of stable isotopes together with molecular trophic markers used by Leal et al. (2014a) contributes to the growing evidence that the small autotrophic and heterotrophic planktonic fraction importantly contributes to the nutrition of symbiotic scleractinian corals (Houlbrèque et al. 2004b, Naumann et al. 2009, Tremblay et al. 2012). These new data on the feeding preferences of symbiotic scleractinian corals may change our understanding of trophic interactions in coral reefs because pico- and nanoplankton have been overlooked as a potential food source for symbiotic corals.

7.5 Acknowledgments

M.C.L. was supported by a PhD scholarship (SFRH/BD/63783/2009) funded by the Fundação para a Ciência e Tecnologia (QREN-POPH-Type 4.1 – Advanced Training, subsidized by the European Social Fund and national funds MCTES). Partial support was also provided by the US National Science Foundation to M.E.F. (awards OCE 0825999 and OCE 1031263), J.C.N. (award OCE 0824499) and J.A.B. (award OCE 1031263), and CFP was supported by the government of the Principality of Monaco. We are also grateful to Greg McFall and NOAA's Gray's Reef National Marine Sanctuary for access to and help collecting the corals used in this study, and to three anonymous reviewers for their comments. *Oculina arbuscula* corals were collected at Gray's Reef National Marine Sanctuary under the manager's permit.

7.6 References

Alamaru A, Yam R, Shemesh A, Loya Y (2009) Trophic biology of *Stylophora pistillata* larvae: evidence from stable isotope analysis. Mar Ecol Prog Ser 383:85-94

Anthony KRN, Fabricius KE (2000) Shifting roles of heterotrophy and autotrophy in coral energetics under varying turbidity. J Exp Mar Biol Ecol 252:221-253

Cocito S, Ferrier-Pagès C, Cupido R, Rottier C, Meier-Augenstein W, Kemp H, Reynaud S, Peirano A (2013) Nutrient acquisition in four Mediterranean gorgonian species. Mar Ecol Prog Ser 473:179-188

Fabricius KE, Benayahu Y, Genin A (1995) Herbivory in asymbiotic soft corals. Science 268:90-92

Fabricius KE, Yahel G, Genin A (1998) *In situ* depletion of phytoplankton by an azooxanthellate soft coral. Limnol Oceanogr 43:354-356

Falkowski P, Dubinsky Z, Muscatine L, Porter J (1984) Light and the bioenergetics of a symbiotic coral. BioScience 34:705-709

Ferrier-Pagès C, Gattuso J-P (1998) Biomass, production and grazing rates of pico- and nanoplankton in coral reef waters (Miyako island, Japan). Microbial Ecol 35:46-57

Ferrier-Pagès C, Witting J, Tambutté E, Sebens KP (2003) Effect of natural zooplankton feeding on the tissue and skeletal growth of the scleractinian coral *Stylophora pistillata*. Coral Reefs 22:229-240

Ferrier-Pagès C, Peirano A, Abbate M, Cocito S, Negri A, Rottier C, Riera P, Rodolfo-Metalpa R, Reynaud S (2011) Summer autotrophy and winter heterotrophy in the temperate symbiotic coral *Cladocora caespitosa*. Limnol Oceanogr 56:1429-1438

Fitt WK, McFarland FK, Warner ME, Chilcoat GC (2000) Seasonal patterns of tissue biomass and densities of symbiotic dinoflagellates in reef corals and relation to coral bleaching. Limnol Oceanogr 45:677-685

Fry B, Brand W, Mersch FJ, Tholke K, Garritt R (1992) Automated analysis system for coupled $\delta^{13}C$ and $\delta^{15}N$ measurements. Anal Chem 64:288-291

Furnas MJ, Mitchell AW, Gilmartin M, Revelante N (1990) Phytoplankton biomass and primary production in semi-enclosed reef lagoons of the central Great Barrier Reef, Australia. Coral Reefs 9:1-10

Glynn PW (1973) Ecology of a caribbean coral reef. The *Porites* reef-flat biotope: part II. Plankton community with evidence for depletion. Mar Biol 22:1-21

Grottoli AG, Rodrigues LJ, Juarez C (2004) Lipids and stable carbon isotopes in two species of Hawaiian corals, *Porites compressa* and *Montipora verrucosa*, following a bleaching event. Mar Biol 145:1-11

Grottoli AG, Rodrigues LJ, Palardy JE (2006) Heterotrophic plasticity and resilience in bleached corals. Nature 440:1186-1189

Houlbrèque F, Tambutté E, Ferrier-Pagès C (2003) Effect of zooplankton availability on the rates of photosynthesis, and tissue and skeletal growth in the scleractinian coral *Stylophora pistillata*. J Exp Mar Biol Ecol 296:145-166

Houlbrèque F, Tambutte E, Allemand D, Ferrier-Pages C (2004a) Interactions between zooplankton feeding, photosynthesis and skeletal growth in the scleractinian coral *Stylophora pistillata*. J Exp Biol 207:1461-1469

Houlbrèque F, Tambutte E, Richard C, Ferrier-Pages C (2004b) Importance of a micro-diet for scleractinian corals. Mar Ecol Prog Ser 282:151-160

Houlbrèque F, Delesalle B, Blanchot J, Montel Y, Ferrier-Pagès C (2006) Picoplankton removal by the coral reef community of La Prévoyante, Mayotte Island. Aquatic Microb Ecol 44:59-70

Houlbrèque F, Ferrier-Pagès C (2009) Heterotrophy in tropical scleractinian corals. Biol Rev 84:1-17

Hughes AD, Grottoli AG, Pease TK, Matsui Y (2010) Acquisition and assimilation of carbon in non-bleached and bleached corals. Mar Ecol Prog Ser 420:91-101

Hughes AD, Grottoli AG (2013) Heterotrophic compensation: a possible mechanism for resilience of coral reefs to global warming or a sign of prolonged stress? PLoS One 8:e81172

Hunt J (1974) The geology and origin of Gray's Reef, Georgia continental shelf. MSc thesis, University of Georgia, Athens, GA

Hyland J, Cooksey C, Balthis WL, Fulton M, Bearden D, McFall G, Kendall M (2006) The soft-bottom macrobenthos of Gray's Reef National Marine Sanctuary and nearby shelf waters off the coast of Georgia, USA. J Exp Mar Biol Ecol 330:307-326

Lalli C, Parsons TR (1997) Biological oceanography: An introduction (2nd edn). Elsevier Butterworth-Heinemann, Oxford, 320 pp.

Leal MC, Nunes C, Kempf SC, Reis A, Silva TL, Serôdio J, Cleary DFR, Calado R (2013) Effect of light, temperature and diet on the fatty acid profile of the tropical sea anemone *Aiptasia pallida*. Aquacult Nutr 19:818-826

Leal MC, Ferrier-Pagès C, Calado R, Thompson ME, Frischer ME, Nejstgaard JC (2014a) Coral feeding on microalgae assessed with molecular trophic markers. Mol Ecol 23:3870-3876

Leal MC, Nejstgaard JC, Calado R, Thompson ME, Frischer ME (2014b) Molecular assessment of heterotrophy and prey digeston in zooxanthellate cnidarians. Mol Ecol 23:3838-3848

Miller M (1995) Growth of a temperate coral - Effects of temperature, light, depth, and heterotrophy. Mar Ecol Prog Ser 122:217-225

Muscatine L, McCloskey L, Marian R (1981) Estimating the daily contribution of carbon from zooxanthellae to coral animal respiration. Limnol Oceanogr 26:601-611

Muscatine L, Porter JW, Kaplan IR (1989) Resource partitioning by reef corals as determined from stable isotope composition. I. $\delta^{13}C$ of zooxanthellae and animal tissue *vs* depth. Mar Biol 100:185-193

Muscatine L, Goiran C, Land L, Jaubert J (2005) Stable isotopes (^{13}C and ^{15}N) of organic matrix from coral skeleton. PNAS 102:1525-1530

Naumann MS, Richter C, el-Zibdah M, Wild C (2009) Coral mucus as an efficient trap for picoplanktonic cyanobacteria: implications for pelagic–benthic coupling in the reef ecosystem. Mar Ecol Prog Ser 385:65-76

Palardy JE, Grottoli AG, Matthews KA (2006) Effect of naturally changing zooplankton concentrations on feeding rates of two coral species in the Eastern Pacific. J Exp Mar Biol Ecol 331:99-107

Palardy JE, Rodrigues LJ, Grottoli AG (2008) The importance of zooplankton to the daily metabolic carbon requirements of healthy and bleached corals at two depths. J Exp Mar Biol Ecol 367:180-188

Parsons TR, Maita Y, Lalli CM (1984) A manual of chemical and biological methods for seawater analysis, Pergamon Press, Oxford, UK

Piniak G (2002) Effects of symbiotic status, flow speed, and prey type on prey capture by the facultatively symbiotic temperate coral *Oculina arbuscula*. Mar Biol 141:449-455

Piniak G, Lipschultz F, McClelland J (2003) Assimilation and partitioning of prey nitrogen within two anthozoans and their endosymbiotic zooxanthellae. Mar Ecol Prog Ser 262:125-136

Porter JW (1976) Autotrophy, heterotrophy, and resource partitioning in Caribbean reef-building corals. Am Nat 110:731-742

R Development Core Team (2013) R: A language and environment for statistical computing. R Foundation for Statistical Computing. R Foundation for Statistical Computing, Vienna, Austria (http://www.R-project.org)

Reynaud S, Ferrier-Pagés C, Sambrotto R, Juillet-Lecrec A, Jaubert J, Gattuso JP (2002) Effect of feeding on the carbon and oxygen isotopic composition in the tissues and skeleton of the zooxanthellate coral *Stylophora pistillata*. Mar Ecol Prog Ser 238:81-89

Reynaud S, Martinez P, Houlbrèque F, Billy I, Allemand D, Ferrier-Pagès C (2009) Effect of light and feeding on the nitrogen isotopic composition of a zooxanthellate coral: role of nitrogen recycling. Mar Ecol Prog Ser 392:103-110

Ribes M, Coma R, Rossi S (2003) Natural feeding of the temperate asymbiotic octocoral-gorgonian *Letpgorgia sarmentosa* (Cnidaria: Octocorallia). Mar Ecol Prog Ser 254:141-150

Riera P, Richard P, Grémare A, Blanchard G (1996) Food source of intertidal nematodes in the Bay of Marennes-Oléron (France), as determined by dual stable isotope analysis. Mar Ecol Prog Ser 142:303-309

Riera P (1998) d^{15}N of organic matter sources and benthic invertebrates along an estuarine gradient in Marennes-Oléron Bay, France. Implication for the study of trophic structures. Mar Ecol Prog Ser 166:143-150

Riera P, Stal LJ, Nieuwenhuize J, Richard P, Blanchard G, Gentil F (1999) Determination of food sources for benthic invertebrates in a salt marsh (Aiguillon Bay, France) by carbon and nitrogen stable isotopes: importance of locally produced sources. Mar Ecol Prog Ser 187:301-307

Rocha RJM, Serôdio J, Leal MC, Cartaxana P, Calado R (2013) Effect of light intensity on post-fragmentation photobiological performance of the soft coral *Sinularia flexibilis*. Aquaculture 388-391:24-29

Rodolfo-Metalpa R, Richard C, Allemand D, Bianchi CN, Morri C, Ferrier-Pages C (2006) Response of zooxanthellae in symbiosis with the Mediterranean corals *Cladocora caespitosa* and *Oculina patagonica* to elevated temperatures. Mar Biol 150:45-55

Rodrigues L, Grottoli A (2007) Energy reserves and metabolism as indicators of coral recovery from bleaching. Limnol Oceanogr 52:1874-1882

Sebens KP, Vandersall KS, Savina LA, Graham KR (1996) Zooplankton capture by two scleractinian corals, *Madracis mirabilis* and *Montastrea cavernosa*, in a field enclosure. Mar Biol 127:303-317

Seemann J, Berry KL, Carballo-Bolaños R, Struck U, Leinfelder RR (2013) The use of ^{13}C and ^{15}N isotope labeling techniques to assess heterotrophy of corals. J Exp Mar Biol Ecol 442:88-95

Swart PK, Saied A, Lam K (2005) Temporal and spatial variation in the δ^{15}N and δ^{13}C of coral tissue and zooxanthellae in *Montastraea faveolata* collected from the Florida reef tract. Limnol Oceanogr 50:1049-1058

Tada K, Sakai K, Nakano Y, Takemura A, Montani S (2003) Size-fractionated phytoplankton biomass in coral reef waters off Sesoko Island, Okinawa, Japan. J Plankton Res 25:991-997

Tremblay P, Naumann MS, Sikorski S, Grover R, Ferrier-Pagès C (2012) Experimental assessment of organic carbon fluxes in the scleractinian coral *Stylophora pistillata* during a thermal and photo stress event. Mar Ecol Prog Ser 453:63-77

Veal CJ, Carmi M, Fine M, Hoegh-Guldberg O (2010) Increasing the accuracy of surface area estimation using single wax dipping of coral fragments. Coral Reefs 29:893-897

Verity PG, Yoder JA, Bishop SS, Nelson JR, Craven DB, Blanton JO, Robertson CY, Tronzo CR (1993) Composition, productivity and nutrient chemistry of a coastal ocean planktonic food web. Cont Shelf Res 13:741-776

Verity PG, Paffenhofer GA, Wallace D, Sherr E, Sherr B (1996) Composition and biomass of plankton in spring on the Cape Hatteras shelf, with implications for carbon flux. Cont Shelf Res 16:1087-1116

Yahel R, Yahel G, Genin A (2005) Near-bottom depletion of zooplankton over coral reefs: I: diurnal dynamics and size distribution. Coral Reefs 24:75-85

Chapter 8 Symbiont type influences trophic plasticity of a model cnidarian-algal symbiosis

Abstract

Symbiotic associations represent critical drivers of ecological function and evolutionary processes. The association between cnidarians and photosynthetic dinoflagellates within genus *Symbiodinium* is a prevalent and ecologically important relationship in tropical and subtropical marine environments. Although the remarkable diversity of *Symbiodinium* provides an axis for niche diversification, increased functional range, and resilience to changing climate, how such diversity relates to the balance between autotrophy and heterotrophy remains unknown. Here we show inter- and intraspecific variability of carbon fixation and subsequent translocation by *Symbiodinium* to the model cnidarian host *Aiptasia pallida*. Symbiont identity defines trophic plasticity through its individual metabolic requirements, capacity to fix carbon, quantity, and possibly quality, of translocated photosynthates, and ultimately the host's capacity to feed and digest prey. A positive correlation between carbon translocation and host feeding across symbiotic combinations contrasts with the paradigm of heterotrophic compensation when autotrophy declines. The lack of a shift toward greater heterotrophy when carbon translocation is low suggests that the metabolic demand of feeding and digestion may overwhelm nutritional stores when autotrophy is reduced, and raises questions of the generalized role of heterotrophy in resiliency and resistance to the effects of climate change in more obligate symbioses such as reef corals.

Keywords

Symbiodinium; Functional diversity; Nutrition; Photosynthesis.

Submitted: Leal MC, Hoadley K, Pettay DT, Grajales A, Calado R, Warner ME (submitted) Symbiont type influences trophic plasticity of a model cnidarian-algal symbiosis. Journal of Experimental Biology.

8.1 Introduction

Throughout evolutionary history, several animals have thrived in oligotrophic environments, such as coral reefs, by capitalizing on the photosynthetically-fixed carbon of endosymbiotic unicellular algae (Venn et al. 2008). The association between coral reef cnidarians and dinoflagellates within the genus *Symbiodinium* represents one such key cosmopolitan symbiosis in the oceans (Coffroth and Santos 2005, Weis et al. 2008).

While the interspecific diversity and flexibility within *Symbiodinium* is well known (Coffroth and Santos 2005, Sampayo et al. 2008), the functional diversity of *Symbiodinium* and its consequences to the nutritional balance of the host remains unexplored. Symbiotic cnidarians are reliant on both autotrophically and heterotrophically derived carbon (Falkowski et al. 1984), from the photoautotrophic products of their symbionts and nutrients acquired through feeding on planktonic organisms, respectively. This trophic plasticity is critical for the health, fitness, and resilience of these symbiotic associations (Grottoli et al. 2006). While a shifting reliance from auto- to heterotrophy with light attenuation has been observed within different coral species (Muscatine et al. 1989, Anthony and Fabricius 2000), others suggest that autotrophy is either unrelated (Davy and Cook 2001) or inversely related to heterotrophic contribution (Grottoli et al. 2006, Hughes and Grottoli 2013).

Symbiont genotypic diversity affects the quantity and quality of translocated material to the host (Loram et al. 2007, Starzak et al. 2014), but it is unknown how this diversity relates to the trophic status of the holobiont (i.e. the combination of animal host and algal symbiont). Notably, no direct simultaneous comparisons exist between auto- and heterotrophic performance that accounts for symbiont identity. Here we address the consequences of inter- and intraspecific variability of *Symbiodinium* and its relationship to the trophic plasticity of the association as defined by the interaction of autotrophic and heterotrophic performance. The symbiotic sea anemone *Aiptasia pallida* was used while individually hosting three isoclonal lines (i.e. strains) of its naturally occurring clade B symbiont, *Symbiodinium minutum* (ITS2 type B1), a mixture of one *S. minutum* strain and *Symbiodinium psygmophilum* (ITS2 type B2), or a single isolate of *Symbiodinium* from the putatively thermally tolerant ‘D’ lineage (ITS2 type D4-5) (Rowan 2004, Lajeunesse et al. 2010a). Due to its global distribution and symbiont flexibility, this anemone has become a model organism to understand the physiology and coevolution of cnidarian-*Symbiodinium* symbioses (Weis et al. 2008, Thornhill et al. 2013). Photosynthetic performance and carbon translocation of the symbionts, together with host prey capture and digestion provided the proxies to score nutritional plasticity of the symbiosis. To gauge heterotrophic performance alone, results were then compared to anemones lacking symbionts (aposymbiotic).

8.2 Materials and Methods

8.2.1 Animal models

Anemones consisted of a monoclonal line of aposymbiotic (Burriesci et al. 2012) *Aiptasia pallida* (clone CC7) provided by the Pringle Lab (Stanford University, USA). Aposymbiotic anemones were kept in constant darkness over two years in a closed system containing filtered seawater (1 µm FSW) and fed brine shrimp weekly. Different combinations of *A. pallida* symbioses were generated by infecting aposymbiotic anemones (similar to Schoenberg and Trench (1980), minus the seawater extract of *Artemia*) with genetically distinct cultures of *Symbiodinium* originating from

various symbiotic cnidarians (Table 8.1). Two of the symbionts used are recently described species of clade B *Symbiodinium*, *S. minutum* and *S. psygmophilum* (Lajeunesse et al. 2012), while the third, D4-5, represents a stress tolerant clade of symbionts (Glynn et al. 2001, Lajeunesse et al. 2010b). Three strains (designated at strains 1, 2 & 3) within the species *S. minutum* (ITS2 type B1) were chosen because they are the dominant symbiont of wild *Aiptasia pallida* (Thornhill et al. 2013), and *S. psygmophilum* (ITS2 type B2) was included to investigate the effects of a mixed symbiont infection between two species within the same clade. Another monoclonal line of *A. pallida*, originally collected in Bermuda, was used as well and hosted one of the unique strains of *S. minutum* (strain 3). All associations of *A. pallida* symbiosis were stable for over 1 year and kept in flow-through systems using FSW under normal growth conditions (26ºC, ~33 ‰, 150 µmol m^{-2} s^{-1} photosynthetic photon flux, 12-h light-dark cycle) and fed brine shrimp weekly. Associations with each symbiont(s) genotype were confirmed before experiments (see below). Aposymbiotic anemones were confirmed to be free of algae by periodic microscopic examination as well as after shifting several anemones into lighted incubators over several months.

Table 8.1 Culture name, cnidarian host and corresponding ITS2 Genbank numbers for the different symbiont strains

Symbiont	Culture name	Host	Corresponding ITS2 Genbank #
S. minutum strain 1	FLAp2	*Aiptasia pallida*	AF333511
S. minutum strain 2	Unknown	Unknown	AF333511
S. minutum strain 3	N/A	*Aiptasia pallida*	AF333511
S. psygmophilum	Unknown	Unknown	AF333512
D4-5	Ap31	Unknown anemone	AF499802 (4) EU812743 (5)

8.2.2 Genetic identification of algal types

One representative anemone from each of the five algal combinations was sampled from batch isoclonal cultures prior to the experiment to confirm the genetic identity of the symbionts. Following the heterotrophic feeding (see below), symbiont identity was again confirmed for all five replicates per host/symbiont combination by extracting total DNA from 100 µL of the anemone homogenate (LaJeunesse 2002). The partial 5.8S and ITS2 region of each sample was fingerprinted using PCR-DGGE and the fingerprints characterized by Sanger sequencing of the fingerprint (LaJeunesse 2002). The symbionts, and their corresponding ITS2 fingerprints, used in this study are detailed in Table 8.1. Additional diversity and resolution within the B1 ITS2 lineage that better approximates species-level diversity can be gained by sequencing the microsatellite locus B7Sym15 (Finney et al. 2010, Lajeunesse et al. 2012). Therefore, the three strains used were characterized based on flanker region sequence of this locus to definitively place them within the species *S. minutum* (matching genbank# JX263427). To further elucidate the genetic diversity within *S. minutum* and characterize each strain (i.e. multilocus genotype) used in this study, fragment analysis was conducted on five microsatellite loci (B7Sym15, B7Sym34, B7Sym36, CA4.86 and CA6.38) for the samples prior to the experiment (Table 8.2) (Santos and Coffroth 2003, Pettay and LaJeunesse 2007). Two of these loci (B7Sym15 and B7Sym36) were further used at the conclusion of the feeding experiment (see below) to confirm the identity of the genetically distinct *S. minutum* strains and verify that the symbioses had remained stable at both the ITS2 and strain level. Lastly, to verify that the *Aiptasia* clones were genetically distinct, fragment analysis was conducted on six microsatellite loci (AIPT6, AIPT8, AIPT14, AIPT15, AIPT17 and AIPT20) developed for *Aiptasia* spp. Briefly, microsatellite loci were developed from EST sequences of *A. pallida* (Sunagawa et al. 2009) that were vectored screened (using VecScreen & the UniVec NCBI vector library) and

assembled (CAP3; Huang and Madan 1999). Contigs and singlent sequences were screened for SSR of di, tri, tetra, penta and hexanucleotides with more than 6 repeats (WebSat; Martins et al. 2009). Primers were designed for candidate loci (Primer3; Rozen and Skaletsky 2000) and the loci screened on *A. pallida* samples from the Florida Keys and Bermuda collected in 2011. The two clones used in this study differed by at least one allele at all loci except AIPT14, proving that the clonal lines are genetically different (Table 8.3).

Table 8.2 Alleles for the *Symbiodinium minutum* microsatellites used to resolve strain diversity.

Strain or MLG	Microsatellite Loci				
	B7Sym15	B7Sym34	B7Sym36	CA4.86	CA6.38
Strain 1	263	281	196	182	101
Strain 2	263	267	163	199	103
Strain 3	259	271	169	182	101
mixture	263	267	163	199	103

[a] Microsatellites loci for the B1 strain present in the mixture with B2

Table 8.3 Alleles for the *Aiptasia* microsatellites used to resolve clone divrersity.

Aiptasia clone	Microsatellite Loci					
	AIPT6	AIPT8	AIPT14	AIPT15	AIPT17	AIPT20
CC7	302	293	188	319	292	334
	302	295	191	322	292	334
Bermudas	302	293	188	319	294	339
	318	293	191	319	296	341

8.2.3 Carbon uptake and translocation

Starved anemones of each algal combination genotype were placed in separate 7 mL scintillation vials containing 2 mL of seawater spiked with 15 µL of ^{14}C Bicarbonate (specific activity 17 µCi µmol^{-1}) following previously described procedures (Davy and Cook 2001). Five anemones were used for each algal combination and treatment. All vials were then placed on a LED light-table (Cool White Cree XPG-R5; 150 µmol photons m^{-2} s^{-1}; 28°C) for 90 minutes. Two additional anemones from each algal combination were placed in vials with spiked seawater and maintained in the dark for 90 minutes to account for carbon uptake in the dark. Three additional vials containing only the spiked seawater were also included for measurement of total activity. After incubations each anemone was ground up in 1 mL of seawater with a 1.5 mL Ten Broeck tissue grinder. A 100 µL sample of the resulting homogenate was removed and fixed with 10 µL of 1% gluteraldehyde (Acros Organics) and utilized for symbiont cell counts (see below). The remaining homogenate was centrifuged at 5000 g for 5 min to separate the host and symbiont fractions. A 500 µL sample of the host supernatant (H_s) was removed and the remaining supernatant was stored for downstream calculation of protein content. The symbiont pellet (S) was then resuspended in 400 µL of FSW. Dissolved organic carbon (DOC) released from the organism was also calculated by removing 200 µL of seawater from each anemone-containing vial. All samples were acidified using an equal volume of 2N HCL for 24 hours, then dosed with 5mL of scintillation cocktail. After an additional 24-hour period, radioactivity was determined with a liquid scintillation counter (Beckman LS-6500). Calculations were made using the mean specific activity (gC dpm^{-1}), which was estimated from the carbon content of 0.024 g C L^{-1} of seawater (Davy and Cook 2001). All samples were background and dark uptake corrected. Translocation (T_L) was calculated as (DOC+H_s) normalized to host protein (see below). Photosynthesis (P_{net}) was calculated as

(DOC+H_s+S) normalized to total symbiont cells per anemone (see below). The fraction of photosynthate translocated to the host was calculated as (DOC+H_s)/(DOC+H_s+S).

8.2.4 Heterotrophic feeding

A. pallida individuals starved over one week were placed in 1.2 L Plexiglas chambers with unidirectional flow (0.1 m s^{-1}) (Leal et al. 2014) and each replicate consisted of a separate feeding chamber with one individual each for each symbiont genotype tested and aposymbiotic anemones. Newly hatched *Artemia* nauplii (24 h) were added at a final concentration of 2 nauplii mL^{-1} to each chamber once the polyps were expanded. After 15 min feeding time, anemones were sampled and thoroughly rinsed three times in FSW to detach any prey that were captured but not ingested. Five individuals were immediately flash-freeze and stored at -80 ºC for molecular assessment of prey ingestion, and other five individuals were transferred to a prey-free environment where they were allowed to digest ingested prey over 24 h before sampling as previously described. Unfed *A. pallida* from each algal combination were also sampled prior to feeding incubations as negative controls. Samples (n = 5) of a known number of *Artemia* nauplii (varying from 5 to 100 individuals) were also flash-freeze and stored at -80 ºC for genomic DNA (gDNA) extraction.

Each individual stored during feeding incubations was thawed at room temperature, grind with ultra turrax (IKA, Staufen, Germany) in 1 mL of FSW, and 300 µL transferred for gDNA extraction. The remaining 700 µL were centrifuged (5 min, 4 ºC, 6000 rpm) to pellet the symbionts. The supernatant composed of the cnidarian host fraction was transferred to a new tube and stored at -80 ºC for later protein quantification. The pellet was re-suspended in 400 µL of FSW and 100 µL were aliquot to a new tube with 10 µL of gluteraldehyde (1%, Acros Organics) and stored at 4 ºC for determination of symbiont cell density.

Total animal protein was assessed using Pierce BCA Protein Assay Kit (Thermo Scientific, Rockford, IL) following the manufacturer's instructions for microplate readings. Absorbance (562 nm) was measured using a FluoStar Omega reader (BMG Labtech GmbH, Ortenberg, Germany). Symbiont cell density was recorded by light fluorescence microscopy. Six independent replicate counts were performed for each sample on a haemocytometer. Samples were photographed using a Nikon microphot-FXA epifluorescent microscope (100x magnification). Photographs were then analyzed by computer software ImageJ (Schneider et al. 2012) with the analyze particles function.

Extraction of gDNA was performed using the MoBio UltraClean Tissue and Cells DNA isolation Kit (Carlsbad, Ca, USA) following the manufacturer's instructions, apart from the bead beating step that used approximately 100 µL of 0.5 mm glass beads for each extraction. After extraction, gDNA was quantified using a Nanodrop 2000c spectrophotometer (Thermo Scientific, New York, NY, USA). Total gDNA from *Artemia* nauplii samples was used to estimate the gDNA content per individual prey (Leal et al. 2014). Prey DNA content in each anemone sample was estimated through qPCR amplification of *Artemia* DNA using the primers Af18s-1298F and Af18S-1373R (Leal et al. 2014). For each qPCR reaction, a dilution series of extracted gDNA from *Artemia* nauplii was run as a quantitative standard. The appropriate amount of template DNA in all assays was achieved using 1 µL of gDNA extract. qPCR reactions were performed using a 7500 RealTime PCR System (Applied Biosystems, Foster City, Ca, USA) in 96-well plates with each reaction well containing 5 uL of SensiMix SYBR Hi-ROX reaction mix (Bioline, UK), 400 nM of primers and template gDNA. Amplification conditions included an initial denaturation step (10 min, 95 ºC) followed by 40 amplification cycles (15s, 94 ºC; 30s 60 ºC annealing/extension temperature). Each reaction was followed by a melt-curve thermal profile from 60 to 95 ºC to evaluate specificity of the primers. All reactions were run in triplicate and PCR-grade water was used as a template for negative control, as well as gDNA from unfed anemones. Mean primer efficiency in all qPCR reactions was 99.2% ± 1.0%. To estimate prey DNA breakdown, all samples were also run in

qPCR reactions using primers Af18s-1298F and Af18S-1422R (Leal et al. 2014). Anemones break down *Artemia* nauplii prey during digestion, which results in decreasing quantity with increasing amplicon size. Thus, the ratio between prey DNA content obtained with the two primer sets amplifying amplicon sizes of 73 and 112 bp will be 0% if all prey DNA is degraded (no prey DNA detected using the primer set amplifying the 112 bp amplicon) and 100% if no prey DNA is broken down (equal amount of prey DNA detected using both primer sets) (Leal et al. 2014). Digestion rate was assessed through the ratio between prey DNA content detected in samples collected immediately after ingestion and after 24 h digestion, and calculated as a percentage. A digestion rate of 100% indicates that no prey DNA was detected after 24h digestion, whereas 0% is obtained when identical prey DNA contents are observed immediately after ingestion and after 24 h digestion. Prey DNA content was normalized to animal protein.

8.2.5 Statistics

All measured parameters were compared among host/algal combinations with a one-way ANOVA. Tukey's HSD post-hoc test used when statistical differences were observed ($p<0.05$). Pearson's correlation was used to assess the relationship between different parameters measured in the same *Aiptasia* individuals. Due to the necessarily destructive nature of the methods, carbon translocation and prey ingestion were measured on different individuals; hence some statistical comparisons were not possible. Patterns of symbiont genotype and photosynthesis or symbiont cell density on carbon translocation per cell or per host protein, respectively, were tested using ANCOVA. Model residuals were checked to verify assumptions of normality and homogeneity of variance; transformations were not required (Zuur et al. 2009). Statistical analyses were performed with R (R Development Core Team 2013).

8.3 Results

While substantial differences were observed in symbiont density (ANOVA, $n = 25$, $F = 13.16$, $p<0.001$), all symbiont combinations displayed a significant positive correlation between the rate of cellular carbon fixation (photosynthesis) and the carbon translocated to the animal (Fig. 8.1; Pearson correlation, $n = 25$, $r = 0.89$, $t = 9.368$, $df = 23$, $p<0.001$). Photosynthesis was a good predictor of carbon translocation across genotypes and the slopes were significantly different among genotypes, particularly D4-5 symbionts ($p<0.05$; Table 8.4). Individual photosynthetic performance of each animal-algal combination, together with symbiont density, resulted in greater carbon translocated to the host as algal density increased (Fig. 8.2; Pearson correlation, $n = 25$, $r = 0.75$, $t = 5.4352$, $df = 23$, $p<0.001$). While this affected total carbon translocated to the host across symbiont genotype (ANOVA, $n = 25$, $F = 4.006$, $p<0.05$), the relationship between symbiont density and carbon translocated (Fig. 8.2) were similar among clades (Table 8.4).

Table 8.4 Summary statistics for slopes from multiple linear regressions of carbon translocation as a function of photosynthesis or symbiont density

Carbon translocation (µg C cell^{-1}hour^{-1})			Total carbon translocation (µg C host protein^{-1}hour^{-1})		
	F value	*p* value		*F* value	*p* value
Photosynthesis	388.89	< 0.001	Cell density	35.93	< 0.001
Symbiont genotype	6.81	< 0.01	Symbiont genotype	1.48	0.26
Interaction	12.77	< 0.001	Interaction	1.76	0.19
Residual d.f.	15		Residual d.f.	15	

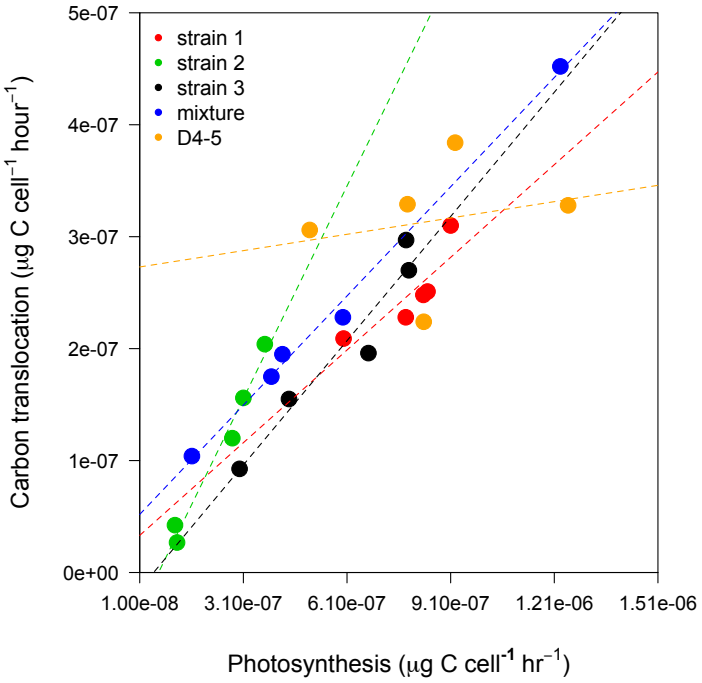

Fig. 8.1 Relationship between maximal photosynthesis and carbon translocation to the host. Photosynthesis and carbon translocation rates normalized to algal cell number in individual *Aiptasia pallida* hosting a single unique strain of *Symbiodinium minutum* (denoted by strain 1, 2 or 3) or a mixture of *S. minutum* strain 2 and *S. psygmophilum* or D4-5 (n = 5 • algal genotype combination^{-1}; strains 1, 2 & 3 = *S. minutum*). Dashed lines correspond to linear regression for each strain.

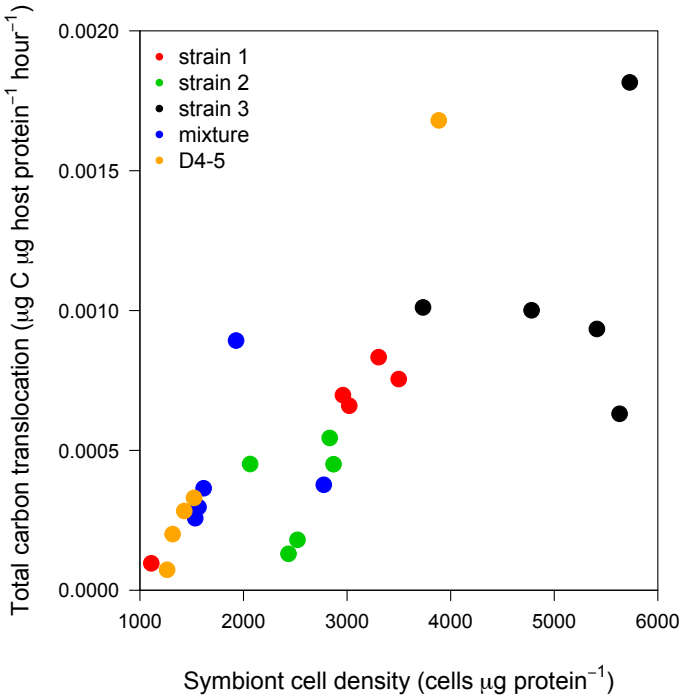

Fig. 8.2 Relationship between symbiont density and total carbon translocated to the host. Algal cell densities and the rate of carbon translocation normalized to anemone protein measured in individuals hosting a single unique strain of *Symbiodinium minutum* (denoted by strain 1, 2 or 3) or a mixture of *S. minutum* strain 2 and *S. psygmophilum* or D4-5 (n = 5 • algal genotype combination^{-1}; strains 1, 2 & 3 = *S. minutum*).

The relationship between carbon translocated from the symbiont to the host and prey ingestion shows that heterotrophy is positively associated with autotrophy with the exception of anemones hosting D4-5 symbionts (Fig. 8.3a). Although this pattern fits across symbiont genotypes within clade B, inter- and intraspecific differences were observed for prey ingestion and prey DNA breakdown among the different symbiotic combinations (Fig. 8.3b,c). Particularly, high prey ingestion and slow prey digestion (supplementary material Table S2) was observed for aposymbiotic individuals and anemones hosting *S. minutum* strain 3 and D4-5 symbionts.

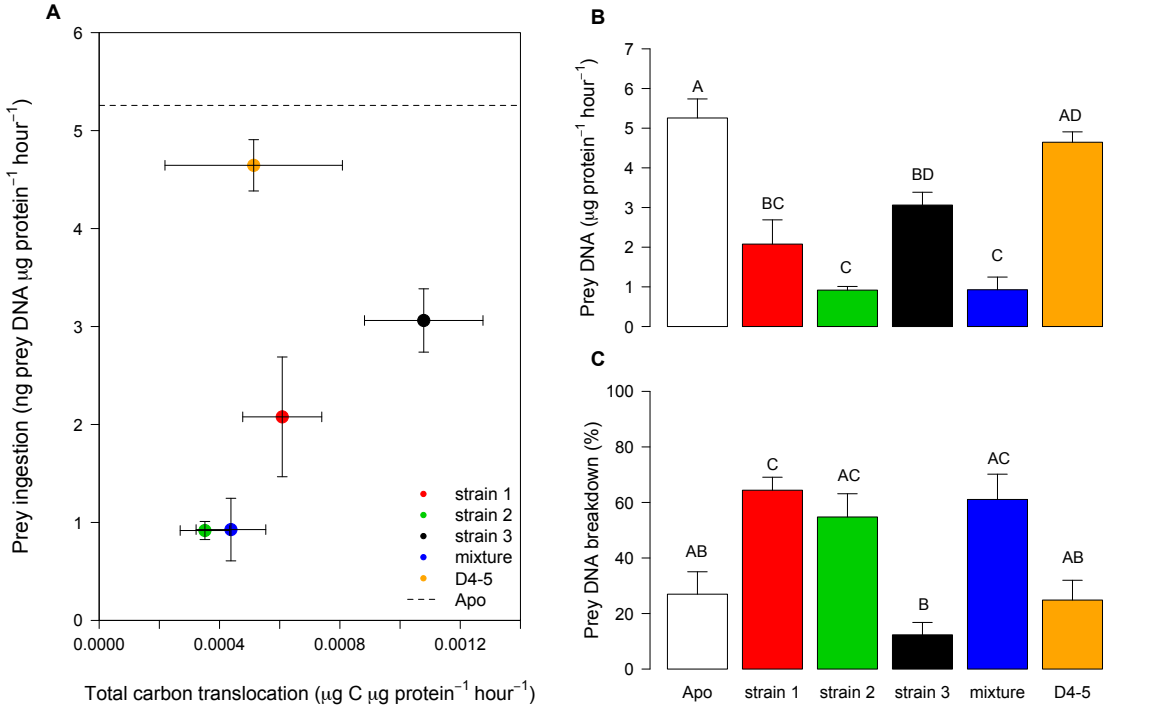

Fig. 8.3 Autotrophy and heterotrophy. Measured in individuals (n = 5) hosting a single unique strain of *Symbiodinium minutum* (denoted by strain 1, 2 or 3) or a mixture of *S. minutum* strain 2 and *S. psygmophilum* or D4-5. Total carbon translocation and prey ingestion rates (mean ± SE) (a). Prey ingestion rate (mean ± SE.; estimated through prey DNA content) (b). Prey DNA breakdown (mean ± SE; 100% denotes no prey DNA breakdown and 0% denotes total prey DNA breakdown) (c). *Apo* denotes aposymbiotic anemones (dashed line; a). Different superscript letters (b, c) denote significant differences among genotypes (Tukey's HSD, p<0.05).

8.4 Discussion

This study shows that the genetic identity of *Symbiodinium* influences the nutritional plasticity of cnidarian-algal symbioses. Host prey feeding and digestion is associated with both photoautotrophic carbon translocation and symbiont type, even at the symbiont sub-species level. The marked differences in symbiont density and translocation among algal strains within *S. minutum* alone underscore the functional diversity within these algae, and that broad physiological generalizations for entire clades of *Symbiodinium* (e.g. Fabina et al. 2013) are likely not warranted.

We expected that symbiotic associations with lower autotrophic contribution (i.e. less C-translocated) would compensate for such losses by increasing heterotrophy (Grottoli et al. 2006, Ferrier-Pagès et al. 2011, Hughes and Grottoli 2013). However, with the exception of the D4-5 symbiont that does not fit this pattern, results suggest that higher autotrophy is strongly associated to increased heterotrophy (Fig. 8.3a). In contrast, the association with the D alga resulted in relatively low total carbon translocated but high prey ingestion (Fig. 8.3a). Similarly, aposymbiotic anemones receive no autotrophic input and consequently rely on prey capture and ingestion efforts

as their only source of nutrients (Grottoli et al. 2006). Similar prey ingestion and digestion between aposymbiotic *Aiptasia* and anemones hosting D4-5 symbionts (Fig. 8.3b,c) suggests that both groups of anemones increase their heterotrophic efforts through prey capture and ingestion but subsequent prey breakdown and digestion is relatively slow. While not directly tested here, such similarities may be explained by the reduced autotrophic contribution of D4-5 symbionts to support their host's metabolism (Fig. 8.2).

The lack of congruence between high carbon fixation and translocation per algal cell and total translocation to the host in the anemones harbouring the D symbiont is also a consequence of their low cell density (Fig. 8.1 and Fig. 8.2), suggesting that increased photosynthetic rates are needed to translocate the same amount of carbon (Fig. 8.1). Symbiont cell density is determined, in part, by the photosynthetic carbon flux and individual metabolic requirements of symbionts, which varies with symbiont type (Dubinsky and Berman-Frank 2001, Starzak et al. 2014). Likewise, possible space constraints, or other as yet uncharacterized, control elements of the animal and cellular recognition signals between the partners and may play a defining role here (Schoenberg and Trench 1980, Smith and Muscatine 1999). As such, the D4-5 symbiont is efficient at fixing carbon (i.e. photosynthesis) but performs poorly at translocating it. While the symbiosis with D4-5 cells is temporally stable in isolation, it may represent a suboptimal symbiosis between host and symbiont lineages that have not coevolved together. This may cause the strong relationship between autotrophy and heterotrophy noted in the other holobionts to breakdown in this particular symbiosis (Fig. 8.3a). If true, this symbiont may be an inefficient competitor against homologous symbionts of *Aiptasia* like *S. minutum*. While not measured in this study, a difference in the quality of translocated material between different *Symbiodinium,* as has been noted in another tropical anemone harbouring different clades of *Symbiodinium* (Loram et al. 2007), could also contribute to this pattern.

The positive association between autotrophy and heterotrophy for the different *S. minutum* strains and the mixed clade B infections may be due to two non-mutually exclusive reasons: i) increased heterotrophy is the result of autotrophic energy supply that is available to support metabolically demanding heterotrophic processes (Sebens 2002), and ii) increased heterotrophic contribution is critical to the assimilation of photosynthetic carbon into host biomass (Falkowski et al. 1984, Dubinsky and Jokiel 1994). Conversely, the increased prey ingestion with slower digestion in aposymbiotic and D4-5 anemones may be the result of heterotrophy being a partial energetic sink in itself. Such quantitative and qualitative differences may have implications to energy budgets of the symbiosis. Further, widely used models quantifying autotrophic and heterotrophic contributions to animal respiration, known as CZAR (Muscatine et al. 1981) and CHAR (Grottoli et al. 2006) respectively, may need further modification to address the important metabolic costs of feeding and digestion (Sebens 2002).

In conclusion, heterotrophy is positively associated with autotrophy, and the latter is significantly correlated with the symbionts' capacity to fix and translocate carbon in a density dependent manner (Fig. 8.2), which is in turn affected by individual metabolic requirements of the symbiont. Physiological variability within a single *Symbiodinium* species thus results in a change in the nutritional status of the cnidarian host where both auto- and heterotrophy play a pivotal role. The influence of symbiont type in contributing to this trade-off between auto- and heterotrophy is especially important in the context of coral bleaching events, as not all stable algal/animal symbioses are equally nutritionally advantageous to the animal. Bleached corals may increase their feeding rates (Grottoli et al. 2006, Hughes and Grottoli 2013) but may not take advantage of heterotrophic opportunities if host metabolic processes associated with prey digestion are affected by symbiont competency and consequent autotrophic capacity. *Symbiodinium* functional diversity, which can extend below the species-level, is thus critical to the nutritional plasticity of cnidarian-

algal symbioses, influencing their resilience and acclimation, and having ecological implications for the success of these symbioses in marine environments.

8.5 Acknowledgments

The authors would like to thank J. Pringle for the CC7 *A. pallida* clone. M.C.L. was supported by a PhD scholarship (SFRH/BD/63783/2009) funded by the Fundação para a Ciência e Tencologia (QREN-POPH-Type 4.1-Advanced Training, subsidized by the ESF and national MED funds). This project was supported by project SYMBIOCoRe (FP7-PEOPLE-2011-IRSES, 295191), and by the National Science Foundation (IOS 1258065 and EF 1316055).

8.6 References

Anthony KRN, Fabricius KE (2000) Shifting roles of heterotrophy and autotrophy in coral energetics under varying turbidity. J Exp Mar Biol Ecol 252:221-253

Burriesci MS, Raab TK, Pringle JR (2012) Evidence that glucose is the major transferred metabolite in dinoflagellate-cnidarian symbiosis. J Exp Biol 215:3467-3477

Coffroth MA, Santos SR (2005) Genetic diversity of symbiotic dinoflagellates in the genus *Symbiodinium*. Protist 156:19-34

Davy S, Cook C (2001) The relationship between nutritional status and carbon flux in the zooxanthellate sea anemone *Aiptasia pallida*. Mar Biol 139:999-1005

Dubinsky Z, Jokiel PL (1994) Ratio of energy and nutrient fluxes regulates symbiosis between zooxanthellae and corals. Pacific Sci 48:313-324

Dubinsky Z, Berman-Frank I (2001) Uncoupling primary production from population growth in photosynthesizing organisms in aquatic ecosystems. Aquat Sci 63:4-17

Fabina NS, Putnam HM, Franklin EC, Stat M, Gates RD (2013) Symbiotic specificity, association patterns, and function determine community responses to global changes: defining critical research areas for coral-*Symbiodinium* symbiosis. Global Change Biol 19:3306-3316

Falkowski P, Dubinsky Z, Muscatine L, Porter J (1984) Light and the bioenergetics of a symbiotic coral. BioScience 34:705-709

Ferrier-Pagès C, Peirano A, Abbate M, Cocito S, Negri A, Rottier C, Riera P, Rodolfo-Metalpa R, Reynaud S (2011) Summer autotrophy and winter heterotrophy in the temperate symbiotic coral *Cladocora caespitosa*. Limnol Oceanogr 56:1429-1438

Finney JC, Pettay DT, Sampayo EM, Warner ME, Oxenford HA, LaJeunesse TC (2010) The relative significance of host-habitat, depth, and geography on the ecology, endemism, and speciation of coral endosymbionts in the genus *Symbiodinium*. Microbial Ecol 60:250-263

Glynn PW, Maté JL, Baker AC, Calderón MO (2001) Coral bleavhing and mortality in Panama and Ecuador during the 1997-1998 El Niño-southern oscilation event: spatial/temporal patterns and comparisons with the 1982-1983 event. Bull Mar Sci 69:79-109

Grottoli AG, Rodrigues LJ, Palardy JE (2006) Heterotrophic plasticity and resilience in bleached corals. Nature 440:1186-1189

Huang X, Madan A (1999) CAP3: A DNA sequence assembly program. Genome Res 9:868-877

Hughes AD, Grottoli AG (2013) Heterotrophic compensation: a possible mechanism for resilience of coral reefs to global warming or a sign of prolonged stress? PLoS One 8:e81172

LaJeunesse T (2002) Diversity and community structure of symbiotic dinoflagellates from Caribbean coral reefs. Mar Biol 141:387-400

Lajeunesse TC, Pettay DT, Sampayo EM, Phongsuwan N, Brown B, Obura D, Hoegh-Guldberg O, Fitt WK (2010a) Long-standing environmental conditions, geographic isolation and host-symbiont specificity influence the relative ecological dominance and genetic diversification of coral endosymbionts in the genus *Symbiodinium*. J Biogeography 37:785-800

Lajeunesse TC, Smith R, Walther M, Pinzon J, Pettay DT, McGinley M, Aschaffenburg M, Medina-Rosas P, Cupul-Magana AL, Perez AL, Reyes-Bonilla H, Warner ME (2010b) Host-symbiont recombination versus natural selection in the response of coral-dinoflagellate symbioses to environmental disturbance. Proc R Soc Lond, Ser B: Biol Sci 277:2925-2934

Lajeunesse TC, Parkinson JE, Reimer JD (2012) A genetics-based description of *Symbiodinium minutum* sp. nov. and *S. psygmophilum* sp. nov. (Dinophyceae), two dinoflagellates symbiotic with cnidaria. J Phycol 48:1380-1391

Leal MC, Nejstgaard JC, Calado R, Thompson ME, Frischer ME (2014) Molecular assessment of heterotrophy and prey digeston in zooxanthellate cnidarians. Mol Ecol 23:3838-3848

Loram JE, Trapido-Rosenthal HG, Douglas AE (2007) Functional significance of genetically different symbiotic algae *Symbiodinium* in a coral reef symbiosis. Mol Ecol 16:4849-4857

Martins WS, Lucas DCS, Souza Neves KF, Bertioli DJ (2009) WebSat: A web software for microsatellite marker development. Bioinformation 3:282

Muscatine L, McCloskey L, Marian R (1981) Estimating the daily contribution of carbon from zooxanthellae to coral animal respiration. Limnol Oceanogr 26:601-611

Muscatine L, Porter JW, Kaplan IR (1989) Resource partitioning by reef corals as determined from stable isotope composition. I. δ13C of zooxanthellae and animal tissue vs depth. Mar Biol 100:185-193

Pettay DT, LaJeunesse TC (2007) Microsatellites from clade B *Symbiodinium* spp. specialized for Caribbean corals in the genus Madracis. Mol Ecol Notes 7:1271-1274

R Development Core Team (2013) R: A language and environment for statistical computing. R Foundation for Statistical Computing. R Foundation for Statistical Computing, Vienna, Austria (http://www.R-project.org)

Rowan R (2004) Coral bleaching thermal adaptation in reef coral symbionts. Nature 430:742

Rozen S, Skaletsky H (2000) Primer 3 on the WWW for general users and for biologist programmers. Methods Mol Biol 132:365-386

Sampayo E, Ridgway T, Bongaerts P, Hoegh-Guldberg O (2008) Bleaching susceptibility and mortality of corals are determined by fine-scale differences in symbiont type. PNAS 105:10444

Santos SR, Coffroth MA (2003) Molecular genetic evidence that dinoflagellates belonging to the genus *Symbiodinium* Freudenthal are haploid. Biol Bull 204:10-20

Schneider C, Rasband W, Eliceiri K (2012) NIH Image to ImageJ: 25 years of image analysis. Nat Methods 9:671-675

Schoenberg DA, Trench RK (1980) Genetic variation in *Symbiodinium* (=*Gymnodinium*) *microadriaticum* Freudenthal, and specificity in its symbiosis with marine invertebrates: III. Specificity and infectivity of *Symbiodinium microadriaticum*. Proc Nat Acad Sci 207:445-460

Sebens KP (2002) Energetic contraints, size gradients, and size limits in benthic marine invertebrates. Integr Comp Biol 42:853-861

Smith G, Muscatine L (1999) Cell cycle of symbiotic dinofagellates: variation in G1 phase-duration with anemone nutritional status and macronutrient supply in the *Aiptasia pulchella-Symbiodinium pulchrorum* symbiosis. Mar Biol:1-14

Starzak DE, Quinnell RG, Nitschke MR, Davy SK (2014) The influence of symbiont type on photosynthetic carbon flux in a model cnidarian-dinoflagellate symbiosis. Mar Biol 161:711-724

Sunagawa S, Wilson EC, Thaler M, Smith ML, Caruso C, Pringle JR, Weis VM, Medina M, Schwarz JA (2009) Generation and analysis of transcriptomic resources for a model system on the rise: the sea anemone *Aiptasia pallida* and its dinoflagellate endosymbiont. BMC genomics 10:258

Thornhill DJ, Xiang Y, Pettay DT, Zhong M, Santos SR (2013) Population genetic data of a model symbiotic cnidarian system reveal remarkable symbiotic specificity and vectored introductions across ocean basins. Mol Ecol 22:4499-4515

Venn A, Loram J, Douglas A (2008) Photosynthetic symbioses in animals. J Exp Bot 59:1069-1080

Weis V, Davy S, Hoegh-Guldberg O, Rodriguez-Lanetty M, Pringle J (2008) Cell biology in model systems as the key to understanding corals. Trends Ecol Evol 23:369-376

Zuur AF, Ieno EN, Walker NJ, Saveliev AA, Smith GM (2009) Mixed effects models and extensions in ecology with R, Springer, New York, 663 pp.

Chapter 9 Final remarks and future directions

9.1 Final remarks

The overall goal of this thesis is to increase our understanding of the role of auto- and heterotrophy in the ecophysiology of the cnidarian-dinoflagellate symbiosis, and the ecological implications of this trophic plasticity. However, our understanding of any scientific question is inherently limited by the methods available to address postulated hypotheses. Therefore, in order to tackle new questions on the trophic plasticity of the cnidarian-algal symbiosis, the first component of this thesis was dedicated to develop new methodological approaches (**Chapters 2-5**). The methods here developed were associated with photophysiology (**Chapter 2**), biomass production of the model organism *Aiptasia pallida* (**Chapters 3-4**) and heterotrophy in zooxanthellate cnidarians (**Chapter 5**). The optimization of *Aiptasia pallida* production was successfully used in **Chapter 5** and **Chapter 8**, whereas the molecular methods to investigate heterotrophy were used in **Chapter 6** and **Chapter 8**. The developed methods allowed unravelling key findings associated with symbiotic corals and the functioning of this symbiosis. Microalgae were confirmed as a potential food source for symbiotic corals (**Chapter 6**), which contrasts with current knowledge on their potential heterotrophic food sources (Houlbrèque & Ferrier-Pagès 2009). This finding, combined with the *in situ* assessment of the trophic ecology of *Oculina arbuscula*, contributes to the growing evidence that small (<10 µm) autotrophic planktonic organisms may play a major contribution to the nutrition of symbiotic corals (**Chapter 7**). Lastly, the molecular trophic methods (**Chapter 5**) were applied in a laboratory experiment devoted to experimental comparative physiology of a model cnidarian-algal symbiosis (**Chapter 8**). This investigation tackled fundamentally important questions concerning the functional diversity of *Symbiodinium* symbioses with broad implications for the understanding of the balance between auto- and heterotrophy on tropical symbiotic organisms such as reef forming corals.

Five research questions were proposed in the introductory chapter (**Chapter 1**). Here, I briefly summarize the answer to each specific question in the context of the observed results:

1. *How can we non-invasively assess the photophysiological spatial heterogeneity within the cnidarian-dinoflagellate symbiosis?*

The modification of an imaging pulse amplitude fluorometer using differential excitation light and selectively detecting spectral bands allowed a high-resolution characterization of the spatial relationship between key parameters (chlorophyll variable fluorescence, chlorophyll *a* content and green fluorescent protein-like proteins). Spatial patterns were identified and interesting results open new questions on the photophysiology of zooxanthellate cnidarians.

2. *How can we maximize biomass production of the model organism Aiptasia pallida to use in the study of the cnidarian-dinoflagellate symbiosis, and what are the biochemical implications of culturing these organisms in laboratory?*

The conditions that resulted in faster biomass production were 26 ºC water temperature, total darkness and using a diet of *Artemia* nauplii. Initial stocking density was also important to produce a larger number of anemones (low initial stocking density) or increase biomass of anemone individuals (high initial stocking density). However, *Aiptasia pallida* should be reared under light conditions to increase fatty acid content, as it drives the production of alpha-linolenic acid (18:3*n*-3) and docasohexaenoic acid (22:6*n*-3) by *Symbiodinium*.

3. *Can we use molecular methods to improve the study of heterotrophy in zooxanthellate cnidarians, and what ecological insights can these methods provide?*

We were able to use molecular trophic markers to assess prey ingestion and digestion in zooxanthellate cnidarians. This method allowed us to identify prey digestion times of 1-3 days depending on the type of prey, cnidarian species and predator feeding history. These findings have important implications for bioenergetic and trophodynamic studies of zooxanthellate cnidarians, particularly energy budgets in the cnidarian-algal symbiosis.

4. *Are symbiotic corals able to feed on phytoplankton under laboratory and field conditions?*

Herbivory was confirmed for symbiotic corals in laboratory. Field data suggest that the facultative symbiotic coral *Oculina arbuscula* rely on nutrients translocated from their symbionts and from pico- and nanoplanktonic prey. These findings have implications for trophic interactions and benthic-pelagic coupling in coral reefs.

5. *How does Symbiodinium diversity affect trophic plasticity of the cnidarian-dinoflagellate symbiosis?*

Different *Symbiodinium* species and sub-species provide variable amounts of carbon from photosynthesis to the animal host, and this trophic relationship directly influences animal feeding and prey digestion. Symbiont identity defines this nutritional plasticity through its individual metabolic requirements, capacity to fix carbon, quantity of translocated carbon and, ultimately, the host's capacity to feed and digest prey.

The cnidarian-dinoflagellate symbiosis is an ecologically important association, particularly in oligotrophic reef ecosystems where nutrients are scarce. As other metazoans that are metabolically impoverished, cnidarians overcame this limitation by hosting autotrophic organisms that provide organic carbon molecules (Porter 1976). This association granted the cnidarian host with alternative metabolic pathways to overcome deprivation of environmental food. Both autotrophic and heterotrophic pathways have an important role on the metabolism, growth and energy reserves of the cnidarian host (Anthony & Fabricius 2000, Houlbrèque et al. 2003, Grottoli et al. 2004). However, the effects of the functional diversity of *Symbiodinium* in this nutritional regulation and the ecological consequences of this trophic plasticity still remain poorly explored.

The work presented here provides new methodological approaches and addresses poorly studied issues of the cnidarian-dinoflagellate symbiosis. Consequently, important findings are here presented. Pico- and nanoplankton were confirmed as important items on the trophic ecology of symbiotic corals, particularly autotrophic organisms that have long been an overlooked food source. Prey digestion was assessed for the first time using molecular methods and revealed an effect of predator and prey species on digestion time and prey digestion processes. Lastly, this work culminated with an integrated approach that investigated auto- and heterotrophy simultaneously and revealed that closely related sub-species of symbionts directly influence the trophic plasticity of the cnidarian-dinoflagellate symbiosis. This suggests that not all algal/animal symbioses are equally nutritionally advantageous to the animal and evidence the functional implications of how *Symbiodinium* diversity extends beyond the species level. These results have broad implications for understanding the balance between auto- and heterotrophy in the cnidarian-dinoflagellate symbiosis, and note the role of *Symbiodinium* diversity on the resilience and recovery of zooxanthellate cnidarians.

9.2 Future directions

Three main directions can be followed after this study:

- **Herbivory in symbiotic corals**. Using an established method, i.e. stable isotopes, and a new methodological approach, i.e. molecular trophic markers, we confirmed the importance

of small planktonic organisms (<10 µm), particularly microalgae, to the trophic ecology of symbiotic corals. As this group of organisms has been overlooked as a potential food source, this opens new perspectives on the role of phytoplankton for the nutrition of symbiotic corals. Fundamental ecological questions involving microalgae prey remain overlooked, such as feeding rates, digestion times and prey selectivity. Extrapolation of such question to an ecosystem scale are also important in order to accurately assess the role of phytoplankton on coral reef food webs, tropical biogeochemical cycling and benthic-pelagic coupling.

- **Heterotrophy and molecular trophic markers**. The use of molecular trophic markers has been changing our understanding of food-web ecology (Pompanon et al. 2012). The use of this approach to investigate heterotrophy in cnidarian-dinoflagellate symbiosis may allow researchers to unravel underlying mechanisms of coral reef trophic ecology. Investigating ingested prey items *in situ* can be more accurately performed using these molecular tools, as well as the investigation of tropical marine food webs and resource partitioning in nutrient-depleted reef ecosystems. Moreover, the use of molecular tools to investigate prey ingestion and digestion may also be used to assess metabolic costs associated with this energy-demanding mechanism, and its implications to energy budgets. Furthermore, accurate molecular methods may be used to investigate the conclusions of **Chapter 8** related with heterotrophy acting as an energetic sink and its implications to the recovery of zooxanthellate cnidarians from bleaching events.
- **Functional diversity of *Symbiodinium***. While still controversial, the fundamental role of Symbiodinium in the regulation of the cnidarian-dinoflagellate symbiosis is becoming clearer with increasing research efforts (Davy et al. 2012, Lesser et al. 2013, Wooldridge 2013). Future research will certainly address the diversity of *Symbiodinium* and its specificity towards the cnidarian host (Thornhill et al. 2013). The functional diversity of *Symbiodinium* and its implications to the symbiosis is also an important topic that is currently being investigated. The differential quantity and quality of translocated products by different *Symbiodinium* species to their cnidarian host (Loram et al. 2007), as well as species-specific variability of underlying mechanisms of resilience and resistance to stress associated with future climate change (Palumbi et al. 2014) are still being debated and thoroughly explored.

The cnidarian-dinoflagellate symbiosis has been thoroughly investigated in tropical environments. However, this association also occurs in subtropical and temperate environments (Baker et al. 2003). It is important to understand if the functioning of this symbiosis outside tropical areas remains similar, as well as the underlying mechanisms that affect its fitness and resilience. This is especially relevant from a nutritional point of view, as temperate environments are usually eutrophic, which contrasts with oligotrophic tropical systems. The functional diversity of *Symbiodinium* in temperate environments is also relevant to further investigate, as different strains within this genus may have different implications to the trophic plasticity of the symbiosis.

9.3 References

Anthony KRN, Fabricius KE (2000) Shifting roles of heterotrophy and autotrophy in coral energetics under varying turbidity. J Exp Mar Biol Ecol 252:221-253.

Baker AC (2003) Flexibility and specificity in coral-algal symbiosis: Diversity, ecology, and biogeography of *Symbiodionium*. Annu Rev Ecol Evol S 34: 661-689.

Davy SK, Allemand D, Weis VM (2012) Cell biology of cnidarian-dinoflagellate symbiosis. Microb Molec Biol Rev 76:229-261.

Grottoli AG, Rodrigues LJ, Juarez C (2004) Lipids and stable carbon isotopes in two species of Hawaiian corals, *Porites compressa* and *Montipora verrucosa*, following a bleaching event. Mar Biol 145:1-11.

Houlbrèque F, Ferrier-Pagès C (2009) Heterotrophy in tropical scleractinian corals. Biol Rev 84:1-17.

Houlbrèque F, Tambutté E, Ferrier-Pagès C (2003) Effect of zooplankton availability on the rates of photosynthesis, and tissue and skeletal growth in the scleractinian coral *Stylophora pistillata*. J Exp Mar Biol Ecol 296:145-166.

Lesser MP, Stat M, Gates RD (2013) The endosymbiotic dinoflagellates (*Symbiodinium* sp.) of corals are parasites and mutualists. Coral Reefs 32:603-611.

Loram JE, Trapido-Rosenthal HG, Douglas AE (2007) Functional significance of genetically different symbiotic algae *Symbiodinium* in a coral reef symbiosis. Molec Ecol 16:4849-4857.

Palumbi SR, Barshis DJ, Traylor-Knowles NG, Bay RA (2014) Mechanisms of reef coral resistance to future climate change. Science 344:895-898.

Pompanon F, Deagle BE, Symondson WOC, Brown DS, Jarman SN, Taberlet P (2012) Who is eating what: diet assessment using next generation sequencing. Molec Ecol 21:1931-1950.

Porter JW (1976) Autotrophy, heterotrophy, and resource partitioning in Caribbean reef-building corals. Am Nat 110:731-742.

Thornhill DJ, Xiang Y, Pettay DT, Zhong M, Santos SR (2013) Population genetic data of a model symbiotic cnidarian system reveal remarkable symbiotic specificity and vectored introductions across ocean basins. Molec Ecol 22:4499-4515.

Wooldridge SA (2013) Breakdown of the coral-algae symbiosis: towards formalising a linkage between warm-water bleaching thresholds and the growth rate of the intracellular zooxanthellae. Biogeosciences 10:1647-1658.